THESIS

NUMERICAL MODELING INVESTIGATION OF LONG-TERM HYDROLOGIC CHANGE DUE TO SURFACE WATER AND GROUNDWATER WITHDRAWALS FROM A HIGH ANDEAN HEADWATER BASIN, SOUTHERN PERU

Submitted by

William J. Stansfield

Department of Geosciences

In partial fulfillment of the requirements

For the Degree of Master of Science

Colorado State University

Fort Collins, Colorado

Fall 2024

Master's Committee:

Advisor: Michael J. Ronayne

David Cooper
William Sanford

ABSTRACT

NUMERICAL MODELING INVESTIGATION OF LONG-TERM HYDROLOGIC CHANGE DUE TO SURFACE WATER AND GROUNDWATER WITHDRAWALS FROM A HIGH ANDEAN HEADWATER BASIN, SOUTHERN PERU

Reliable surface water and groundwater resources are of critical importance in the arid central Andes of Southern Peru. Low elevation cities and towns in coastal regions are dependent on water derived from relatively humid mountains and high elevation basins on the Andean Altiplano. The Huaytire Basin, located on the Altiplano at approximately 4,450 meters above mean sea level, is a headwater basin that has experienced hydrologic change in recent years. Surface water diversions from the perennial Lake Suches began in the 1960s, followed by groundwater pumping starting in the 1980s. These water development activities have been accompanied by observations of declining surface water quantity in the downgradient Rio Callazas and deteriorating phreatophytic vegetation within the basin itself. A review of precipitation and pan evaporation data from weather stations in the region did not reveal any clear climate-related trends that would impact water resource availability. A numerical groundwater flow model was constructed using MODFLOW to estimate the impact of long-term pumping on local hydrology and to investigate the sustainability of the Huaytire Basin pumping regime. The model accounted for groundwater-surface water interaction, including lake-aquifer exchange and stream-aquifer exchange along three major streams that originate within the basin. Surface water levels and flow rates were computed as part of the numerical solution, dependent on the simulated hydraulic head in the aquifer, which controls the amount of groundwater-surface water exchange. Three different recharge scenarios were considered to acknowledge uncertainty associated with groundwater recharge rates on the Altiplano. All three scenarios resulted in the study area converting from an open basin with surface water outflow to a closed basin within 50 years of the start of development. Other simulated impacts of pumping include a reduction in the stage and areal extent of Lake Suches and significant reductions in head-dependent outflows for the aquifer system. Relative to predevelopment conditions, groundwater discharge to Lake Suches, groundwater discharge to gaining stream reaches, phreatophytic evapotranspiration, and underflow out of the basin were all lower at the end of the 63-year transient simulation (by ~ 9.5, 50, 18, and 51%, respectively, using base-case recharge rates). It was concluded that groundwater development in the Huaytire Basin is a key factor that explains the observed hydrologic changes and that current pumping rates may be unsustainable.

ACKNOWLEDGEMENTS

I would like to express my deep gratitude to my advisor, Dr. Michael Ronayne, for his patient guidance and support throughout my time at Colorado State University. I am also grateful to Dr. David Cooper for his collaboration with our Peruvian partners, his assistance with fieldwork, and for serving on my master's committee, and to Dr. William Sanford for his valuable insight and for joining the committee on short notice.

I would like to extend special thanks to Eduardo Oyague for his indispensable knowledge and for serving as a translator during fieldwork in Peru, and to Ana Perez for her help with translating technical documents. I am also thankful to Dr. Ben Vining for providing helpful information about the study area.

Finally, I am deeply appreciative of Dr. Pablo Franco León and the faculty, staff, and undergraduate students from his lab group at Jorge Basadre Grohmann National University for their hospitality and critical assistance in the field. This research was funded by Jorge Basadre Grohmann National University.

TABLE OF CONTENTS

CHAPTER 1: INTRODUCTION

Water resources in mountainous regions can be affected by a variety of hydrologic stresses including climate changes, groundwater pumping, and surface water diversions for agricultural or industrial purposes. Mountains, especially those in or near arid and semiarid regions, provide a high proportion of water to lowland human population centers. Mountain areas are projected to become increasingly important zones in water resource management due to population expansion and the impacts of climate change (Viviroli et al., 2020; Viviroli et al., 2007). Reliable surface water and groundwater resources derived from mountain regions are of particular importance in Peru, where large cities located near the Pacific Ocean in the Atacama Desert are largely dependent on water flowing from the central Andes Mountains (Gies, 2021). Peru is one of the most water stressed nations in the world, due in part to its diverse geography and uneven distribution of water resources – nearly 70% of the Peruvian population lives in the Pacific hydrographic basin which receives only approximately 2% of the country's available water (OECD, 2021; Salem et al., 2021). Water stress has led to water related conflict across several economic sectors in Peru, including mining, one of the most economically important industries in the country (Bebbington and Williams, 2008).

1.1 Background

The Huaytire Basin in southern Peru is an example of a hydrologically vulnerable, high elevation basin that has experienced environmental change in recent decades. The 430 square kilometer basin is located in the Department of Tacna, the southernmost region of Peru, and ranges in elevation from approximately 4,450 to 5,800 meters above mean sea level (amsl) (Figure 1.1).

The climate is generally cold due to its extreme altitude and features strong diurnal temperature fluctuations. Precipitation is highly seasonal, with annual totals ranging from 300 to 400 mm/y (Garreaud et al., 2003; Oyague and Cooper, 2020). These climatic and environmental characteristics are typical of the dry puna grassland – a xeric South American biome dominating Andean landscapes from 4,000 to 4,800 meters amsl in the Altiplano of Peru, Bolivia, and Chile (Olson et al., 2001). The puna is characterized by harsh growing conditions and sparse vegetation (Josse et al., 2009).

The Huaytire Basin also supports high elevation peat accumulating wetlands locally called bofedals. Bofedals typically occur in the Andes from 3,200 to 5,000 m amsl (Squeo et al., 2006). They form in valley bottoms and depressions on the puna and function as biotic oases in the otherwise sparsely vegetated landscape. Bofedals are groundwater dependent ecosystems that persist through long seasonal periods of dry conditions on the climatically extreme and highly seasonal puna. Bofedals are sensitive to fluctuating groundwater levels and may desiccate due to changes in the hydrologic regime (Earle et al., 2003). In contrast with the sparsely vegetated puna grassland, bofedals can support plant coverage of 70% or greater, making them a critical component of successful camelid husbandry in the Huaytire Basin (Vining, 2011) and elsewhere in the Andes. In addition to providing high quality pasture for livestock and wildlife, bofedals rapidly accumulate peat and may be important for sequestration of atmospheric carbon (Hribljan et al., 2015).

Modern settlement in the basin is anchored by the rural village of Huaytire, which has a population of approximately 400 people and is economically sustained primarily through camelid husbandry as well as aquaculture in nearby Lake Suches (Benavides, 2014). Surface water resources make human occupation of the environmentally challenging Huaytire Basin possible. Settlement patterns inferred from the archeological record demonstrate a preference for sites near springs and the margins of bofedals, which provide drinking water to inhabitants as well as vegetation for grazing llama and alpaca. Initial settlement of the Huaytire Basin may have been encouraged by the abundance of bofedals in the basin relative to other regions. Bofedal coverage in the Huaytire Basin has been estimated at 6%, compared to approximately 2.5% of the overall puna in the Altiplano region (Vining et al., 2019; Kuznar, 1995; Vining, 2011).

Lake Suches, located 3 km southwest of Huaytire, is an approximately 1,000-hectare perennial lake that contributes to the habitability of the Huaytire Basin. Sediment cores collected from Lake Suches and analyzed by Vining et al. (2019) indicated that the lake water level has been relatively stable over the last 14,000 years. This period includes a known phase of extreme Andean aridity during the Holocene that desiccated other lakes in the region. This information, combined with archeological evidence of nearly continuous human occupation in the basin provide support for Vining's hypothesis that Huaytire Basin functioned as a refugia for human settlement throughout the Holocene, largely as a consequence of reliable and abundant surface water resources (Vining et al., 2019).

Likely the first instance of surface water management in the Huaytire Basin was performed by indigenous people related to the management of bofedals. Squeo et al. (2006) notes that local inhabitants often divert water to expand bofedals or create new pastures. However, the indigenous population of Huaytire Basin has not placed a significant stress on local water resources, with a modern water right of just 1 L/s (Meneses, 2018). The first industrial water use license in the basin was granted to the Southern Peru Copper Corporation (SPCC) in 1955, and allowed for extraction of up to 2,000 L/s from Lake Suches to support activities at the Caujone copper mine, located approximately 33 km west of the Huaytire Basin. This action was accompanied by approval for construction of hydraulic infrastructure, including a pipeline to transfer water out of the basin. Construction of hydraulic infrastructure on Lake Suches was complete by 1961, and extraction of surface water commenced shortly thereafter. SPCC did not initially use its full water use license, and in 1988 the Lake Suches surface water use license was reduced to 300 L/s (Meneses, 2018). Between 1984 and 2005, SPCC acquired additional water use licenses to extract groundwater from eight production wells in the basin to supplement surface water extraction, with a total additional water use license of 890 L/s. This brought the company's total water use licenses in Huaytire Basin, including both surface water and groundwater, to 1,090 L/s (Meneses, 2018). Pumping records collected by the local water administration authority indicate that actual modern groundwater extraction from the eight wells installed in the Huaytire Basin is approximately 667 L/s (ALA, 2022).

1.2 Motivation

This study was motivated by reports of recent hydrologic changes in the Huaytire Basin and downstream communities. Surface water historically flowed southeast from the Huaytire Basin down the Rio Callazas to the agricultural region of Candarave (Figure 1.1). Groundwater pumping in the Huaytire Basin has been cited as a potential cause of declining surface water quantity and quality in the Rio Callazas watershed, and a reduction in vegetation cover in bofedal wetlands within the basin (Bahamontes et al., 2021; Meneses, 2018, Oyague and Cooper, 2020). The perceived degradation of surface water quality in the Rio Callazas may be attributed to a reduction in high quality surface and groundwater flowing from the Huaytire Basin that historically offset contributions of low-quality water from tributaries of the Rio Callazas (Delgado, 2020). While several authors have speculated about a relationship between groundwater extraction in Huaytire Basin, desiccated bofedals, and deteriorating water quality and quantity in the Rio Callazas (Perla, 2012; Meneses, 2018), this relationship has not been quantified, and supporting evidence is mostly anecdotal.

1.2.1 Water Quality

The Huaytire Basin has often been characterized as containing good water quality relative to nearby basins in southern Peru. Several water quality sampling campaigns have been conducted on Lake Suches since the mid-1980s that have reported persistently high water quality results (Balvin, 1995; Delgado, 2020; Beas, 1996; INGEMMET, 2009). Water quality in the Rio Callazas rapidly deteriorates downstream of the basin due to contributions of low quality groundwater and surface water associated with nearby volcanic activity, notably containing unsafe levels of boron, arsenic, and cadmium (Meneses, 2018; INGEMMET, 2009; CRL, 2017)

Water quality testing performed by Balvin (1995) on samples collected from Lake Suches showed low levels of copper, boron, and iron, and did not detect cadmium, arsenic, lead, or zinc. Testing indicated that surface water in Lake Suches was compliant with World Health Organization (WHO) water quality guidelines and was appropriate for human consumption after minimal treatment. A sampling event summarized in Delgado (2020) found similar results, indicating that water from Lake Suches could be used for human consumption after a disinfection process. Arsenic and boron concentrations in the Huaytire Basin were shown to be low in a study published by INGEMMET in 2009, and Lake Suches was shown to be relatively less saline than other high-altitude lakes in southern Peru due to its persistent supply of groundwater and relatively high precipitation inputs (Beas, 1996; INGEMMET, 2009).

Water quality in the Rio Callazas deteriorates downstream of the study area, especially after the contribution of several streams with naturally high concentrations of boron, cadmium, arsenic, and other constituents (Meneses, 2018; INGEMMET, 2009; CRL, 2017). For this reason, the contribution of high-quality water from the Huaytire Basin, either as direct surface water outflow in the Rio Callazas or as subsurface outflow, is critical for diluting low-quality water downstream that is not suitable for drinking or agricultural irrigation. While long term water quality monitoring data for the Rio Callazas is not publicly available, water extraction from Huaytire Basin has negatively impacted water quality in Rio Callazas and created a decline in the area used for cultivated crops and population in Candarave (Isch and Gentes, 2006). Geng (2018) noted that 86% of localities evaluated in Candarave, including the town of Candarave, used water that presented a high risk for human consumption, and pumping from Huaytire Basin has caused a decline in water quality in the Rio Callazas. The Observatory of Transnational Corporations (OET) similarly reported that water quality in the Rio Locumba, for which the Rio Callazas is a tributary, has decreased due to the extraction of high-quality water from the headwaters (OET, 2008).

1.2.2 Water Quantity

Observations of reduced water quality have been accompanied by observations of reduced water quantity in the Rio Callazas and in Huaytire Basin. Several reports have identified a reduction in area or complete desiccation of bofedals in the study area (Oyague and Cooper, 2020; Bahamondes et al., 2021; Isch and Gentes, 2006; Pérez-Jiménez, 2018; McCall et al., 2021). Bofedals respond rapidly to changes in hydrologic regime (Earle et al., 2003), suggesting they may be sensitive to land and water management. Desiccated bofedals in Huaytire Basin have been documented by Oyague and Cooper (2020). Bahamondes et al. (2021) reported a decrease in the vigor of bofedal vegetation around Huaytire based on an analysis of normalized difference vegetation index (NDVI) using remote sensing data spanning a 45-year period between 1975 to

2020. Other authors have described bofedal degradation in Huaytire Basin and highlighted water level decline as a likely factor (Isch and Gentes, 2006; Pérez-Jiménez, 2018; McCall et al., 2021). Bofedal condition may be impacted by overgrazing, climate change, or human activity such as surface water diversions and groundwater pumping; however, the causes of bofedal desiccation in the Huaytire Basin remain poorly understood.

In addition to a reduction in bofedal area, a trend of declining streamflow in Rio Callazas has been documented. An interview in 2012 with residents of Candarave indicated that water scarcity has become more common in recent decades, and dry years are more common today than in the past (Perla, 2012). Meneses (2018) observed that, between 1999 and 2016, agricultural production in Candarave decreased by 52%, and beef production decreased by 48%. Although it was acknowledged that the cause of this decline has not been rigorously studied, Meneses (2018) observed that it may be connected to declining water availability and water quality in the Rio Callazas. A 2012 national agricultural census, which conducted interviews with Candarave residents, indicated that the main perception of the cause for decline in agricultural production was water scarcity (Meneses, 2018).

1.3 Research Objectives

The objective of this thesis is to investigate the cause of observed groundwater and surface water change within the Huaytire Basin and in downgradient systems using a physically based numerical groundwater flow model. Modeling was performed to investigate the effects of groundwater pumping and, specifically, to evaluate changes in the aquifer water budget and Lake Suches water budget due to pumping. Simulated changes to the aquifer water budget will be used to infer the potential cause of hydrologic change on the downstream Rio Callazas drainage basin. By incorporating phreatophytic vegetation in the model, simulations can also be used to assess the impact of pumping on groundwater-dependent ecosystems in the basin. This study will provide a foundation for informed water resources management within Huaytire Basin and in similar mountain hydrogeologic settings subjected to environmental stress associated with water withdrawals.

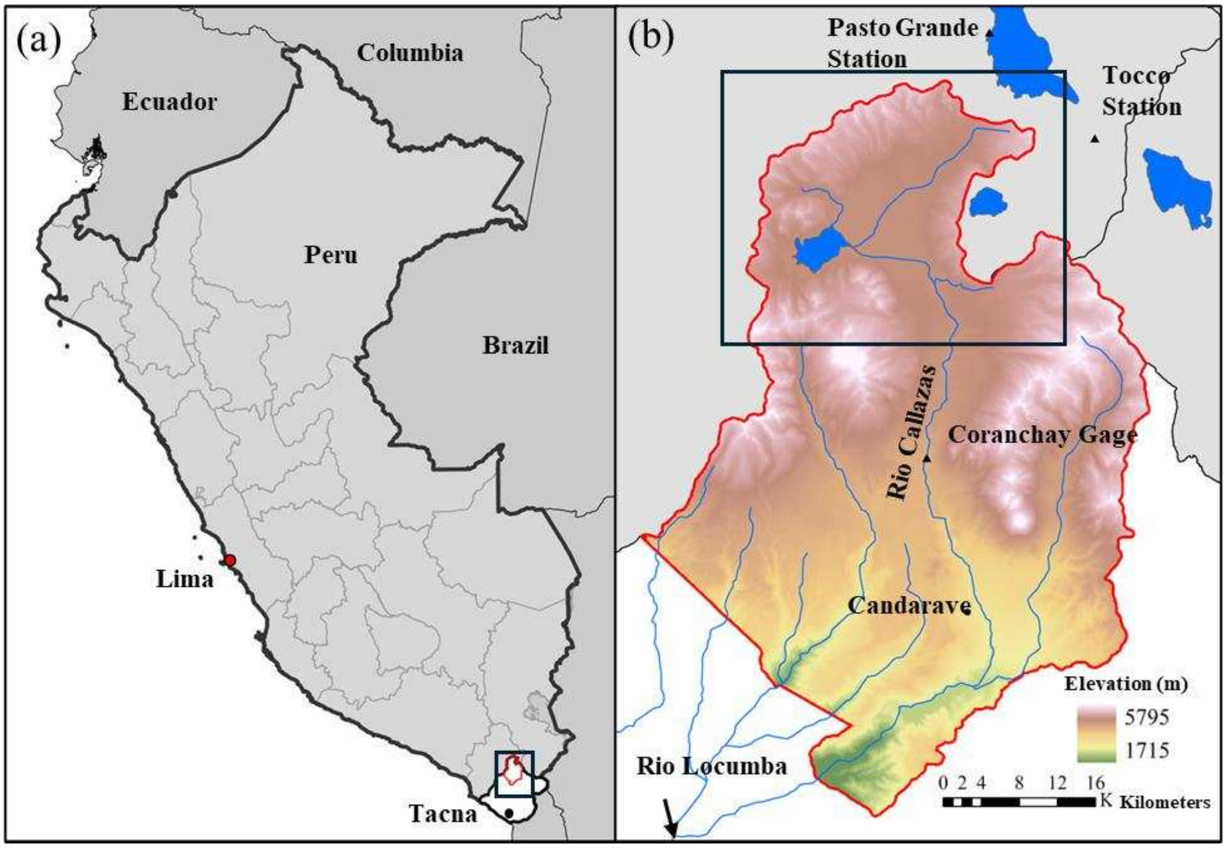

Figure 1.1: (a) Location of Candarave Province within Peru. (b) Location of the study area within Candarave Province. The town of Candarave and relevant weather stations are also pictured.

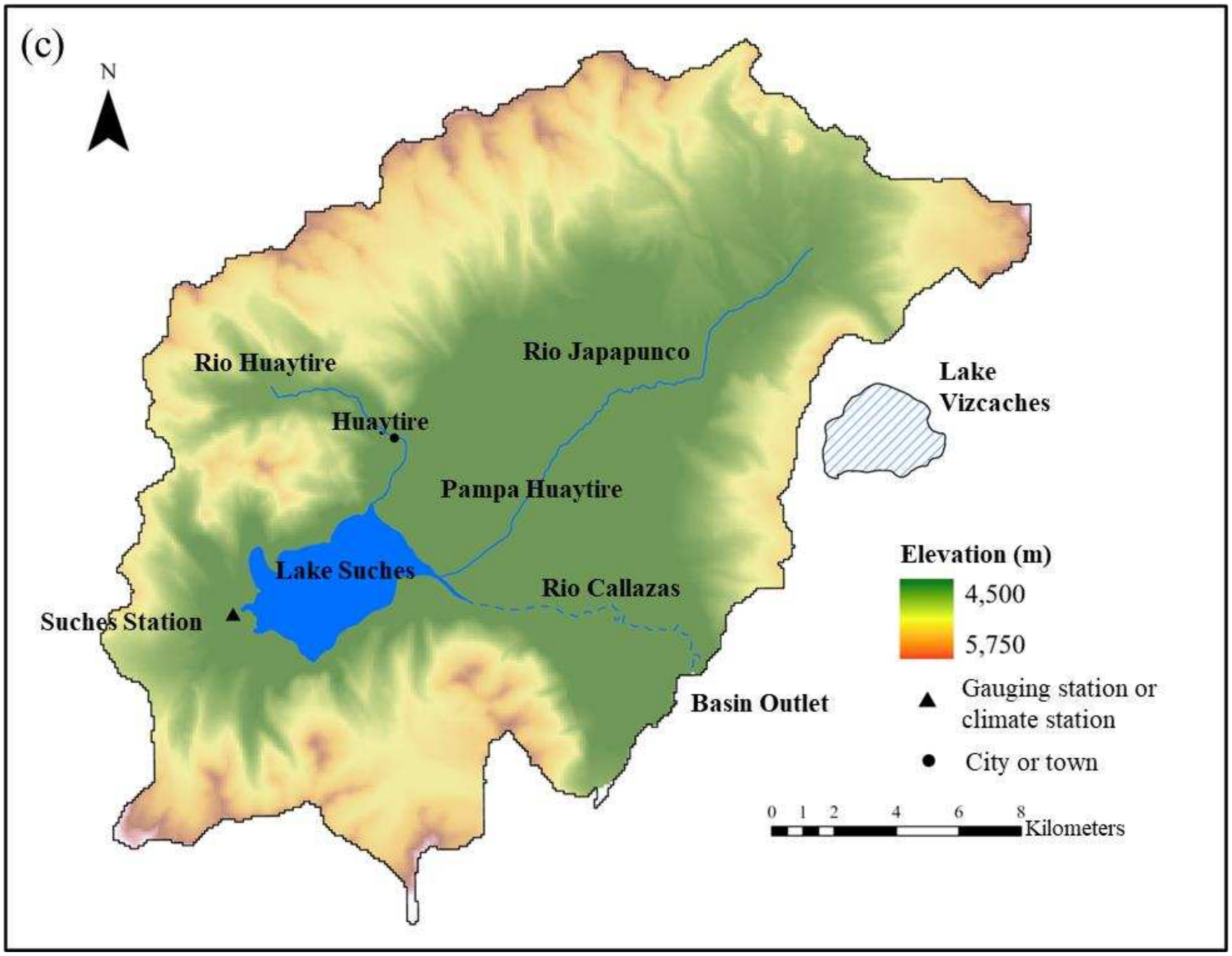

Figure 1.1: (c) The Huaytire Basin study area. The Suches weather station, elevation, and other geographic features are also depicted.

CHAPTER 2: STUDY AREA DESCRIPTION AND CONCEPTUAL MODEL

This chapter reviews physical aspects of the study area, including climate, topography, vegetation, surface waters, land use, and the hydrogeologic setting. In addition, a conceptual hydrogeologic model for Huaytire Basin is presented, based on a review and interpretation of relevant literature describing aquifer characteristics. The information summarized below was used to guide decisions related to the selection of boundary conditions and aquifer properties during the creation of the numerical model (Chapter 3).

2.1 Climate

Precipitation on the puna is strongly seasonal, with 70% or more of total precipitation occurring between December and April and pronounced dry seasons lasting between 7 and 9 months through the austral winter (Garreaud et al., 2003; Oyague and Cooper, 2020; Vining et al., 2019). Despite occupying tropical and subtropical latitudes, mean annual temperatures in the extreme elevation of the puna create cold temperatures, ranging from 0 to 7 ºC with strong diurnal fluctuation, and precipitation falls in the form of rain and snow (Sandweiss and Richardson, 2008; Vining, 2011). Temperature records collected at a SPCC weather station located near Lake Suches ranged from a monthly mean of approximately 6 ºC in January, the warmest month, to approximately 0 ºC in July, the coolest month, with diurnal variation of up to 25 ºC (Vining, 2016; Vining et al., 2019). Data collected from 1954 to 2008 at the same weather station indicate that annual precipitation generally ranged from 300 to 400 mm, with an overall mean of 389 mm/y (Vining, 2016). No long-term trend in precipitation was observed in the 54-year Lake Suches dataset (Figure 2.1). Long-term temperature records were not available for the Lake Suches weather station, but records collected at the nearby Pasto Grande weather station indicate no trend in maximum monthly temperatures, and a weak increasing trend in minimum monthly temperatures recorded between 1965 and 2001 (Figure 2.2). Twenty-two years of evaporation data collected between 1986 and 2008 was evaluated from the Tocco weather station, located approximately 30 km northeast of Lake Suches, and no significant trend was observed in evaporation rate over the measurement period (SPCC, 2009) (Figure 2.3).

2.2 Vegetation

Vegetation in the Huaytire Basin is limited by cold temperatures, high elevations, low mean annual precipitation, and high insolation rates producing a treeless landscape supporting only sparse vegetation cover (Vining, 2011). The Huaytire Basin would be classified as being in the *alta puna* (arid-alpine) phytogeographic zone, characterized by cold adapted vegetation able to withstand low moisture availability (Tosi, 1960). Upland puna vegetation consists primarily of woody shrubs including *Parastrephia lepidophyllum* and *Parastrephia quandrangularis* and bunchgrasses including *Calamogrostis* sp., *Stipa* sp., and *Festuca* sp. Less abundant upland species include the cushion plant *yareta* and the cactus *oreocerus* (Vining, 2011; Franco et al., 2022). Although upland puna vegetation is used as forage for camelid livestock, it is considered inferior by local herders to the more productive and nutritious vegetation in bofedal wetlands (Vining, 2016).

Bofedals are typically dominated by two species of Juncaceae cushion plant, *Distichia muscoides* and *Oxychloe andina*, which form a characteristic pool and hummock wetland morphology often exhibiting lawns and dense mats of vegetation (Oyague and Cooper, 2020). Squeo et al. (2006) notes that local pastoralists often divert water in or around pre-existing peatlands to expand bofedals or create new pastures. At least one bofedal in the Huaytire Basin was created in this manner.

The distribution of vegetation shown in Figure 2.4 is based on mapped wetland areas provided by INGEMMET (1978; 2023), with further refinement conducted during this study using Normalized Difference Vegetation Index (NDVI) analysis. The more sparsely vegetated Pampa Huaytire was delineated using a wetland shapefile published in INGEMMET 2023, and the more densely vegetated bofedal vegetation was delineated using a wetland shapefile published in INGEMMET (1978). Bofedal areas not captured by the wetland polygons published in INGEMMET (1978) were identified using a Normalized Difference Vegetation Index (NDVI) analysis performed using Landsat data collected in 1983 (USGS Earth Explorer, 2024). NDVI is a commonly used metric for describing vegetation that measures the difference in near infrared (NID) and red light reflected by vegetation (Kriegler et al. 1969). The index ranges between -1 and 1, with numbers closer to 1 representing healthier and more vigorous vegetation. A polygon of NDVI cells with a value of greater than 0.1 over a known bofedal complex were aggregated into a polygon and appended to the bofedal shapefiles depicted in Figure 2.4.

2.3 Land Use

The Huaytire Basin is sparsely populated, but contains several small villages generally comprised of 10 or fewer buildings. The largest settlement is the community of Huaytire, located near the Rio Huaytire 3 km northeast of Lake Suches (Figure 1). Contemporary demographic information for Huaytire is not available, but the village has been estimated to have a population of approximately 370 (Benavides, 2014). Low mean annual temperature makes cultivated agriculture impossible in Huaytire, and the local economy is supported primarily by trout aquaculture in Lake Suches and camelid husbandry. Herds are primarily alpacas managed in herds of 50 to 200 animals, although llama and sheep are also present in smaller numbers

(Vining, 2011). Herding is concentrated on comparatively productive bofedal wetlands that provide high quality forage for livestock relative to the more sparsely vegetated upland puna.

Water resources in the Huaytire Basin have been exploited by the metal mining industry since the 1960s. The Southern Peru Copper Corporation (SPCC) maintains a permanently staffed compound comprised of several structures near the southern end of Lake Suches that serves to maintain pumping infrastructure and oversee the security of company property. Eight pumping wells are installed in the basin, at least two of which discharge directly into Lake Suches, which effectively functions as a water storage reservoir. Surface water is pumped directly from Lake Suches to the Cuajone copper mine approximately 33 km west of Lake Suches for use in the processing of copper ore. Several municipal pumping wells are also present in the neighboring Vizcaches basin, located east of the Huaytire Basin and used for supplementing water supplies in cities at lower elevations. Land ownership in the Huaytire Basin is split between private landowners, community holdings, and land owned and managed by the SPCC.

2.4 Topography

The Huaytire Basin is an intermontane basin rimmed by the high elevation peaks of the Barroso Range to the north, south and west. Lake Suches, an endorheic lake, occupies a depression in the southwestern region of the basin floor at an elevation of approximately 4,450m amsl. Northeast of Lake Suches is a large and relatively flat deltaic plain of fluvioglacial and alluvial material locally known as the Pampa Huaytire (Figure 1.1). The land surface is generally steeper south and west of Lake Suches, rising to an elevation of over 5,800m amsl at Mount Tutupaca volcano, located 8km south of Lake Suches. Beyond the Pampa Huaytire to the north and east, basin topography is impacted by outcrops of horizontally deposited upper strata of the clastic Capillune Formation. Watercourses in this part of the basin are generally bedrock confined and incised. The edge of the basin is dominated by steeper and more rugged crystalline volcanic rock associated with the Barroso Group, which is in turn associated with the regionally extensive Barroso mountain range. The continuity of the Barroso Range is interrupted east of Lake Suches by a relatively low elevation valley occupied by the Rio Callazas – an ephemeral channel draining Lake Suches. This relatively low relief and low elevation region is dominated by clastic geology and referred to as the basin outlet (Figure 1.1).

2.5 Surface Water Features

The largest surface water feature in the Huaytire Basin is Lake Suches, a natural perennial endorheic lake that also is used as a storage reservoir for extracted groundwater and for the local aquaculture industry. The surface area of Lake Suches varies seasonally and inter-annually depending on the magnitude of wet season precipitation and rate of pumping from the lake. Bahamondes et. al (2021) calculated the surface area variability of Lake Suches by performing a Normalized Differential Water Index (NDWI) analysis and found that, over the 35-year period between 1975 and 2020, the lake area has ranged from a minimum of approximately 800 hectares in 2015 to a maximum of approximately 1,500 hectares in 1975. The maximum depth in Lake Suches is approximately 15 meters, and its bathymetry has been described as bowl shaped, with generally steeper banks near the edge of the lake (Vining, 2011).

Vining (2011) presented evidence from a Lake Suches sediment core analysis to suggest that water levels in Lake Suches remained stable throughout the Holocene, despite known periods of aridity that had larger impacts on other lakes in the region. Modern fluctuation of lake level is not monitored or not publicly available, but a historic high-water mark was observed by Vining (2011) approximately 2.5m above the “current mean shoreline”.

Although Lake Suches has been described as the source of the Rio Callazas in some publications (CRL, 2017; INGEMMET, 1998), under modern conditions it exists as a closed basin with no surface water outlet. Disconnected pools of standing water were observed in what appeared to be the deepened and straightened outlet channel of Lake Suches during my June 2023 site visit; however, surface water was not observed to flow between pools, which are likely fed by groundwater directly. Flowing water was not noted in any observed reaches of the Rio Callazas during any site visits conducted as part of this study.

SPCC maintains a surface water use license on Lake Suches of 300 liters/second (L/s), or approximately 9,500,000 m^3/y, for use in mining operations outside of the basin (Meneses, 2018). In addition to this surface water right, SPCC utilizes Lake Suches as a storage reservoir for groundwater extracted from nearby pumping wells, which are authorized under a separate water use license, with at least two production wells discharging directly into the lake. In 1959, a dike was constructed on the outlet of Lake Suches to increase the storage capacity of the lake in preparation for eventual surface water diversion (Beas, 1996; OET, 2008; Meneses, 2018). Water rights held by the SPCC are summarized in Table 1.

Table 1: Summary of water rights maintained by the Southern Peru Copper Corporation. Data from the SPCC (2022).

Wells	Water Right	Date
TP-11 and TP-12	Adequacy of the water use license granted to in the R.M. N ° 00899-79-AA/DGAS and R.A. N ° 002-94-DISRAG/ATDRL-S up to 9,744,624 m3	4/1/2003
	License for the use of an annual mass of 5,991,840 m3 of groundwater captured from tubular wells TP-11 and TP-12 drilled in the "Huaitire-Gentilar" hydrographic basin	1994
TP-14 and TP-15	Groundwater use license with a flow of 162.2 L/s equivalent to an annual mass of 5,115,139 m3 captured by two tubular wells TP-14 and TP-15 located in the Huaitire Gentilar basin	1/8/2005
Remaining Wells: TP-5, TP-8, TP-9A, TP-3A	License to use an annual mass of up to 13,268,966 m3 of groundwater extracted through four tube wells from the "Huaitire" basin	6/15/1983
	License to use a mass of 15,736,464 m3 of groundwater through tubular wells drilled in the "Vizcachas" and "Titijones" hydrographic basins	7/9/1974

Lake Suches is fed by two streams commonly considered perennial in the Huaytire Basin – the Rio Huaytire, which flows towards Lake Suches from the northwestern edge of the basin, and the Rio Japopunco, which flows towards Lake Suches from the northeastern edge of the basin. Both streams are generally gaining over high relief, bedrock constrained reaches higher in the watershed and transition to losing streams over the alluvial and fluvioglacial deltaic material of the Pampa Huaytire. Streambeds are generally coarse-grained material ranging in size from sand to boulders in upper reaches and fine-grained material ranging from silt to coarse sand in lower reaches. The Rio Huaytire was observed to discharge directly to Lake Suches during site visits in January 2023 and June 2023, albeit at a considerably reduced flow rate relative to upstream flow, and the mouth of the Rio Japapunco was not observed. It has been reported by Vining (2011) that both streams go completely dry on the Pampa Huaytire during dry periods, suggesting that water in Lake Suches is fed primarily through subsurface inputs for part of the year.

In addition to the two perennial streams described above, the basin is drained by numerous named and unnamed ephemeral channels which flow only during and after periods of high precipitation. Many of these streams are tributary channels that provide flow to the Rio Japapunco and Rio Huaytire during the wet season, including the Quebrada Ancocachi, Quebrada Cotarine, the Quebrada Callapa, which flow into the Rio Japapunco, and the Quebrada Ancobichinga, which flows into the Rio Huaytire. Some channels flow directly into Lake Suches, including the Quebrada Livecalani, which flows across the Pampa Huaytire, and the Quebrada Challuma, Quebrada Irocahua, and Quebrada Vilacahua, which flow into Lake Suches from the south and west (INGEMMET, 1998). These channels only provide low volume and episodic input to the lake and shallow aquifer system.

Many springs have been observed in the Huaytire Basin, some of which have been documented and named in CRL (2017) and INGEMMET (2009). INGEMMET (2009) indicates that nine springs occur within the Huaytire Basin, while CRL (2017) identifies only five springs in the basin. One flowing spring located west of Lake Suches was observed during the January and June sampling events that is not listed in either publication, suggesting that both lists are likely incomplete.

2.6 Regional Geology and Hydrogeologic Characteristics

The study area is part of the Andean Cordillera – a continuous chain of mountains nearly 6,000 km long and 700 km wide at its widest point occupying the western region of South America. The Andean Cordillera is the result of a convergent tectonic boundary along the western margin of South America where the oceanic Nazca plate is subducted below the South American continent. The Huaytire Basin occurs within the Central Andes, which includes much of the cordillera between Peru, Bolivia, and northern Chile, and generally divided into three physiographic regions: the Cordillera Occidental, the Altiplano, and the Cordillera Oriental (USGS, 1992; Porter GeoConsultancy, 2010).

The Eastern Cordillera (Cordillera Oriental) is a fold and thrust belt composed largely of Paleozoic marine faces that have been uplifted and deformed during at least three mountain building events related to the subduction of the Nazca plate, most recently the Mesozoic – Cenozoic Andean Orogeny, and the Western Cordillera (Cordillera Occidental) is a Cenozoic magmatic arc also associated with the subduction of the Nazca plate as part of the Andean orogeny (USGS, 1992; Porter GeoConsultancy, 2010). The western cordillera is composed largely of lava flows and volcanoclastic rock associated with late Oligocene and Holocene volcanism. The crest of the Cordillera Occidental is occupied by andesitic to dacitic stratovolcanoes of the Central Volcano Zone, many of which are active in the modern era. Between the eastern and western cordilleras is the Altiplano – a series of continuous intermontane foreland basins associated with crustal shortening and thickening which have been subject to Cenozoic continental deposition of sediments and volcanic material. Fluvial and lacustrine deposits of sandstone, shale, claystone, and conglomerate interbed with tuff and other volcanic material up to 15,000 m thick in some areas of the Altiplano. The region appears as an undulating but relatively flat high-altitude plateau, second in elevation only to the Tibetan plateau. The Huaytire Basin study area is located near the poorly defined transition zone between the Cordillera Occidental and the Altiplano and contains both relatively young volcanic rock associated with the Cordillera Occidental as well as older clastic rocks more characteristic of the Altiplano (INGEMMET, 1978).

Geologic units within the study area range in age from the Neogene through the Quaternary Period (CRL, 2017). The rim of the basin is occupied by the Barroso Group (Figure 2.5), which is composed primarily of upper Neogene age volcanic rocks. The Barroso Group intruded through older Neogene sedimentary and volcanic sequences of the Sencca and Capillune formations. The Sencca, which does not crop out in the study area, is the oldest and lowest unit detailed in the Huaytire Basin and is considered to be an aquitard (CRL, 2017). The Capillune Formation and Barroso Group both outcrop in the basin but are often covered by relatively thin Quaternary sediments generated by fluvial, alluvial, colluvial, fluvioglacial, and glacial processes. The Barroso Group, Capillune Formation, and Quaternary glaciofluvial sediments all serve as important aquifer units within the study area (INGEMMET, 2009). In Figure 2.5, Barroso Group aquifer material is mapped as crystalline igneous rock, which is commonly fractured, whereas the Quaternary sediments are shown as alluvium and fluvioglacial units. Pampa vegetation on the basin floor generally occurs in areas covered by the Quaternary sediment.

Estimates of aquifer thickness, hydraulic conductivity, transmissivity, and/or storativity have been published for all the hydrostratigraphic units described above (Table 2). Estimates across studies are extremely variable, reflecting significant heterogeneity within the study area and uncertainty inherent in the estimation of hydraulic properties.

Table 2: Summary of hydraulic conductivity, transmissivity, and storativity for major aquifer units in the Huaytire Basin.

	Barroso Group	**Capillune Formation**	**Sencca Formation**	**Fluvioglacial Deposits**
Hydraulic conductivity estimates (m/d)				
Number of estimates	7	11	2	5
Minimum	0.01	0.06	0.04	0.89
Maximum	57	16	1.1	10
Median	17	2.2	N/A	1.0
Average	21	4.3	0.57	2.8
Transmissivity estimates (m^2/d)				
Number of estimates	3	7	2	2
Minimum	500	310	10	20
Maximum	21000	7300	50	50
Median	800	990	N/A	N/A
Mean	7500	1800	30	35
Storativity Estimates				
Number of estimates	0	3	0	0
Minimum	N/A	0.001	N/A	N/A
Maximum	N/A	0.11	N/A	N/A
Median	N/A	0.004	N/A	N/A
Mean	N/A	0.038	N/A	N/A
Specific Storage Estimates (m^{-1})				
Number of estimates	0	2	0	0
Minimum	N/A	$6.0x10^{-6}$	N/A	N/A
Maximum	N/A	$2.9x10^{-5}$	N/A	N/A
Median	N/A	N/A	N/A	N/A
Mean	N/A	$1.8x10^{-5}$	N/A	N/A
Estimated Thickness (m)				
	800 - 1000	300	30	0 - 170

2.6.1 Barroso Group

The Barroso Group is a complex of related extrusive igneous rocks dating to the upper Neogene and lower Quaternary Periods (INGEMMET, 1978). The Barroso Group is associated with the more regional Barroso volcanic mountain range, which is generally characterized by highly eroded summits that have been heavily reworked during Pleistocene glaciations (INGEMMET, 2009). Within the study area, Barroso Group rocks occupy the high elevation rim of the basin, and generally include porphyritic and aphanitic andesite and dacite. The Barroso Group is characterized by steeply dipping strata near modern ridgelines that gradually become more horizontal at contacts with underlying horizontally deposited clastic units (INGEMET, 1978). The group has been described by INGEMMET (1978) as a highly fractured intercalation of tuffs and trachytic lava flow deposits, and it was also noted how these fractured volcanic rocks represent an important recharge conduit of meteoric waters to underlying aquifers, namely the Capillune Formation. Similarly, CRL (2017) described the Barroso Group as a fractured aquifer, serving as a recharge conduit and favorable to subsurface flow. The thickness of the Barroso Group has been reported to range between 800 m and 1,000 m (CRL, 2017).

Barroso Group hydraulic property data have been summarized by CRL (2017) (Table 2). Knight Piesold (2000) reported relatively low hydraulic conductivities ranging from 0.01 to 0.1 m/d, but the method of estimation is unknown. Estimated hydraulic conductivities from pumping tests ranged between 9.2 m/d and 17.4 m/d (Knight Piesold, 2012). Near-surface hydraulic conductivity was measured by INGEMMET (2009) using a permeameter, and estimated values ranged between 28 m/d and 51 m/d. Hydraulic conductivity data collected using a permeameter, while useful in some contexts, is likely only representative of near surface geology and may have only limited relevance in this study. No storage property estimates for the Barroso Group were identified during this literature review.

2.6.2 Capillune Formation

The Capillune Formation is a regionally extensive clastic unit dating to the Upper Pliocene that constitutes the primary aquifer of the Huaytire Basin (CRL, 2017). The regional continuity of the Capillune Formation is interrupted by the younger Barroso Group, which intrudes through and overlies the Capillune Formation around the edge of the basin on an erosional unconformity. The Capillune Formation outcrops near the center of the basin along the banks of the Rio Japapunco (Figure 2.5), though much of the unit is covered by Quaternary glaciofluvial material or by the Barroso Group (INGEMMET, 2023).

The Capillune Formation formed in a continental basin that received sediment inputs from the adjacent Cordillera Occidental and Cordillera Oriental with episodic input of volcanic materials (INGEMMET, 1978; USGS, 1992). It is a heterogeneous lacustrine sequence consisting of intercalated sedimentary and igneous members with variable hydraulic properties. Its composition is reported to be of poorly consolidated fine-grained sandstones, conglomerates, siltstones, clays, and thick sequences of pyroclastic material and tuffs (INGEMMET, 1978; INGEMMET, 2009). The rocks of the Capillune Formation are oriented horizontally to sub horizontally and are mostly undeformed, locally dipping slightly to the south. The tuffaceous sandstone members of the formation have been described as productive aquifers, while clay and ash members are considered aquitards (CRL, 2017). The thickness of the Capillune Formation in the Huaytire Basin is thought to be approximately 300 m thick on average (CRL, 2017).

Hydraulic property estimates for the Capillune Formation were published in CRL (2017), Knight Piesold (2000, 2012), INGEMMET (2009), and SPCC (1974). Hydraulic conductivity estimates range from 0.06 m/d and 16.28 m/d, and specific storage was estimated to range between $6.0x10^{-}$

^{6} and $2.9x10^{-5}$ m^{-1}. A complete summary of published hydraulic property estimates that were identified for the Capillune Formation is presented in Table 2.

2.6.3 Sencca Formation – lower confining unit

The Sencca Formation is a volcanic unit underlying the Capillune as a paraconformity and dates to the Upper Pliocene (INGEMMET, 1978). The Sencca is made up of relatively thin, horizontally deposited, poorly compacted rhyolitic, andesitic, and dacitic tuffs, as well as pyroclastic material, with a maximum thickness of approximately 100 m and an average thickness of approximately 30 m (CRL, 2017). The Sencca is characterized by very low permeability ash, thus forming an aquitard below the more permeable overlying Capillune aquifer (INGEMMET, 2009).

Reported hydraulic conductivities for the Sencca Formation range between 0.04 m/d and 1.1 m/d (Knight Piesold, 2012; CRL, 2017). Other hydraulic property information for the Sencca Formation is summarized in Table 2. No storage estimates for the Sencca Formation were identified during the literature review.

2.6.4 Quaternary Deposits

Much of the landscape in the Huaytire Basin is covered by unconsolidated or semi-consolidated Quaternary deposits related to Pleistocene glaciation and Holocene alluvial and fluvial processes (CRL, 2017). The thickness of unconsolidated Quaternary deposits in the Huaytire Basin is variable and dependent on the depositional process and underlying geomorphology, ranging from 0 to 170m thick. Average thickness of Quaternary deposits across the Huaytire Basin has been estimated between 20 m and 30 m (CRL, 2017).

The most common Quaternary materials present in the Huaytire Basin are glaciofluvial deposits formed by ice age glacial meltwater. Fluvioglacial deposits in the study area are characterized as fine conglomerates intercalated with sands up to 30 m thick. In the Huaytire Basin, fluvioglacial deposits occupy the lower slopes of the volcanic Barroso Group and the flanks of the Pampa Huaytire. Fine glacial sediments deposited in ancient periglacial lakes are more dominant near the center of intermontane pampas (INGEMMET, 1978; INGEMMET, 2009; CRL, 2017).

Glacial moraines dating from the Pleistocene are mapped by INGEMMET (2023) on the ridgeline southwest of Lake Suches. Terminal and lateral moraines in the Huaytire Basin are composed of poorly sorted angular volcanic gravels, sand, and clay deposited by retreating glaciers (INGEMMET, 2009). Moraines have been categorized by INGEMMET (2009) as medium productivity aquifers for their unconsolidated nature and generally large grain size.

Alluvial and fluvial deposits are commonly observed in the floodplains of streams in the Huaytire Basin and on the Pampa Huaytire near the center of the basin. Alluvial materials are unconsolidated and heterogeneous, generally consisting of interbedded gravels, sands, and silts of variable thickness transported by water from adjoining hillslopes (INGEMMET, 2009; CRL, 2017). Alluvial and fluvial deposits are typically very permeable and may constitute an important surficial aquifer in the Huaytire Basin.

Other minor Quaternary units exist in the Huaytire Basin including eluvial deposits, volcanic ash, and bofedals. Bofedals in the study area have been geologically characterized as spatially discrete deposits of moderately permeable clayey sands and histosol organic soils (INGEMMET 2009; CRL, 2017; Oyague and Cooper, 2020)

A pumping test conducted by Knight Piesold (2012) in quaternary fluvioglacial deposit yielding an estimated hydraulic conductivity of 0.6 m/d (CRL, 2017). Knight Piesold also reported that the hydraulic conductivity of fluvioglacial deposits ranged from 1 to 10 m/d. Hydraulic conductivity tests using an infiltrometer were also conducted on quaternary fluvioglacial material yielding a conductivity of 0.89 m/d and 1.32 m/d (CRL, 2017). Hydraulic conductivity as measured using the "hand auger method" was measured at to range between 2.1 m/d and 3.6 m/d, ranging between 0.92 m/d and 15 m/d across the study area. The exact location of these permeameter tests was not specified. Other hydraulic property data for Quaternary materials is summarized in Table 2.

2.7 Water Budget

Defining a water budget is a useful exercise for understanding groundwater inflows and outflows of an aquifer system and how the system may change under different hydrologic stress scenarios. As Anderson et. al (2015) summarizes, in its simplest form, the water budget for an aquifer can be defined as follows:

$$\Delta Storage = Inflow - Outlfow$$

Where *Inflow* and *Outflow* are both lumped terms comprised of many individual flows. If water is removed from the system at a faster rate than it is recharged, then the rate of storage change is negative and there will be a net decline in hydraulic head within the aquifer. Under pre-development conditions, inflows are roughly balanced by outflows (during an average year) such that the ΔStorage value is zero, indicating that the system is at steady state.

There is insufficient data available for the Huaytire Basin to accurately quantify each term of the water budget, so the following sections are a qualitative discussion of the known aquifer inflows and outflows. The transient aquifer water budget for Huaytire Basin may be expressed as follows:

$$\Delta S = R_p + Q_{sw\ in} + Q_{gw\ in} - \ Q_{sw\ out} - Q_{gw\ out} - ET - Q_p$$

where ΔS = change in aquifer storage, R_p = recharge derived from precipitation, $Q_{sw\ in}$ = inflows to the aquifer from surface water sources (Lake Suches and losing stream reaches), $Q_{gw\ in}$ = underflow into the modeled area from adjacent aquifers, $Q_{sw\ out}$ = outflows from the aquifer to surface water bodies (Lake Suches and gaining stream reaches), $Q_{gw\ out}$ = underflow out of the modeled area to adjacent aquifers, ET = evapotranspiration, and Q_p = groundwater pumping discharge.

2.7.1 Recharge Derived from Precipitation

Assuming poor inter-basin connection between regional aquifer units such as the Capillune Formation, most of the water entering the Huaytire Basin is ultimately derived from precipitation (Figure 2.6). Precipitation at the Lake Suches meteorological station operated by SPCC is reasonably well constrained, averaging 300 to 400mm per year, and mostly occurs during the summer wet season. Precipitation at higher elevations is not well constrained but will likely increase with elevation due to orographic rainout. Recharge derived from precipitation is applied in the numerical model as a diffuse areal recharge flux across the entire model domain. Only a fraction of actual precipitation reaches the water table in this way due to runoff, water retention in unsaturated soils, evapotranspiration, and direct evaporation; for this reason, diffuse areal recharge will be estimated as some percentage of total precipitation.

2.7.2 Evapotranspiration

Freeze and Cherry (1979) define evapotranspiration (ET) as a combination of evaporation from open bodies of water and soil surfaces, and transpiration from the soil by plants, often reported as a length per time flux. Evapotranspiration is sensitive to many environmental conditions including vegetation type and density, net solar radiation, wind speed, surface water area, and temperature, and therefore can range significantly between regions. It is generally typical for a large fraction of precipitation to be lost to evapotranspiration. In the numerical model, some evapotranspiration will be accounted for in the term describing recharge derived from precipitation, which will be a fraction of total precipitation. Additional evapotranspiration from phreatophytes – plants that draw water directly from the saturated zone – will be applied to the model as a negative flux.

2.7.3 Subsurface Outflow

Groundwater is assumed to leave the study area through the subsurface across the basin outlet at the southeast edge of the Huaytire Basin. The amount of water leaving the system across this boundary under predevelopment conditions is unknown, but it has been reduced under modern conditions due to groundwater extraction. The magnitude of this reduction in flow is unknown and is one of the motivating questions of this study. Hydraulic connection with adjacent hydrographic basins is assumed to be minimal, though if present this could account for additional subsurface inflows and/or outflows through the system.

2.7.4 Groundwater-Surface Water Exchange

Groundwater – surface water interactions in the Huaytire Basin are complex and spatially variable. As previously discussed, the upper reaches of perennial streams are generally gaining and receive groundwater contributions from the adjacent aquifer and overland flow. The lower reaches of perennial streams are generally losing and contribute surface water back to the adjacent aquifer. Groundwater and surface waters also discharge into Lake Suches, which can then leave the basin via evaporation and surface water pumping. Although the Huaytire Basin is currently a hydrologically closed basin to surface water and has no modern outflow, some water may have also left the basin as surface water in the Rio Callazas under predevelopment conditions.

2.7.5 Groundwater Pumping Flows

Groundwater has been extracted from eight pumping wells operated by the SPCC in the Huaytire Basin since at least the 1980s (Figure 2.4). Exact pumping rates for each well are not publicly available, but the SPCC maintains a water right of 1,950 liters per second (L/s) from surface water and groundwater in the "Huaytire, Vizcachas and Titjones" aquifers (SPCC, 2022). More precise pumping rates estimated for each well are summarized in Chapter 3. Groundwater pumped from the Huaytire Basin is removed from the system as interbasin transfers.

2.8 Groundwater Flow Patterns

Water levels were measured in thirty-seven SPCC piezometers and eight SPCC production wells in the Huaytire Basin between May 30 and May 31, 2015 by the Rio Locumba Consortium. Water level elevation ranged between 4,588.78 m amsl at piezometer C-01 in the northeastern area of the basin to 4,364.71 m amsl at pumping well TP-9A near the basin outlet. Water level elevations were plotted and contoured to illustrate the approximate direction of groundwater flow through the basin (Figure 2.7). A cone of depression is evident in the vicinity of several pumping wells, including around the cluster of four pumping wells located near the basin outlet. There is insufficient data available to accurately contour water levels at a resolution finer than 25 meters, and the interpretation is further complicated by lack of information regarding the elevation and length of piezometer screened intervals. Reported water levels at a few piezometers were inconsistent with the expected head gradient in Huaytire Basin; these measurements may have been erroneous, or the piezometers may be screened in aquifer units not well represented in the water level dataset. These data outliers were not considered in the water level interpretation. The 2015 CRL gaging event indicates that groundwater flows from higher elevation recharge zones around the edge of the basin towards lower elevation discharge zones at Lake Suches, the pumping wells, and the basin outlet.

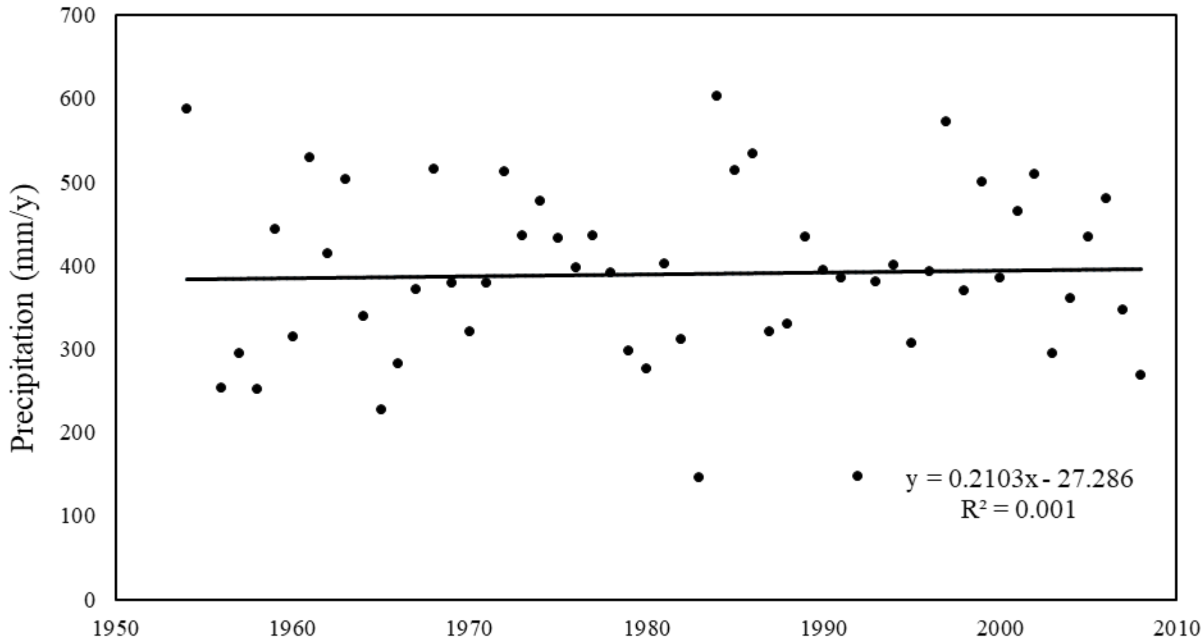

Figure 2.1: Annual precipitation as recorded at the Suches weather station. Data from Vining et al. (2019).

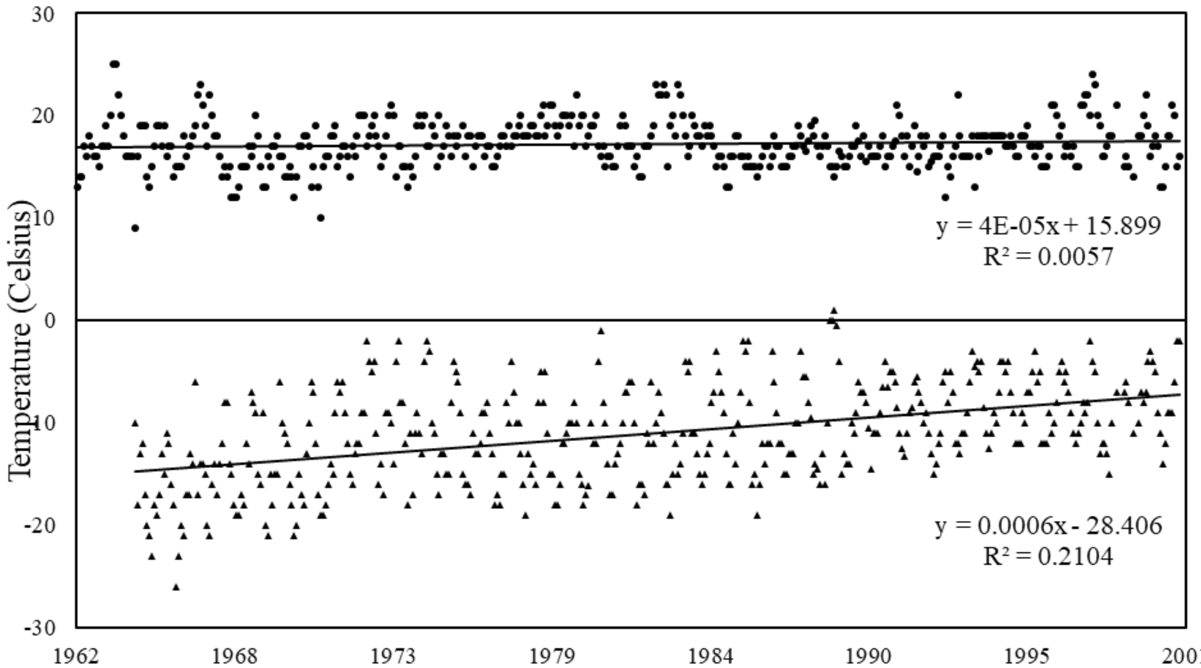

Figure 2.2: Monthly maximum (top panel) and minimum temperature (bottom panel) recorded at the Pasto Grande weather station. Data courtesy of Benjaman Vining.

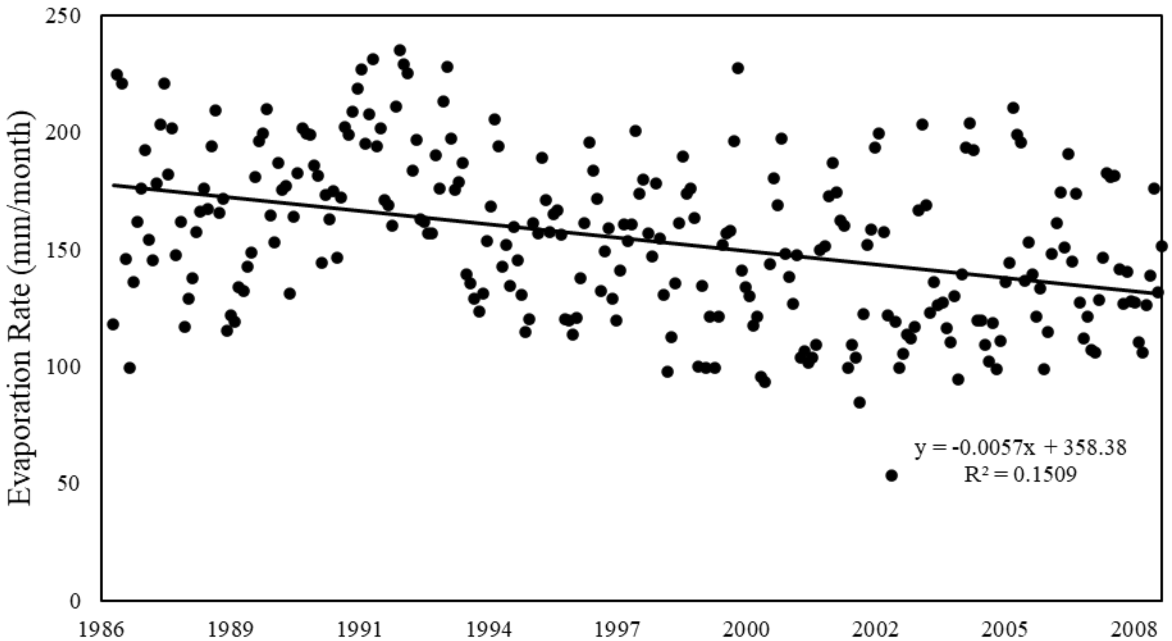

Figure 2.3: Monthly evaporation rates recorded at the Tocco weather station. Monthly values above 250 mm, obtained during the first year of measurement, were deemed outliers and were not considered in the regression. Data courtesy of Benjamen Vining.

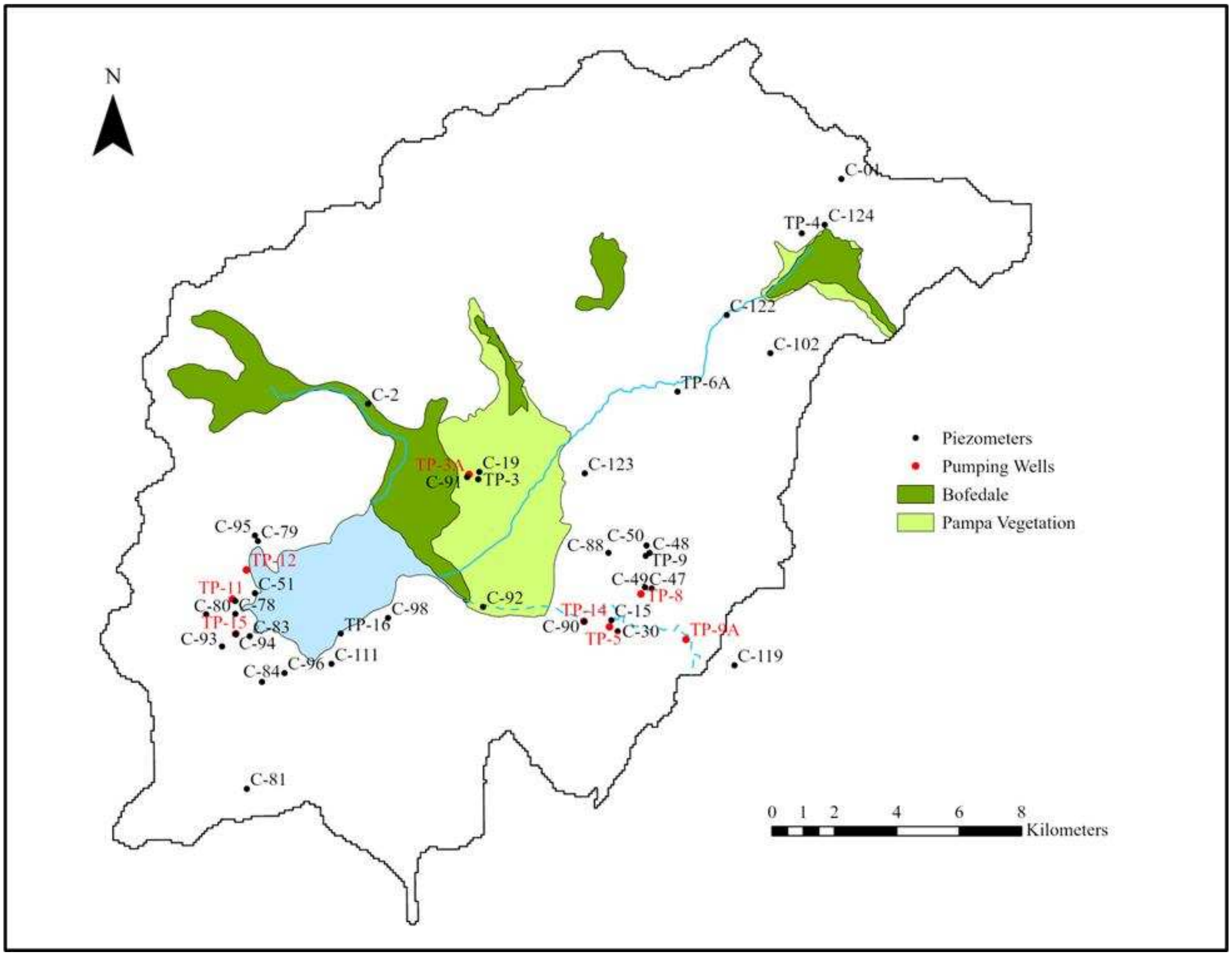

Figure 2.4: Existing pumping wells, piezometers, and vegetation zones within the Huaytire Basin

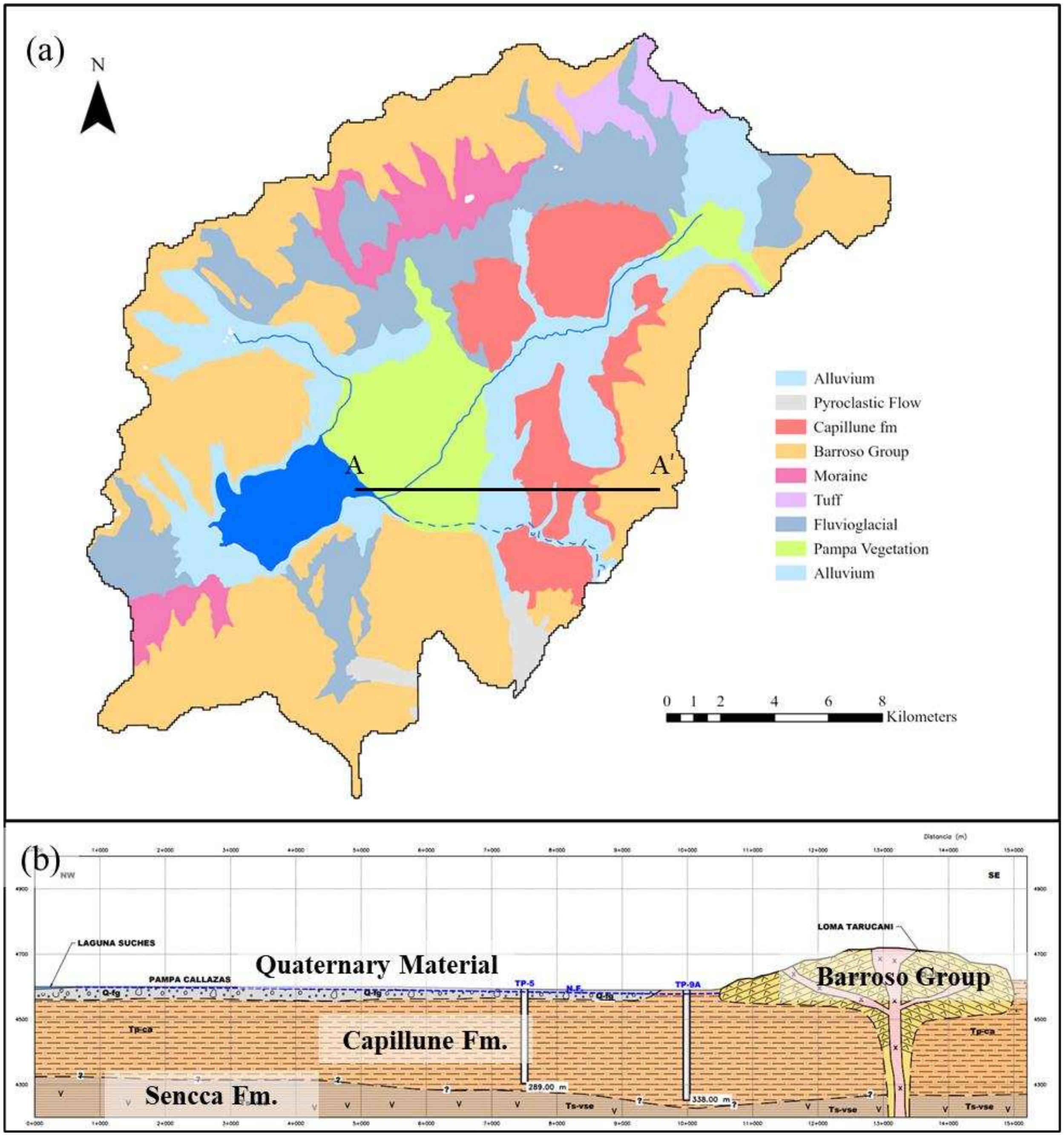

Figure 2.5: (a) Surficial geology within the study area. Data obtained from INGEMMET (2023). (b) Geologic cross section A – A' adapted from CRL (2017).

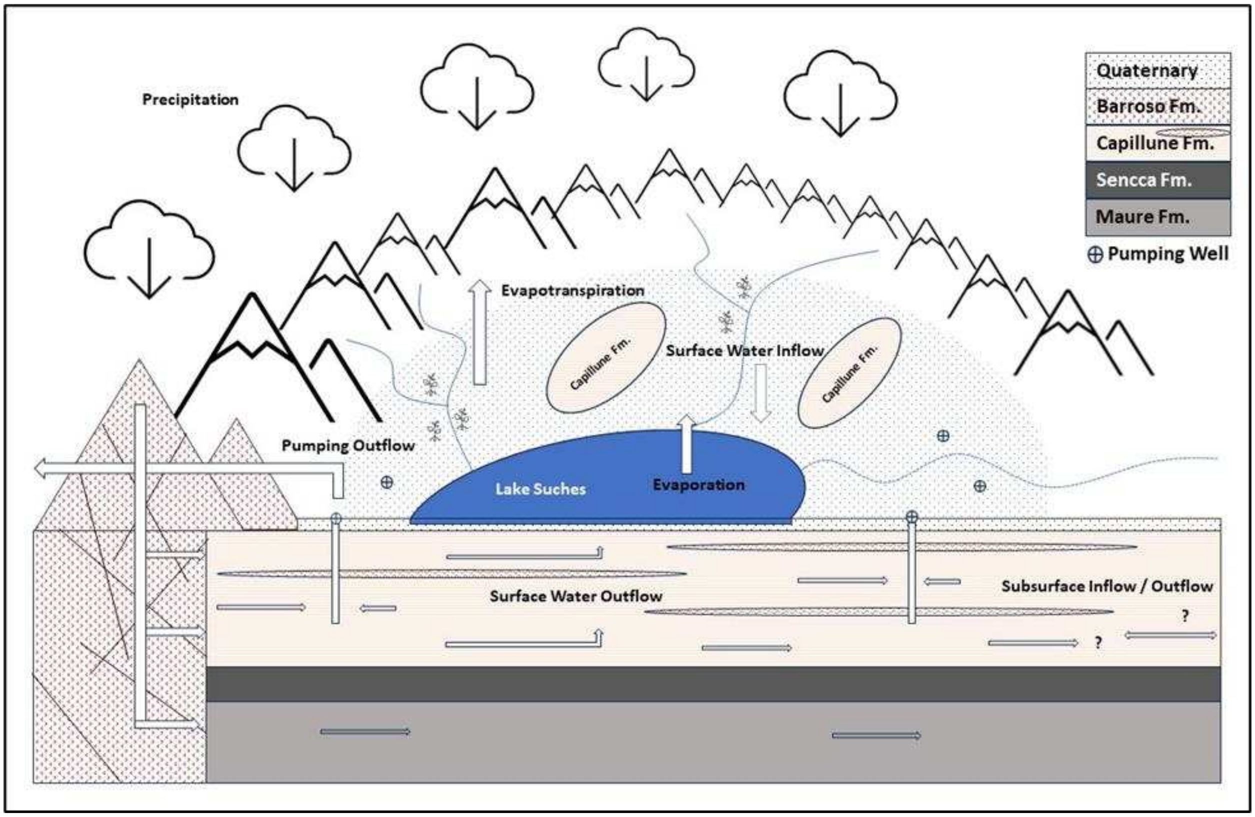

Figure 2.6: Conceptual hydrogeologic model for the Huaytire Basin. Arrows represent regional flow paths and groundwater fluxes. Perennial streams are represented with solid blue lines, and the ephemeral Rio Callaza is represented with a dashed blue line.

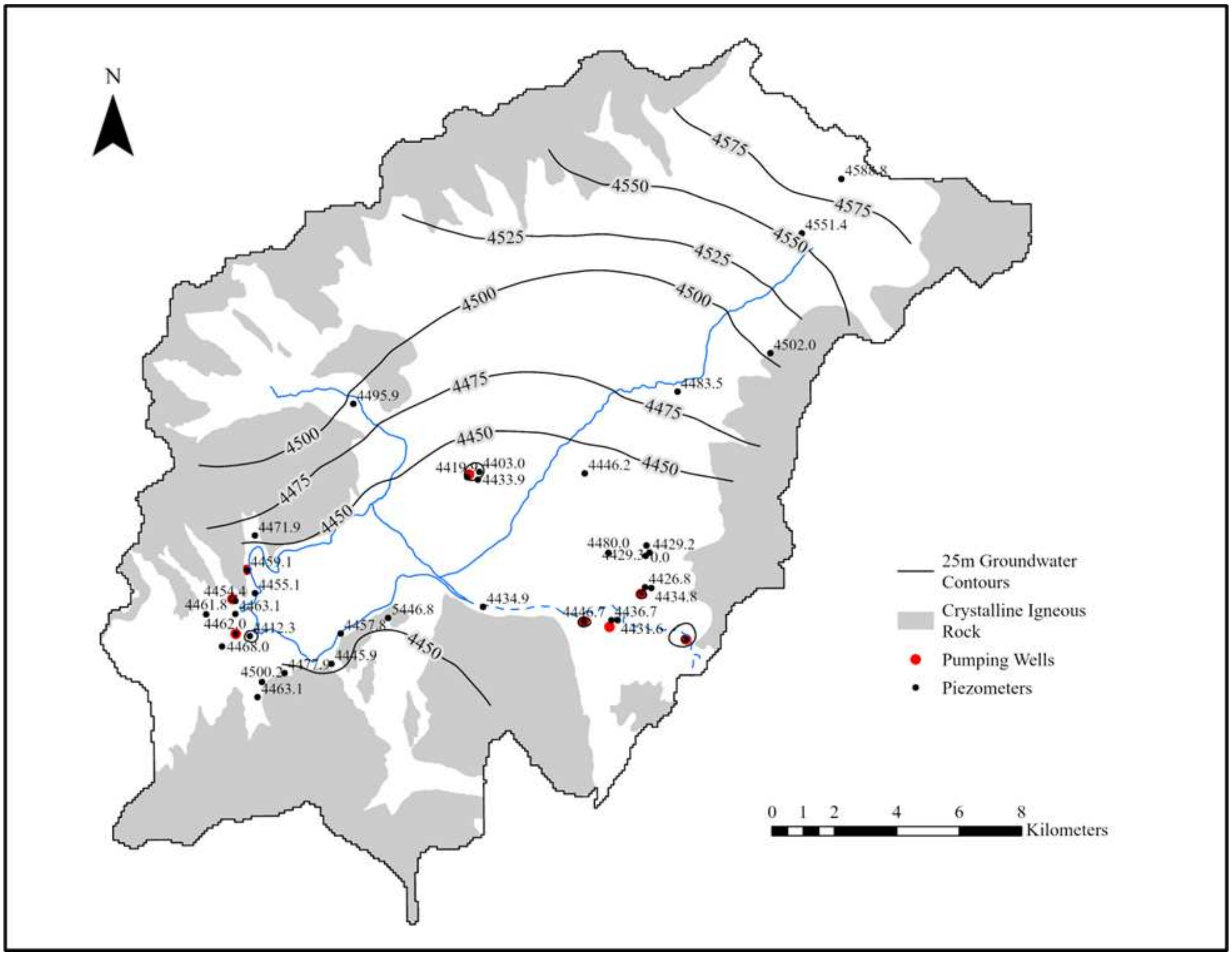

Figure 2.7: Water level elevation contour map of the Huaytire Basin using depth to water data collected on May 30th and May 31st, 2015. Data sourced from CRL (2017).

CHAPTER 3: METHODS

Primary methods employed in this study include water stable isotope analysis, hydrogeologic field data collection, and numerical groundwater modeling. Field activities were conducted between January 2023 and February 2024 and included sampling of surface and groundwater for isotope analysis, installation of shallow monitoring wells, water level measurement, streambed permeameter testing, and stream gaging.

3.1 Water Stable Isotopes

Water stable isotopes (^{1}H, ^{2}H, ^{16}O, and ^{18}O) are environmental tracers commonly used to interpret the dynamics of a hydrologic system. Water stable isotope analysis takes advantage of natural fractionation processes in the water cycle that preferentially sort water molecules containing lighter or heavier isotopes during phase changes. Fractionation creates an isotopically distinct signature in precipitation that can be traced through the water cycle (Clark and Fritz, 1997). In this study, 32 water samples were collected from surface water and groundwater in the Huaytire Basin (Figure 3.1). Samples were collected over two sampling events during the summer wet season (January 2023) and the winter dry season (June 2023). The purpose of this study was to understand the extent of hydraulic connection between surface water and groundwater, to investigate the location of Capillune Formation recharge, and to refine the conceptual hydrogeologic model of the Huaytire Basin.

Samples were collected and stored in accordance with guidance provided by the Utah State University Stable Isotope Ratio Facility for Environmental Research lab (SIRFER) and direction published in Clark and Fritz (1997). Samples were collected in 10 ml vials using a syringe and field filtered using a 0.22 micrometer filter to remove suspended sediments. The syringe was rinsed three times at each location prior to sampling to prevent cross contamination between sample locations. The vials for each sample were filled completely with no headspace and sealed tightly to avoid evaporation from the vial. Samples were stored in a cool location before shipment on ice to the SIRFER lab for processing.

Wet season samples were collected on January 8th and 9th, 2023, from 13 locations in the Huaytire Basin (Figure 3.1). Five samples were collected from perennial streams, four from bofedals, two from pumping wells, one from a spring, and one from Lake Suches. Although it was not possible to sample most of the eight SPCC pumping wells in the basin, two wells, TP-12 and TP-15, discharge groundwater directly to the surface making them available for sampling. Stream samples were collected from moving water as near to the thalweg as possible. Bofedal samples were also collected from moving water whenever possible. One sample was collected from a spring near the northwest corner of Lake Suches close to the spring's discharge location. One sample was collected from the southwest edge of Lake Suches near an access road.

Dry season sampling was completed on June 24th to 27th, 2023. 12 of the original 13 sample locations were repeated during the June 2023 sampling event. One sample location from pumping well TP-15 could not be repeated because the well was not active during the dry season sampling event. Seven new sample locations were added during the June sampling event, including three groundwater samples from recently installed shallow groundwater monitoring wells and four additional surface water sample locations. Sampling procedures for most locations were the same as the previous sampling event. Some repeat surface water locations required breaking through thin ice to reach liquid water. Shallow groundwater samples were collected using a clean plastic bottle taped to a rod. Water samples were collected from the bottle using a syringe.

When comparing water stable isotope results, each sample is generally referred to as being enriched or depleted relative to other samples in the dataset. Enriched water samples have a greater concentration of molecules containing heavy isotopes (^{2}H and ^{18}O), and depleted samples have a lower concentration of molecules containing those isotopes. Isotopes are typically reported as the ratio of the less common isotope to the more common isotope. This document follows the convention of reporting isotopic ratios and comparisons between samples in units of permille, or parts per thousand (‰).

Water stable isotopes are measured using a mass spectrometer and reported as a relative concentration against a standard – Vienna Standard Mean Ocean Water (VSMOW) (Clark and Fritz, 1998). Typically, delta notation (δ) is used when reporting isotope results, as illustrated in Equation 3.1 and 3.2, which describe the permille difference of the ratio of heavy to light isotopes in the sample compared to the reference. Positive delta values indicate that the sample is enriched in the heavy isotope relative to the standard (VSMOW), and negative delta values indicate that the sample is depleted.

$$\delta^{18}O_{sample} = \left(\frac{\frac{^{18}O}{^{16}O}_{sample}}{\frac{^{18}O}{^{16}O}_{reference}} - 1 \right) \times 1000 \qquad \text{(Equation 3.1)}$$

$$\delta^{2}H_{sample} = \left(\frac{\frac{^{2}H}{^{1}H}_{sample}}{\frac{^{2}H}{^{1}H}_{reference}} - 1 \right) \times 1000 \qquad \text{(Equation 3.2)}$$

Craig (1961) performed a linear regression on meteoric water collected from around the world and calculated a Global Meteoric Water Line (GMWL) illustrating the global isotopic relationship in precipitation between deuterium and ^{18}O, which has a slope of 8 and y intercept of 10 permille (Equation 3.3).

$$\delta^2H = 8\times\delta^{18}O + 10 \quad \text{(Equation 3.3)}$$

Water stable isotope results are often visualized by plotting them against the GMWL, with δ^2H on the y axis and δ^{18}O on the x axis.

3.2 Other field activities and measurements

Other field activities and measurements include monitoring well installation and water level measurement, streambed permeameter testing, and stream gaging.

3.2.1 Monitoring Well Installations and Water Level Measurement

Water table observation wells were installed on the Pampa Huaytire to obtain recent water level measurements in the shallow unconfined aquifer. Three observation wells were installed in June 2023 using a hand auger (Figure 3.2). Each well was constructed with 7.6-cm diameter slotted PVC pipe and installed as deeply below the water table as possible. Completed monitoring well depth ranged from 55 to 110 cm below ground surface. Pressure transducers were installed in each well to monitor changes in water table elevation with time. The recorded level data were used as calibration targets in the numerical model (Section 3.3).

3.2.2 Streambed Permeameter Testing

Permeameter testing was conducted to constrain the streambed vertical conductivity parameter in the numerical model. One successful streambed permeameter test was performed on Rio Japapunco (Figure 3.2) in February 2023. Hydraulic conductivity was calculated according to the type E variable head method developed by Hvorslev (1951). The test was performed using a 12.7-cm inner diameter PVC pipe driven between 7.2 cm and 11.1 cm into the streambed. Repeat tests ere performed at three nearby streambed locations (within 5 meters) and the results were averaged.

3.2.3 Stream Gaging

The Rio Japapunco and Rio Huaytire have previously been characterized as gaining streams in high relief and incised upper reaches and as losing streams in low relief downstream reaches where the streams flow across the coarse sediments of the Pampa Huaytire (Vining, 2011). The purpose of further stream gauging in this study was to verify the approximate location of gaining and losing reaches on the perennial streams and to produce discharge data which would be used to constrain simulated streamflow targets in the numerical groundwater model.

Stream gauging was performed over two site visits in the June 2023 dry season and in the February 2024 wet season. Dry season stream gauging was performed at eight locations in the Huaytire Basin, including six locations on the Rio Japapunco and two locations on the Rio Huaytire. Wet season stream gauging was performed at four locations in the basin, including three locations on the Rio Japapunco and one location on the Rio Huaytire. Gauging locations were selected based on proximity to access roads, proximity to other gauging locations, and streambed morphology.

Water velocity was measured using a handheld YSI digital current meter. Total wetted channel width was measured at each location, and water velocity and depth were measured at regular intervals ranging between 20 and 50 centimeters normal to the direction of stream flow. Velocity measurements were collected for each interval at a water depth of approximately 60% the distance between the water surface and the streambed. The cross-sectional area of the stream was estimated as a series of trapezoids, and volumetric flow for each interval was calculated by multiplying mean stream velocity of the interval by the cross-sectional area of the trapezoid. Summing the volumetric flow rate through each trapezoid at each gauging location yields an estimate of volumetric flow through the entire cross section at each location (Turnipseed and

Sauer, 2010). The spatial distribution of gaining and losing reaches was then determined by comparing measured values of streamflow to upstream and downstream measurements.

3.3 Numerical Methods

Numerical modeling was performed to simulate groundwater flow, groundwater-surface water interaction, and the response to historical stresses (pumping) in Huaytire Basin.

3.3.1 Numerical Modeling Overview

Numerical groundwater modeling is a mathematical technique commonly employed by hydrogeologists to understand and analyze groundwater flow systems. Models are often applied by resource managers to forecast aquifer response to changes in hydrologic regime such as groundwater pumping, climate change, managed aquifer recharge, and other hydrologic stresses. The three-dimensional, transient, anisotropic, and heterogeneous governing equation of groundwater flow (Equation 3.4) describes the flow of groundwater through an aquifer and is derived from Darcy's law and the principle of conservation of mass (Anderson et al. 2015):

$$\frac{\partial}{\partial x}\left(K_{xx}\frac{\partial h}{\partial x}\right) + \frac{\partial}{\partial y}\left(K_{yy}\frac{\partial h}{\partial y}\right) + \frac{\partial}{\partial z}\left(K_{zz}\frac{\partial h}{\partial z}\right) - W = S_s\frac{\partial h}{\partial t} \qquad \text{(Equation 3.4)}$$

Where K_{xx}, K_{yy}, *and* K_{zz} are values of hydraulic conductivity in the x, y, and z directions (L/T), *h* is hydraulic head (L), *W* is a source / sink term (1/T), *Ss* is the specific storage (1/L), and *t* is time (T). Groundwater models solve the governing equation for hydraulic head at discrete points in space and time. Numerical solutions allow modelers to simulate three-dimensional systems under transient (time variable) conditions with complex boundary conditions and heterogeneous aquifer materials, as represented in the form of the governing equation illustrated in Equation 3.4, making numerical modeling a useful approach for exploring and understanding a diverse array of hydrogeologic questions.

At steady state, conservation of mass dictates that flow into the aquifer system must equal flow out of the aquifer system, which demands that the solution to a steady state simulation is time invariant and the head distribution and total aquifer storage will not change with time. For a steady-state problem, the time derivative in the governing equation (dh/dt) is equal to zero, which eliminates the storage term and simplifies the governing equation to Equation 3.5, the terms of which have been previously defined:

$$\frac{\partial}{\partial x}\left(K_{xx}\frac{\partial h}{\partial x}\right)+\frac{\partial}{\partial y}\left(K_{yy}\frac{\partial h}{\partial y}\right)+\frac{\partial}{\partial z}\left(K_{zz}\frac{\partial h}{\partial z}\right)+W=0 \qquad \text{(Equation 3.5)}$$

Using initial heads calculated as a steady state solution to the governing equation can greatly improve the accuracy of early time step heads calculated in transient solutions, making steady state predevelopment modeling an important first phase in modeling studies designed to quantify the effects of pumping and/or other transient stresses on an aquifer.

This study utilized MODFLOW, a widely used groundwater modeling program developed and maintained by the United States Geological Survey (USGS), which solves the governing flow equation using the finite difference numerical method (Harbaugh et al., 2000). The implemented numerical method replaces partial derivatives in the governing equation with finite difference approximations, creating a system of linear algebraic difference equations that can be solved using iterative methods. Choices related to grid spacing, time discretization, parameterization, convergence criteria, and boundary conditions can all contribute to the accuracy of the numerical solution and need to be carefully considered by the modeler to produce a meaningful result.

3.3.2 Model Domain and Discretization

The model domain corresponds with the upper watershed of the Rio Locumba, including Lake Suches and its tributaries and the upper ~ 14 km of the Rio Callazas (Figure 3.3). Here, the common assumption that the groundwater divide in the Huaytire Basin is generally congruent with the surface water divide is employed, and the groundwater divide is effectively modeled as a no flow boundary. One exception to this approach is the basin outlet, which was established by considering topography and inferred groundwater flow directions in the southeastern part of the basin. The boundary of the active model domain was placed approximately one kilometer downstream of pumping well TP-9A – the furthest downstream pumping well in the Huaytire Basin and the closest well to the basin outlet.

A structured rectangular grid was used with a regular nodal spacing of 100 by 100 meters. The model domain contains 284 rows and 298 columns for a total of 84,632 cells in each layer of the model. The total dimensions of the model domain are 29.8 km (east to west) by 28.4 km (north to south). Areas within the rectangular model domain that fall outside of Huaytire Basin have been excluded from the active domain with inactive no flow cells. The grid is discretized into four layers, each containing 45,667 active cells, for a total of 182,668 active cells. For transient modeling, time was discretized into 10-day timesteps. The grid resolution of 100 meters by 100 meters is sufficiently fine to accurately simulate surface water – ground water exchange, represent spatially heterogeneous aquifer parameters, and capture complex boundary geometry with acceptable accuracy and without significant overgeneralization. The grid resolution and timestep length are also appropriate to facilitate reasonable MODFLOW runtimes and allow for the clear visualization of results.

The model thickness was discretize" usi'g four layers to simulate vertical groundwater flow, incorporate vertically heterogeneous material property parameters associated with horizontally deposited aquifer stratigraphy, and to accurately represent the general bathymetry of Lake Suches. The top elevation of layer 1 was imported from a 30-meter resolution Copernicus digital elevation model (DEM) (Figure 3.3) (European Space Agency and Sinergise, 2021). The model bottom elevation is set to 4,200 meters across the entire model domain, which corresponds to the approximate elevation of the top of the confining Sencca Formation (CRL, 2017; SPCC, 1974). Layer 1 and Layer 2 have a uniform thickness of 10m and 15m, respectively, over the entire model domain. These relatively thin layers serve to capture the hydraulic properties of thin surficial deposits common throughout the Huaytire Basin and allow for the accurate simulation of near-surface vertical head gradients. Relatively thin layers near the surface also allow for a more accurate representation of Lake Suches bathymetry. The top of model layer 4 is defined at half the distance between the model bottom elevation and the model top elevation across the entire model domain. This method results in thicker cells in model layer 3 and layer 4 in high elevation regions and thinner cells in lower elevation regions.

Time was subdivided using eight stress periods of varying length to accurately simulate the known and quantifiable transient hydrologic stresses in the Huaytire Basin (Table 3). Stress period 1 is a steady state simulation that represents predevelopment conditions prior to Lake Suches diversions starting in 1961. The predevelopment solution obtained during stress period 1 serves as an initial condition for the transient simulation. Stress periods 2 through 8 each represent some change in the Huaytire Basin pumping regime. Long term pumping records with exact commencement dates are not publicly available, so stress periods were established according to the date groundwater licenses were granted to the SPCC by the National Water Authority (Meneses, 2018). Pumping rates were calculated and assigned to each well by analyzing pumping meter records collected from all eight pumping wells in the study area between 2011 and 2022 (ALA, 2023).

Table 3: Transient simulation stress periods with water management information. *Outflow from Lake Suches is reported here as a net outflow (Lake Suches surface water pumping rate – augmentation rate).

Stress Period Number	1	2	3	4	5	6	7	8
Start Date	N/A	1/1/1961	6/15/1983	1/1/1994	1/1/1999	1/1/2003	4/1/2003	5/28/2005
Withdrawal Rate (l/s)								
Lake Suches*	0	300	300	156	89	156	123	89
TP-3A	0	0	56	56	56	56	56	56
TP-5	0	0	41	41	41	41	41	41
TP-8	0	0	150	150	150	150	150	150
TP-9A	0	0	118	118	118	118	118	118
TP-11	0	0	0	91	91	91	91	91
TP-12	0	0	0	53	53	53	53	53
TP-14	0	0	0	0	90	0	45	90
TP-15	0	0	0	0	66	0	33	66
Total (l/s)	0	300	666	666	756	666	711	756
Total (m^3/d)	0	25,920	57,541	57,541	65,359	57,541	61,450	65,359

3.3.3 Boundary Conditions

Boundary conditions describe areas of the model where water enters or leaves the system. The numerical model utilizes both specified flux and head dependent flux type boundaries which can be divided into two categories – internal boundaries and external boundaries. In this model, internal boundary conditions govern hydrologic interactions that occur near streams and lakes within the active model domain, and external boundary conditions govern flows into and out of the system along the edge of the active model domain (Figure 3.3). This section begins with a description of the external boundary conditions represented in the model.

3.3.3.1 General Head Boundary Package

The General Head Boundary, or GHB, is a commonly used external head dependent flux boundary used to simulate flow across a boundary that is dependent on a known constant head specified at some distance from the model external boundary (Anderson et al. 2015). In

MODFLOW, GHBs are simulated using the GHB package (Harbaugh et al., 2000). Flux across a GHB is dependent on the difference in head calculated at the GHB cell relative to the specified head – h_b – located at some distance L from the boundary. The GHB allows for the analysis of flux across a boundary of interest without expanding the active model domain to cover the full extent of adjacent aquifer material. This head-dependent boundary condition allows flow across the boundary to change in magnitude or direction in response to hydrologic stress within the active model domain. Flow across the GHB is calculated according to the relationship illustrated in Equation 3.6:

$$Q = \frac{KA}{L}(h_b - h_{i,j,k}) \qquad \text{(Equation 3.6)}$$

where Q is the simulated flow across the boundary (L^3/T), K is hydraulic conductivity (L/T), A is the cross sectional area (L^2), L is distance from the boundary to h_b (L), h_b is the specified external boundary head, known head at some external location (L), and $h_{i,j,k}$ is the head calculated for a GHB cell along the edge of the model (L).

212 GHB cells were specified to simulate underflow near the basin outlet along the southeast edge of the active model domain. The location of the GHB was determined using surficial topography and geology illustrated in Figure 1.1 and Figure 2.5. The ephemeral channel of the Rio Callazas exits the basin through an approximately six-kilometer gap in the high elevation hills associated with the igneous Barroso Group, and GHB cells were placed in expected lower elevation aquifer material between higher elevation igneous outcrops. Aquifer parameters outside of the study area are not known, and hydraulic conductivity in the area represented by the GHB was assumed to be similar to the Capillune Formation, and was set to 2 meters per day in layers 1 through 3 and 1 meter per day in layer 4. H_b was set to the elevation of a point selected

approximately 2 kilometers downstream of the GHB on the Rio Callazas where flow has been reported to be perennial (CRL, 2017). Analyzing the simulated flow across the GHB will be important for understanding the nature of hydrologic change in the Huaytire Basin and nearby communities.

3.3.3.2 Stream Flow Routing Package

Stream Flow Routing, as simulated using the SFR package in MODFLOW (Prudic et al., 2004), is an internal head dependent boundary condition that is used to simulate interactions between groundwater and streams. Unlike the related River (RIV) package, in which stream stage in a simulated river is specified by the modeler, SFR allows for the simulation of streamflow and stage as part of the model solution. RIV cells can become infinite sources of water and may not be appropriate for modeling small headwater streams – especially small streams near pumping wells. With the SFR package, the quantity of aquifer recharge derived from losing stream cells is constrained by upstream contributions routed from gaining stream cells and may dry up completely when appropriate. Therefore, the SFR package provides a useful tool for accurately constraining the water budget of small headwater streams such as those present in the Huaytire Basin (Anderson et al, 2015). In transient simulations, the SFR package can be used to illustrate flux dynamics between groundwater and surface water features and can be applied to forecast spatial and temporal changes in the location of gaining and losing stream reaches or overall streamflow as a response to hydrologic stress. Groundwater – surface water interactions are an important component of the water budget in the Huaytire Basin, making careful application of the SFR package critical for constructing an accurate simulation.

The mathematical formulation used by MODFLOW to calculate flux between streams and the adjacent aquifer using SFR is similar to that used by other head dependent flux boundaries, and is calculated using a form of Darcy's Law illustrated in Equation 3.7:

$$Q_{GW} = -K_z \frac{h_1 - h_2}{b} \text{LW}$$

Where Q_{GW} is groundwater flow to or from the aquifer (L^3/T), K_z is vertical hydraulic conductivity of the streambed material (L/T), h_1 is head in the aquifer cell that contains the stream (L), h_2 is head in the stream or stream stage (L), *b* is the streambed thickness (L), and LW represents the area of streambed material within the designated SFR model cell (L^2). Unlike the RIV package, the SFR package can calculate streamflow and stream stage converted from water depth using a variety of methods chosen by the modeler. This study used a form of Manning's equation which assumes a wide, rectangular channel (Prudic et al., 2004) (Equation 3.8):

$$Q_s = \frac{C}{n} A R^{2/3} S_0^{1/2} \qquad \text{(Equation 3.8)}$$

In which Q_s is streamflow (L^3/T), C_f is a unit conversion factor (unitless), n is Manning's roughness coefficient (unitless), A is the cross sectional area of the stream channel width (L^2), R is the hydraulic radius of the stream (L), and S_0 is slope of the water surface (unitless), which is assumed to be equal to the slope of the streambed.

Input parameters for the SFR package in MODFLOW include streambed material thickness, channel width, Manning's roughness coefficient, and vertical hydraulic conductivity of the streambed material. Two perennial streams in the Huaytire Basin were modeled using the SFR package – the Rio Huaytire and the Rio Japapunco. Vertical streambed conductivity in both streams was set to 5 meters per day based on the streambed permeameter test performed on the Rio Japapunco. Stream width was measured at several locations on both streams during the June

2023 and February 2024 stream gauging events and was set to the mean stream width measured on each stream – 4.03 meters on the Rio Japapunco and 2.40 meters on the Rio Huaytire. Streambed material depth was not measured directly and was initially set to 1 meter for each stream reach in the model. A Manning's roughness coefficient of 0.04 was assigned for each reach, which describes mountain streams with boulders or clean and straight natural sandy streams (Maidment, 1992).

The Rio Callazas is the outlet channel of Lake Suches and is an ephemeral stream under modern conditions. Field measurements of streambed permeability, thickness, and width were not collected on the Rio Callaza. In the predevelopment simulation, SFR parameters along Rio Callaza, which may have flowed under a historic hydrologic regime, were estimated as equal to those applied to the Rio Japapunco, which is the largest perennial stream in the Huaytire Basin under modern conditions.

3.3.3.3 Lake Package

Lake Suches is represented in the model using the LAK3 package, otherwise called the Lake package, which is also a type of head dependent flux boundary (Merritt and Konikow, 2000). While lakes are commonly simulated using constant head boundaries, the constant head approach does not allow for fluctuation of lake stage in response to hydrologic stresses and, like the RIV package, can potentially supply an infinite amount of recharge to the aquifer under some conditions. Another common method for simulating lakes is the high K method, in which model cells within the lake are assigned a very high hydraulic conductivity and a specific yield value of 1, implying open water, which allows lake stage to change in response to stress (Anderson et al. 2015). The Lake package was selected for its ability to accept inflow from the SFR package, which is impossible to simulate using the high K method, and for the Lake package's more realistic representation of leakance through lakebed materials which may have different physical properties than the adjacent aquifer. Simulation of stage is important for understanding how Lake Suches interacts with the adjacent aquifer as the Huaytire Basin experiences changes under modern conditions, for understanding whether the lake experienced overflowing conditions in a predevelopment scenario, and, if so, for quantifying surface water outflow into the Rio Callaza. Under modern conditions the Lake Suches water budget is also complicated by engineered flows into and out of the lake, which the Lake package is equipped to simulate.

Stage is calculated using the Lake package by assuming a relationship between lake volume and stage, so each component of the lake water budget must be accurately estimated by the modeler for the code to compute lake stage realistically. In lakes occupying more than one layer, lake area is also calculated as a function of stage. The lake water budget is calculated by MODFLOW independently of the aquifer water budget during the numerical solution. Flow rates into or out of the lake describing evaporation, precipitation, surface runoff, and/or anthropogenic withdrawals and augmentation must be specified by the modeler. Some flows, such as evaporation and precipitation, are dependent on lake area and change depending on lake stage. Seepage rates and, when utilizing the SFR package, stream inflows and outflows are computed for each iteration and continually updated in the lake water budget.

The lowest reach of each SFR segment that interfaces with Lake cells are recognized by MODFLOW as stream inflows in the Lake water budget. Channelized surface water outflow from the lake (outflow to streams) is calculated using the version of Manning's equation used by the SFR package. Subsurface flow into or out of the lake, also called seepage, is head dependent and calculated using a method similar to other head dependent flux boundaries such as the GHB package and the SFR package using a variation of Darcy's law, Equation 3.9:

$$Q_{GW} = -K \frac{h_1 - h_2}{\Delta l} A \qquad \text{(Equation 3.9)}$$

Where Q_{GW} is discharge to or from the aquifer, K is the equivalent hydraulic conductivity of geologic material around the lake-aquifer interface, h_1 the hydraulic head of the lake (i.e., lake stage), h_2 is the hydraulic head of the aquifer, and A is the cross-sectional area of a finite difference cell face.

Input parameters for the Lake package that must be specified include lakebed thickness, lakebed hydraulic conductivity, precipitation rate, evaporation rate, anthropogenic inflows, and anthropogenic outflows. In the predevelopment steady state model, anthropogenic inflows and outflows were set to zero. In the transient simulation, pumping from the lake was set as equal to the SPCC surface water right of 300 liters per second, the license for which was approved in 1961 (Meneses, 2018) (Table 3). Pumping wells TP-11, TP-12, and TP-15 are each installed in the immediate vicinity of Lake Suches and are all assumed to discharge directly into the lake. Augmentation from each of these wells was set to begin on the date each groundwater extraction license was approved. Groundwater augmentation of Lake Suches is assumed to be equal to pumping rates calculated for each well, with a maximum total augmentation rate of approximately 211 liters per second (ALA, 2023).

Mean annual precipitation was set to 389 mm as calculated from monthly records collected at a meteorological station maintained by SPCC on the shore of Lake Suches and reported in Vining et al. (2019). Seasonal variation in precipitation was not considered. Lakebed hydraulic conductivity was not measured directly but was estimated to be 0.1 meters per day to simulate typically fine-grained lakebed sediments (Freeze and Cherry, 1979). Lakebed sediment thickness was set to 8 meters as constrained by data published in Vining et al. (2019), which reported lakebed sediment thickness of at least 812 centimeters measured during a sediment coring campaign on Lake Suches. Long term evaporation records were not available for Lake Suches, so evaporation was estimated using a pan evaporation dataset collected over a 21-year period at a SPCC weather station located approximately 30 kilometers northeast of Lake Suches at a similar elevation near the village of Tocco (Figure 1.1). Mean annual pan evaporation measured at the Tocco station is approximately 1.86 meters per year, or approximately 5 millimeters per day (SPCC, 2009). Details regarding the type of pan used to create the dataset were not available, so a standard pan coefficient of 0.70 was used for converting class A pan evaporation to lake evaporation (Kohler et al, 1955). Using the information described above, the evaporation rate in Lake Suches was estimated at approximately 1.3 meters per year, or approximately 3.5 millimeters per day.

Lakebed geometry was extrapolated from bathymetry data published by Vining et al. (2019) and from the Lake Suches polygon depicted in Figure 2.5. Lake cells in Layer 1, which is 10 meters thick, are delineated using the footprint of Lake Suches as represented by the Lake Suches polygon. Layer 2 lake cells are delineated using bathymetry data published by Vining et al. (2019). Only areas of the lake exceeding 10m in depth are delineated as LAK3 cells in layer 2. This two-tiered approach ensures that Lake Suches is accurately represented in the model, and that lake stage and volume are calculated with acceptable precision.

3.3.3.4 Well Package

Groundwater pumping was represented in the model using the standard Well (WEL) package in MODFLOW (Harbaugh et al., 2000). With this approach, the pumping rate for each well is maintained at a constant value during individual stress periods, and the rate is not dependent on the aquifer hydraulic head. Well completion information is not available for the eight groundwater pumping wells installed in the Huaytire Basin, but screened intervals are expected to approximately span the Capillune Formation. Pumping rates for each well were split evenly between model layers 3 and 4. Simulated pumping histories for each well are detailed in Table 3.

3.3.4 Parameter Assignment

Initial aquifer properties, recharge rates, and evapotranspiration rates were assigned to each cell in the finite difference grid during the model setup. Required aquifer properties include hydraulic conductivity, specific storage, and specific yield. Some of these quantities were subsequently adjusted during model calibration, and thus are treated as model parameters. Other parameters, including diffuse areal recharge and evapotranspiration, represent internal sources or sinks for the modeled aquifer system.

3.3.4.1 Recharge

Diffuse areal recharge, as simulated using the MODFLOW Recharge package (Harbaugh et al., 2000), is a specified flux applied to every finite difference cell in the model containing a water table. Recharge was modeled using two zones, constituting lower elevation recharge Zone 1 and higher elevation recharge Zone 2 (Figure 3.4). Although high elevation precipitation data for the Huaytire Basin is not available, recharge flux is expected to increase at higher elevations due to orogenic rainout and more poorly developed soils on the fractured bedrock outcrops of the Barroso Group. This effect was simulated by assigning a higher recharge rate to areas of the model exceeding 4,700 meters amsl. The high elevation recharge rate was estimated as a 10% higher recharge fraction than the low elevation recharge fraction, or 35% of annual valley floor precipitation in the base case scenario. Calibration was performed using a base case recharge rate of 0.097 meters per year in recharge zone 1 and 0.134 meters per year in recharge zone 2, or 25% of low elevation mean annual precipitation in recharge Zone 1 and 35% of low elevation mean annual low elevation precipitation in recharge Zone 2 (Figure 3.4). The base case scenario was analyzed alongside high recharge and low recharge scenarios to acknowledge the substantial uncertainty associated with the recharge parameter. Recharge fractions in highlands and lowlands were increased or decreased by 30% for higher and lower recharge scenarios, for a recharge fraction of 15% to 25% in the low recharge scenario and 32.5% to 45.5% in the high recharge scenario. The model simulates average annual conditions and does not simulate seasonal variability in recharge rate.

3.3.4.2 Evapotranspiration

Evapotranspiration (ET) from phreatophytes was included in the model simulations. In MODFLOW, ET from unconfined aquifers is modeled as a head-dependent flux using the Evapotranspiration package (Harbaugh et al., 2000), which simulates transpiration from phreatophytic plants that draw water directly from the water table. In general, the evapotranspiration flux through phreatophytes only occurs where the water table is shallow, and decreases in magnitude with increasing depth to water. If the water table falls below some critical maximum rooting depth for a phreatophyte species, the ET flux degrades to zero. In the MODFLOW Evapotranspiration package, this critical depth is called the extinction depth, and must be explicitly set by the modeler. When the water table is at or above a maximum ET surface, the phreatophyte plant is fully satisfied and transpiring at its maximum prescribed rate, which also must be specified by the modeler. As the water table falls between the maximum ET surface and the extinction depth, the ET flux is reduced linearly between maximum prescribed ET rate and zero. Two ET zones were delineated in the Huaytire Basin to simulate different types of vegetation present in each zone, constituting the more sparsely vegetated Pampa Huaytire and the more densely vegetated Bofedals (Figure 2.4).

ET rates for vegetation found on the pampas and bofedals of the Huaytire Basin have not been rigorously studied, making extinction depth and maximum ET rate difficult to prescribe. SPCC (1974) estimated evapotranspiration from the Pampa Huaytire at 1 meter per year, but the method of estimation for that value is unclear. Suarez et al. (2024) estimated evapotranspiration from riparian wetlands in a similar high Andean environment approximately 610 kilometers south of the Huaytire Basin using an eddy covariance system, and found altiplano wetland ET to range between 703 and 841 millimeters per year. These values were adopted as maximum ET rates on the pampas (702 millimeters per year) and bofedals (841 millimeters per year) in the Huaytire Basin.

Maximum rooting depth is species dependent and not well understood for vegetation occurring in the Huaytire Basin. While rooting depths for Juncaceae cushion plants have not been explicitly published, bofedal rooting depth was set to 0.8 meters based on observed *Distichia* die-off events in similar Andean peatlands with water table monitoring (Cooper et al. 2019). Rooting depth on the Pampa Huaytire was set to 1.05 meters based on root measurements of a *Tetraglochin cristata* specimen excavated from the Pampa Huaytire. *Tetraglochin cristata* is a common phreatophyte on the Pampa Huaytire.

3.3.4.3 Hydraulic Conductivity and Storage Properties

Initial hydraulic conductivity (K) values were assigned using estimates derived from aquifer tests (Section 2.6) or using reasonable estimates published in the literature for similar materials. Anisotropy – the ratio of vertical to horizontal hydraulic conductivity – is common in aquifers composed of horizontally bedded materials but difficult to measure explicitly (Shepley, 2024). In the Huaytire Basin some degree of anisotropy is expected in the Capillune formation and other horizontally deposited alluvial, fluvial, and volcanoclastic materials. Like hydraulic conductivity, storage properties are assigned to every active cell in the model domain; in confined layers, the relevant storage property is specific storage (S_s), while in unconfined layers the relevant storage property is specific yield (S_y). Both properties must be assigned to each active cell in the model (for convertible layers that can transition between confined and unconfined).

Initial estimates of hydraulic conductivity, specific storage, and specific yield were assigned based on previous estimates and refined during the calibration process described below. Final calibrated values for all hydraulic properties are provided in Chapter 4. Layer 1 hydraulic conductivity and storage zones were delineated using surficial geology published in INGEMMET (2022) (Figure 2.5), which was consolidated into three zones – Zone 1 Capillune Formation, Zone 2 Quaternary Material, and Zone 3 Barroso Group (Figure 3.5). Quaternary materials are thought to be relatively thin and are only represented in model layer 1. Because the igneous Barroso Group overlies the Capillune formation and spreads laterally from volcanic sills, layer 2 and layer 3 are generally defined as igneous wherever the surficial geology is mapped as part of the Barroso Group. Where igneous surficial geology is not mapped at the surface, model layers 2 and 3 were initially defined as having the material properties of the Capillune Formation. Layer 4 was initially defined as Capillune Formation across the entire model domain.

3.2.5 Model Calibration

Model performance is assessed by comparing model results, including simulated heads and fluxes, to measured or observed targets in a real-world system. The process of model calibration involves changing parameters or other structural components of the model to produce the closest possible match between simulated and observed targets through a process called history matching (Anderson et al., 2015). Initial parameter estimates are assigned based on available data and adjusted within a reasonable range to identify sensitive parameters and achieve closer agreement between simulated results and measured head or flux values.

In the Huaytire Basin, available targets for history matching are comprised of less precise soft targets, including streamflow and lake stage, and more robust hard targets, including piezometer and monitoring well water level elevation measurements. With respect to the hard targets, model performance was quantified by analyzing residuals between simulated and measured target values. While several statistics are commonly used to analyze model performance, this study emphasized the mean absolute error (MAE), which captures the total magnitude of model error and avoids the cancellation of residuals with similar magnitudes in opposite directions (Anderson et al., 2015). Dividing the MAE by the range of target observations (max – min observed water levels) is useful for normalizing model performance and aids in the interpretation of model results. Calibration performed in this study was focused on achieving a low MAE/Range, preferably less than 0.1 (10%), which indicates that the average error magnitude is relatively low compared to the observed range in head values.

Hard targets available for the Huaytire Basin include the May 2015 piezometer gauging event published by CRL (2017), groundwater elevation observations inferred from boring logs (SPCC, 1974), and shallow groundwater monitoring wells installed on the pampa as part of this study, constituting target Group 1, Group 2, and Group 3, respectively. Soft targets include lake stage and the presence or absence and magnitude of surface water discharge in perennial streams. Groundwater elevation observations that fall far outside of expected values according to the conceptual site model were not considered in the model calibration. Groundwater elevation observations collected from pumping wells were also not considered.

Group 1 target perforated interval elevations are unknown but are likely to be screened in the Capillune Formation. Group 1 targets are all placed in model layer 4. Group 2 targets represent mean groundwater elevation values recorded on boring logs during monitoring well and pumping well instillation. Group 2 targets are placed in layer 3 and layer 4, depending on the boring depth when the groundwater elevation measurement was collected. Group 3 targets, consisting of three shallow water table observation wells installed on the Pampa Huaytire, were placed in model layer 1 represent the mean water table elevation between June 2023 and February 2024.

Soft targets, including lake stage and streamflow, were compared against stream gauging values collected during the June 2023 and February 2024 gauging events and lake stage information inferred from bathymetry published in Vining (2011) and the Copernicus DEM (European Space Agency, Sinergise, 2021). Surface water discharge and lake stage are seasonally and interannually variable, making exact calibration targets unrealistic. Rather, model results were checked for a reasonable range of values for lake stage and surface water discharge based on measured values and observed general patterns of gaining and losing stream reaches.

Calibration of hydraulic conductivity and storage properties was initiated using the automated parameter estimation software package PEST, which employs a least squares objective function to obtain optimal parameter values (Doherty, 2015). PEST works to minimize the sum of squared residuals between simulated and observed target values by making adjustments to model parameters over many model runs to achieve an optimized value. In PEST simulations, plausible min/max parameter ranges were extended beyond the range of previous estimates (Chapter 2 conceptual model) to allow for optimization without excessive constraint. The model was run with optimal parameters identified by PEST and scrutinized for soft target performance and general adherence to the conceptual model. Final adjustments to the model, including the addition and refinement of hydraulic conductivity zones, simulation of anisotropy, and estimation of base case recharge are summarized in Chapter 4.

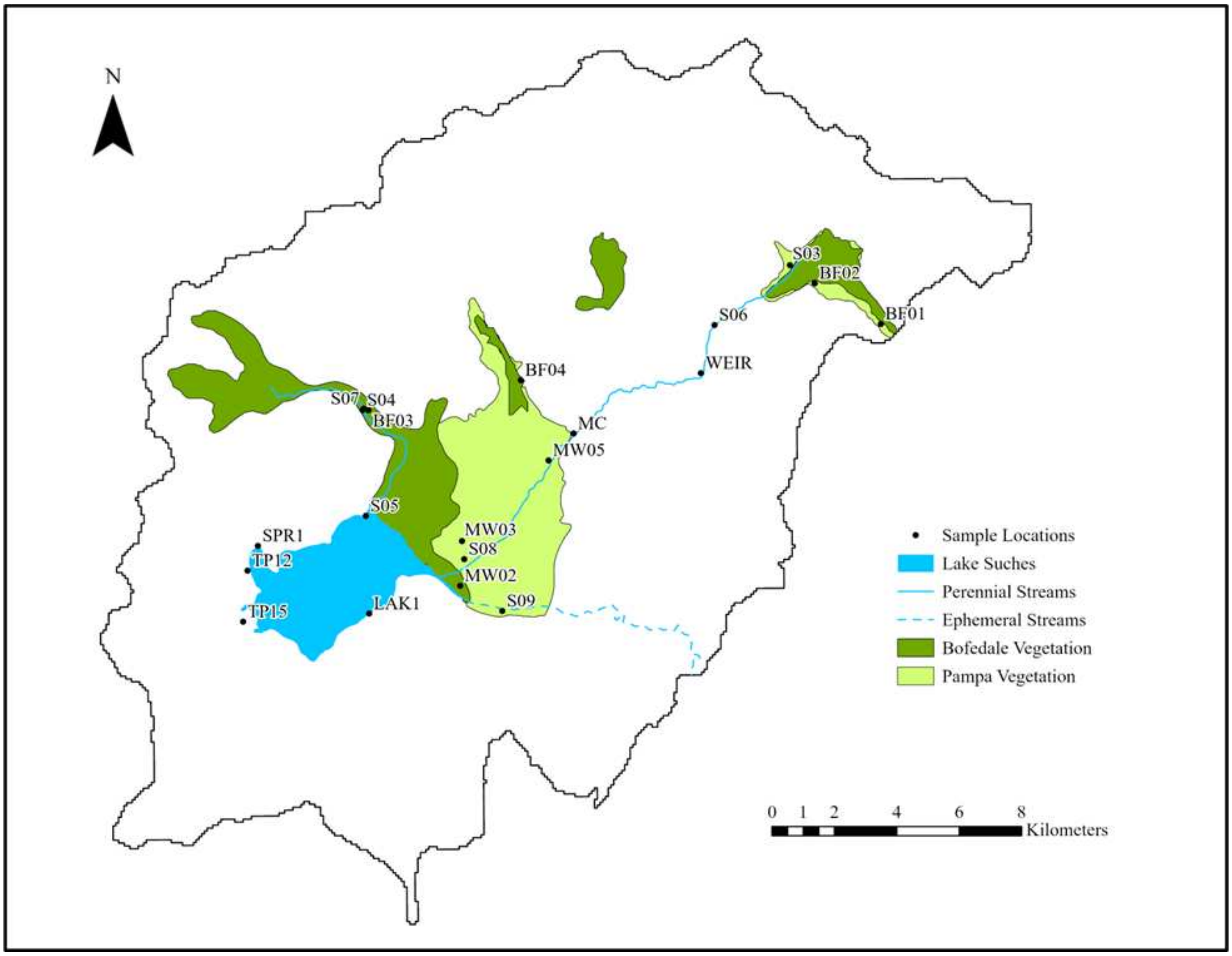

Figure 3.1: Location of groundwater and surface water stable isotope samples collected in the study area in January and June 2023

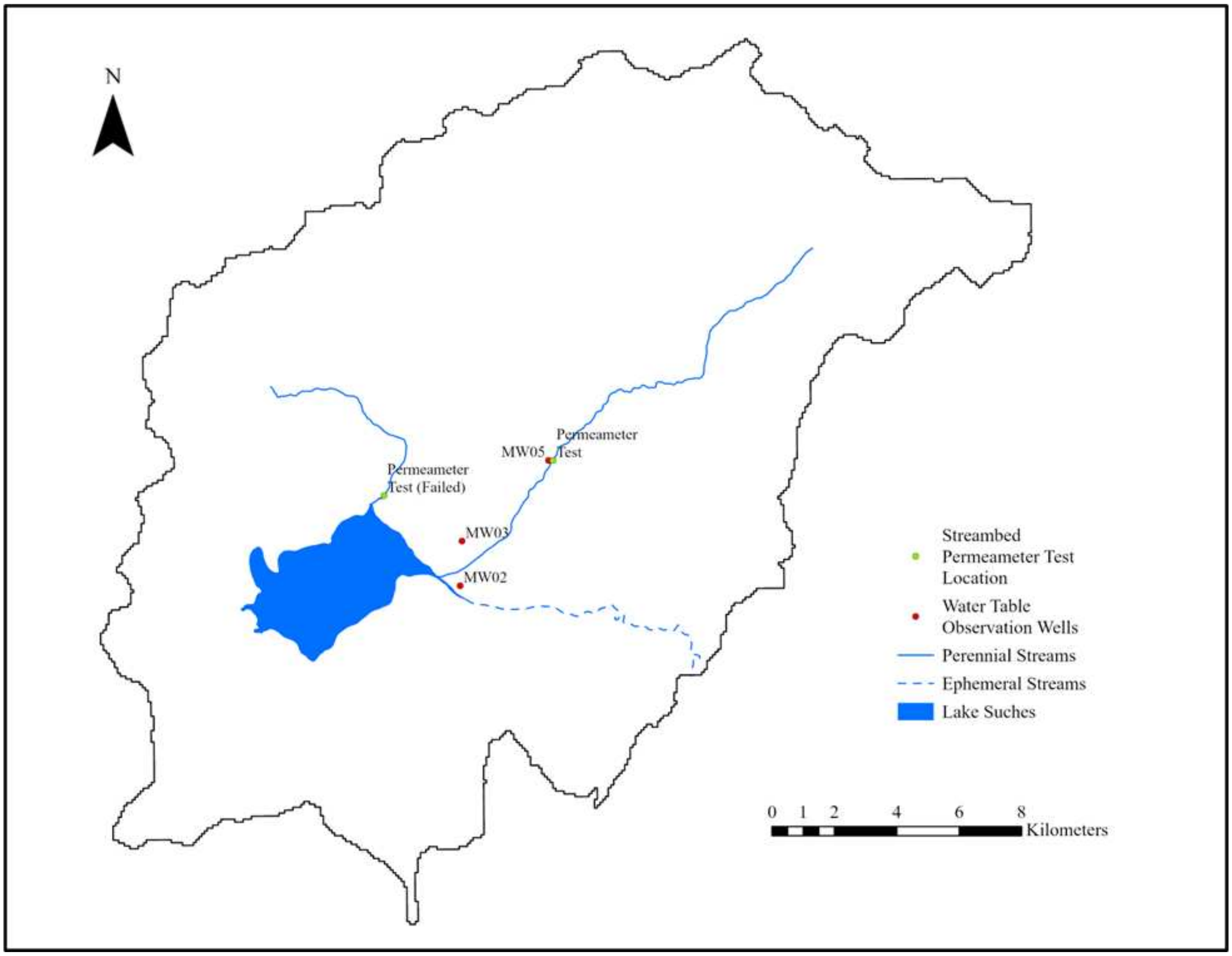

Figure 3.2: Location of June 2023 monitoring well installations and permeameter testing in the Huaytire Basin.

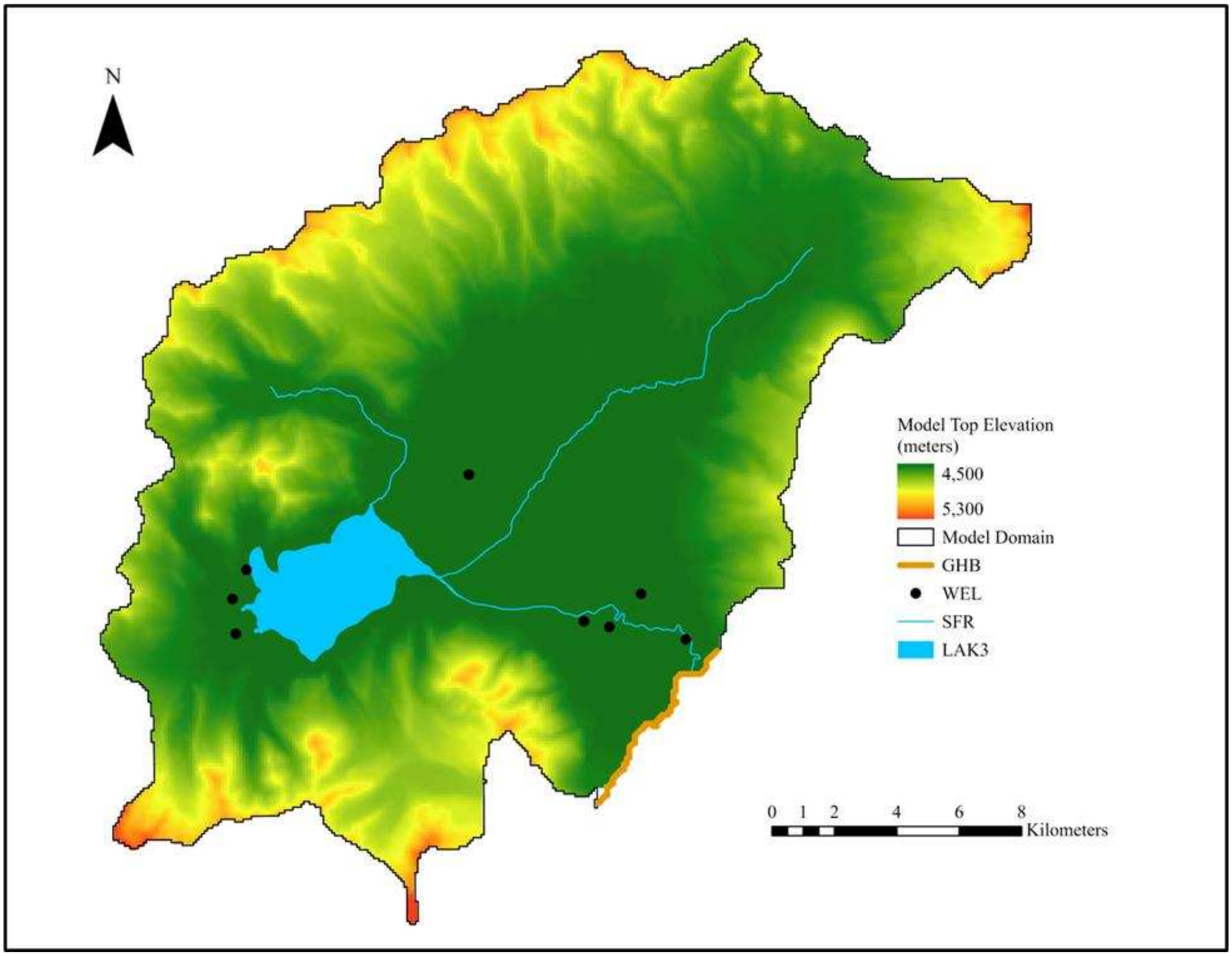

Figure 3.3: Layer 1 boundary conditions, active model domain, and model top elevation.

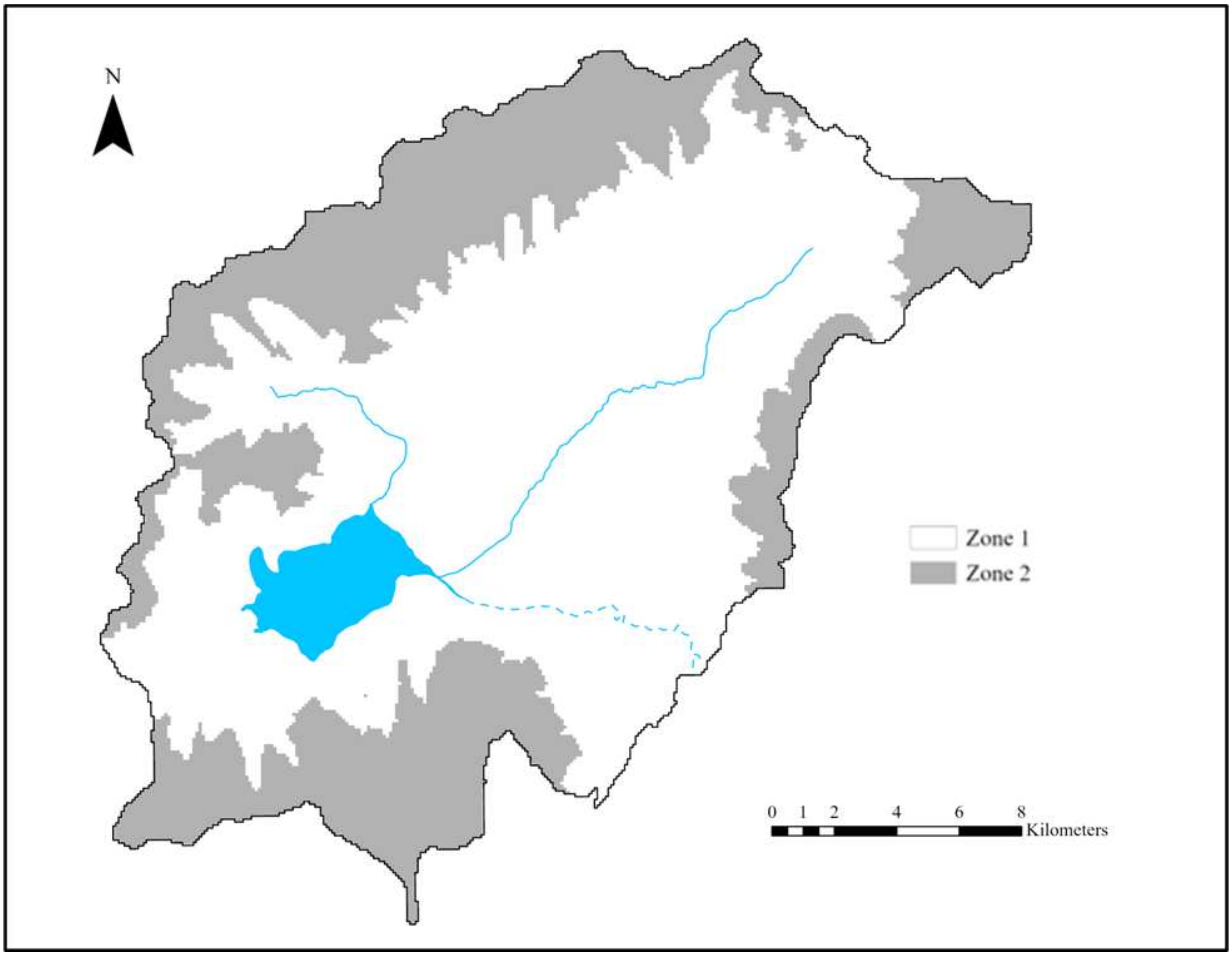

Figure 3.4: Recharge zones. Zone 1 covers the area below 4,700 meters amsl, and Zone 2 includes the area above 4,700 meters amsl.

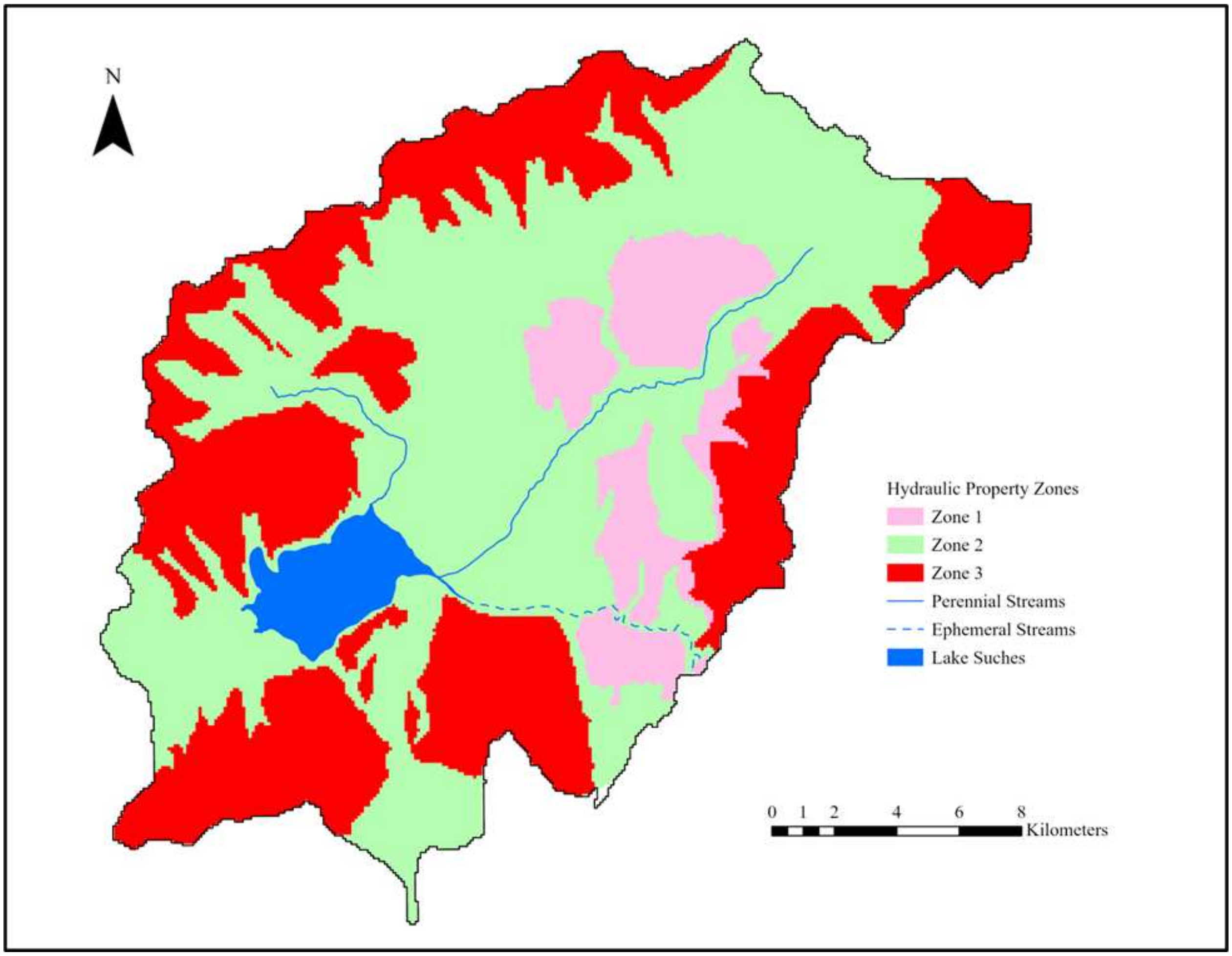

Figure 3.5: Layer 1 hydraulic property zones used to delineate hydraulic conductivity and storage properties.

CHAPTER 4: RESULTS

4.1 Water Stable Isotopes

All surface water and groundwater samples collected during the wet season (January 2023) and dry season (June 2023) sampling events were depleted relative to the approximate mean isotopic composition of worldwide precipitation of $\delta\ ^{18}O$ = -4‰ and $\delta\ ^{2}H$ = - 22‰ (Craig and Gordon, 1965). Wet season $\delta^{2}H$ ranged from the most depleted value of -115.2‰ in TP12 to the most enriched value of -70.6‰ in LAK1, and wet season $\delta^{18}O$ ranged from the most depleted value of -55.6‰ in TP12 to a most enriched value of -6.8‰ in LAK1. Dry season $\delta^{2}H$ ranged from the most depleted value of -120.33‰ in BF01 to the most enriched value of -57.38‰ in S9, and dry season $\delta^{18}O$ ranged from the most depleted value of -16.13‰ in BF01to a most enriched value of -2.83‰ in S9.

All samples from both sampling events plot along an evaporation line with a slope lower than that of the global meteoric water line (Figure 4.1). A linear regression was performed on each dataset yielding a slope of approximately 5.1 and a y intercept of -36.17‰ for the January sampling event and a slope of 4.8 and a y intercept of -40.5‰ for the June sampling event. Both regressions have a coefficient of determination (R^2) value of 0.99.

In general, surface water samples collected from higher elevation sites are more depleted than samples collected from lower elevation sites. Surface water and bofedal samples generally plot as somewhat more enriched than spring and pumping well samples, and bofedal samples generally plot as more depleted than surface water samples in both sampling events (Figure 4.1).

All January 2023 sample locations that were repeated in the June 2023 sampling event were more depleted in ^{18}O and ^{2}H during the June sampling event relative to the January sampling event. On average, samples collected during the June sampling event were 6.9‰ more depleted in deuterium (σ = 4.3‰) and 1.3‰ more depleted in ^{18}O (σ = 0.89‰) than samples collected during the January sampling event. Only locations that were sampled in both sampling events were considered in the above statistics.

4.2 Stream Gaging

The Rio Japapunco and Rio Huaytire have both previously been characterized as gaining streams in their upper reaches and as losing in lower reaches (Vining, 2011). The purpose of the June 2023 gaging event was to verify the flow regime of the Rio Japapunco and Rio Huaytire, to identify the approximate location where perennial streams transition from gaining to losing, and to generate streamflow information that can be used to constrain the numerical model.

Stream gaging was performed at 7 locations during the dry season (June 2023) site visit, including 5 locations on the Rio Japapunco and 2 locations on the Rio Huaytire (Figure 4.2). Four gaging locations were repeated during the wet season (February 2023) site visit, including three locations on the Rio Japapunco and one location on the Rio Huaytire (Figure 4.3). Measured discharge was higher in the wet season gaging event relative to the dry season gaging event for all repeated gaging locations.

Dry season discharge estimates on the Rio Huaytire range between a downstream value of 0.038 m^3/s at gaging location S05 and an upstream value of 0.15 m^3/s at gaging location S04, approximately two kilometers upstream. Location S04 was repeated during the wet season gaging event and discharge was estimated at 0.28 m^3/s.

Dry season discharge estimates on the Rio Japapunco range between 0.042 m^3/s at gaging location S08 and 0.25 m^3/s at gaging location S06, approximately 12-km upstream. Wet season discharge estimates range between 0.33 m^3/s at location WEIR and 0.49 m^3/s at location S08, approximately 11 kilometers downstream.

4.3 Permeameter Testing

Three permeameter tests were performed in the Rio Japapunco near the MW05 stream gaging location (Figure 3.2). Vertical hydraulic conductivity was calculated according to the type E variable head method described in Hvorslev (1951). Results ranged from 2.3 to 6.9 m/d, with a mean of 4.8 m/d.

A second permeameter test was attempted on the lower reach of Rio Huaytire near Lake Suches. This test failed due to a very low infiltration rate requiring the permeameter equipment to remain in situ overnight. Water in the permeameter froze and the data were discarded. It was inferred that fine grained material in the lower reaches of the Rio Huaytire has generally low vertical hydraulic conductivity and is possibly associated with former lakebed sediments.

4.4 Groundwater Modeling

The following section summarizes the model calibration results, steady state model results, and the transient model result for the Huaytire Basin numerical model.

4.4.1 Model Calibration Results

The Huaytire Basin numerical model was calibrated using measured water levels at piezometers and monitoring wells (hard targets) and less precise observations related to streamflow conditions and variable lake stage (soft targets). Calibration was performed using a base case recharge rate defined in Section 3.3. Higher and lower recharge scenarios were also considered due to the uncertainty associated with the recharge parameter. Lower values for the base case recharge rate were considered and ruled out during the calibration process and sensitivity analysis. Base case model calibration results are shown in Figure 4.4 and Table 4. The wors performing targets are generally located near pumping wells The MAE/Range was 8.6%, indicating an acceptable calibration with relatively low model error. In general, the worst performing targets were in the vicinity of TP-3A (C-19, TP-3), north of the Basin Outlet (C-123, C-50, C-48), and south of Lake Suches (C-84).

Table 4: Summarized calibration statistics for the base case recharge scenario model.

Residual Mean (m)	-7.05
Absolute Residual Mean (m)	15.90
Root Mean Squared Error (m^2)	20.10
Minimum Residual (m)	-60.10
Maximum Residual (m)	32.96
Sum of Squared Residuals (m^2)	1,620
Range of Observations (m)	185.75
Mean Absolute Error / Range	8.60%
Root Mean Squared Error / Range (m)	10.80%

4.4.1.1 Hydraulic Conductivity and Zonation

Final calibrated K values for each hydraulic parameter zone are within the range of estimates summarized in Table 2 and within the expected range of values for their respective geologic materials (Table 5). Initial estimates of hydraulic conductivity were assigned to parameter zones depicted in Figure 3.5 based on information previously summarized in Chapter 3. Initial parameter assignments were updated using the parameter estimation software PEST. Model performance was tracked by analyzing the MAE / Range calibration statistic as defined in chapter 3. In certain cases, underperforming regions of the model were assigned new hydraulic conductivity zones and updated with PEST parameter estimates to improve model performance. Soft target performance was checked after each model run to verify reasonable simulated values of streamflow and lake stage.

Table 5: Final calibrated hydraulic conductivity assignments and zone numbers.

	Zone 1	**Zone 2**	**Zone 3**	**Zone 4**	**Zone 5**	**Zone 6**
Geologic Unit	Capillune Fm.	Quaternary Material	Barroso Group	Capillune Fm.	Capillune Fm.	Capillune Fm.
Layer Number	1-3	1	1-4	4	3	4
Horizontal Hydraulic Conductivity	1.7 m/d	10 m/d	0.075 m/d	0.6 m/d	0.1 m/d	0.01 m/d
Vertical Hydraulic Conductivity	0.17 m/d	1 m/d	0.075 m/d	0.06 m/d	0.01 m/d	0.01 m/d
Specific Storage	0.0004 m^{-1}	n/a	0.000001 m^{-1}	0.0004 m^{-1}	0.0004 m^{-1}	0.0004 m^{-1}
Specific Yield	0.1	0.15	0.05	0.1	0.1	0.1

Six final hydraulic parameter zones were delineated in the model domain. Parameter Zone 1, Zone 2, and Zone 3 represent the Capillune Formation, Quaternary Materials, and the Barroso Group, respectively, as depicted in Figure 3.5. Parameter Zone 4 represents the Capillune Formation in Layer 4, which is simulated to have a lower hydraulic conductivity value than Zone 1. Lower conductivity Zone 5 and Zone 6 were created in the Capillune Formation of Layer 3 and Layer 4 because simulated heads in that region were underperforming.

Few head targets are available in the northwestern region of the model near the Rio Huaytire. For this reason, streamflow was used as a soft target and indicator of model performance. In general, areas of the model assigned parameter zone 2 (quaternary materials) in layer 1 are assumed to overlie parameter zone 1 (Capillune Formation) in model layers 2 and 3. Model runs husing initial parameter estimates produced low simulated heads in the northwest region of the model and did not generate streamflow in the Rio Huaytire, indicating that prescribed hydraulic conductivity in that area was too high. Areas initially mapped as parameter zone 1 (Capillune Formation) near the Rio Huaytire in model layers 2 and 3 were rezoned to lower conductivity parameter zone 3 (Barroso Group) to raise heads and induce streamflow. The region near the Rio Huaytire in layer 4 was also rezoned as parameter zone 3.

4.4.1.2 Storage Properties and Zonation

Like hydraulic conductivity, initial estimates for specific storage and specific yield were assigned to parameter zones as depicted in Figure 3.5 and partially based on information summarized in Table 2. Less information was available to inform the assignment of storage properties than there was to inform the assignment of hydraulic conductivity, and initial storage property estimates were generally assigned based on reasonable literature values for each parameter zone. Three storage zones are simulated in the Huaytire Basin, constituting parameter Zone 1, Zone 2, and Zone 3, as summarized in the preceding section. Areas in the northwest region of the model that were rezoned from hydraulic conductivity Zone 1 to Zone 3 were copied to the storage property zones. Initial estimates of the relevant storage properties were assigned and updated with PEST to achieve optimal values. Final calibrated storage properties are presented in Table 5.

4.4.1.3 Streamflow Routing Parameters

With the exception of the lowest segment of the Rio Huaytire, streamflow routing (SFR) parameters were mostly unchanged from initial estimates. In initial model runs, the Rio Huaytire lost all water to the adjacent aquifer on the Pampa Huaytire far from its expected terminus at or near Lake Suches shoreline. The lowest segment of the Rio Huaytire was prescribed a lower vertical hydraulic conductivity value of 0.04 m/d to reduce the amount of leakage between the stream and the adjacent aquifer on the Pampa Huaytire. Low conductivity streambed material in lower reaches of the Rio Huaytire was evidenced in the attempted permeameter test that indicated a low vertical hydraulic conductivity over possible lakebed sediments in near the mouth of the Rio Huaytire.

4.4.2 Steady State Model Results

The simulated groundwater head distribution generated by the predevelopment steady state model is generally consistent with the expected head distribution as presented in the conceptual model (Figure 4.5). In general, as inferred from data presented in CRL (2017), groundwater flows from high elevation areas around the rim of the basin towards low elevation areas near Lake Suches and the southeast basin outlet. This general flow pattern is reproduced in the predevelopment steady state simulation.

The Streamflow Routing package simulated realistic flows for all three perennial streams in the Huaytire Basin (Figure 4.6). The Rio Japapunco is simulated as a gaining stream over most of its course before transitioning to a losing stream on the Pampa Huaytire. The simulated Rio Huaytire is also generally gaining in upper reaches and transitions to losing in lower reaches. The Rio Callazas is generally gaining over its entire course in the predevelopment scenario.

The maximum streamflow simulated on the Rio Japapunco is 0.21 m^3/s, the maximum streamflow simulated on the Rio Huaytire is 0.0086 m^3/s, and the maximum streamflow simulated on the Rio Callazas is 0.25 m^3/s. Simulated flow along Rio Huaytire is significantly lower than the measured streamflows during 2023-24, although general patterns of flow (i.e., transition to losing conditions on Pampa Huaytire) are consistent with observations. Simulated streamflow on the Rio Japapunco is of the same order of magnitude as the maximum observed streamflow measured during the June 2023 and February 2024 gaging events. The Rio Callazas is dry under modern conditions but may have flowed under a historic hydrologic regime.

Simulated predevelopment Lake Suches stage in the base case recharge scenario is 4,450.3 meters – approximately 4 meters below the maximum lake stage as inferred from topography. Modern lake stage is not monitored but is known to fluctuate seasonally and interannually making a direct comparison between simulated and measured values impossible. Because the predevelopment steady state model simulates average annual conditions in the Huaytire Basin, and stage in Lake Suches is known to change throughout the year, the steady state lake stage value of 4,450.3 meters is a realistic result.

The simulated steady-state aquifer water budget is illustrated in Figure 4.7. The largest flow of water entering the aquifer is derived from diffuse areal recharge (~135,000 m^3/d), followed by stream leakage (~21,000 m^3/d). The largest outflows are evapotranspiration (~64,000 m^3/d), followed by discharge to gaining streams (~42,000 m^3/d), groundwater discharge to Lake Suches (~34,000 m^3/d), and subsurface outflow across the general head boundary (~10,000 m^3/d).

When using the Lake Package, a separate water budget is calculated for simulated lakes (Figure 4.7). The largest inflow into Lake Suches is via groundwater discharge (~34,000 m^3/d), followed by precipitation (~16,000 m^3/d) and surface water inflow (~600 m^3/d). Evaporation (~ 55,000 m^3/d) is the only outflow from Lake Suches in the predevelopment simulation.

4.4.3 Transient Model Results

Model results were saved every 100 days in the transient simulation to facilitate the effective visualization of results. Components of the aquifer and lake water budgets were plotted as transient hydrographs to illustrate simulated hydrologic change in the Huaytire Basin (Figure 4.8; Figure 4.9). Aquifer and lake water budgets for higher and lower recharge scenarios were also plotted as transient hydrographs to illustrate the reaction of key model results to changes in prescribed recharge. Simulated lake stage and surface water outflow from the Huaytire Basin for each recharge scenario were also plotted as a function of time (Figures 4.10 and 4.11). Final simulated streamflow transects for the Rio Huaytire, Rio Callaza, and Rio Japapunco were plotted with predevelopment simulated streamflow transects to illustrate changes in streamflow over the duration of the model simulation period (Figure 4.6).

The transient aquifer water budget hydrographs illustrate how water budget components change as stresses, namely groundwater and surface water pumping, are introduced to the system. All head-dependent groundwater outflows in all recharge scenarios are reduced over the course of the simulation to accommodate groundwater pumping (Table 6). Steady state is not achieved in any of the simulated recharge scenarios, and some water leaving the aquifer is derived from storage at the end of all three simulations. In the base case scenario, outflow to streams is reduced by 49.7%, outflow across the GHB is reduced by 50.5%, outflow to Lake Suches is reduced by 9.5%, and outflow to evapotranspiration is reduced by 18.2%. GHB inflow did not exist in the predevelopment steady state model but does occur at the end of the transient simulation. Water is removed from storage at the end of the base case recharge scenario simulation at a rate of approximately 8,400 m^3/d, which corresponds to approximately 15% of the total groundwater pumping rate.

Table 6: Simulated change in aquifer water budget components at steady state and at the end of the transient simulation. Results are provided for the base case model.

	Initial (m^3/d)	Final (m^3/d)	Percent Change
Inflow			
Recharge	134,800	135,600	0.6
Stream Groundwater Inflow	20,560	20,950	1.9
Lake Groundwater Inflow	0	1,560	n/a
General Head Boundary Inflow	0	98	n/a
Outflow			
Pumping	0	57,360	n/a
Evapotranspiration	64,100	52,440	-18.2
General Head Boundary Outflow	9,514	4,707	-50.5
Stream Groundwater Outflow	42,500	21,370	-49.7
Lake Groundwater Outflow	33,880	30,670	-9.5

Similar reductions in each aquifer water budget component are observed in the high recharge and low recharge scenarios (Figure 4.8; Figure 4.9). The low recharge scenario produces some dry WEL cells which are deactivated by MODFLOW and reactivated when heads in adjacent aquifer cells have recovered. In the transient hydrograph, this phenomenon manifests as pumping outflow oscillating between higher and lower values, as pumping wells are deactivated and reactivated in subsequent timesteps. The oscillation between active and inactive pumping wells impacts the rate of storage depletion in a similar way, with early timestep change in pumping locally removing water from or contributing water to storage.

The transient lake water budget hydrographs also illustrate changing water budget components in response to hydrologic stress (Figure 4.10; Table 7). Precipitation and evaporation rates are a function of lake area and therefore change as a function of lake stage. Direct precipitation inflow to Lake Suches is reduced by 43.8%, surface water inflow is reduced by 23.2%, and groundwater seepage inflow is reduced by 9.4% over the duration of the transient simulation period.

Evaporation outflow is reduced by 43.8%. Groundwater seepage outflow did not occur in the steady state model but does occur at the end of the transient simulation.

Table 7: Simulated change in lake water budget components at steady state and at the end of the transient simulation. Results are provided for the base case model.

	Initial (m^3/d)	Final (m^3/d)	Percent Change
Inflow			
Precipitation	16,390	9,206	-43.8
Augmentation	0	18,200	n/a
Groundwater Inflow	33,860	30,680	-9.4
Surface Water Inflow	556	427	-23.2
Outflow			
Pumping	0	25,920	n/a
Groundwater Outflow	0	1,560	n/a
Evaporation	55,340	31,080	-43.8

Surface water outflow through the Rio Callazas across the basin outlet falls to zero in all three recharge scenarios (Figure 4.11a). Initial surface water outflow in the base case scenario is approximately 21,450 m^3/d, initial surface water outflow in the high recharge scenario is approximately 39,100 m^3/d, and initial surface water outflow in the low recharge scenario is approximately 14,280 m^3/d. Simulated surface water outflow ceases in 1995, 2013, and 1985, in the base case, high-recharge, and low-recharge scenarios, respectively. Streamflow in the Rio Callazas and the Rio Japapunco is generally lower in all reaches at the end of the simulation compared with simulated streamflow at the start of the simulation.

Simulated lake stage in the base case scenario falls from approximately 4,450 meters to approximately 4,443 meters over the duration of the transient simulation (Figure 4.11). Simulated lake stage in the high recharge scenario falls by only 1.3 m during the transient simulation. In the low-recharge scenario, simulated lake stage falls from approximately 4,445 meters to 4,438.6 meters before recovering to 4,441.8 meters at the end of the simulation.

Simulated layer 4 heads at the end of the transient simulation are depicted in Figure 4.12, while Figures 4.13 and 4.14 illustrate the simulated drawdown in Layers 4 and 1, respectively. Simulated drawdown of up to 10 meters is evident around each group of pumping wells in layer 4.

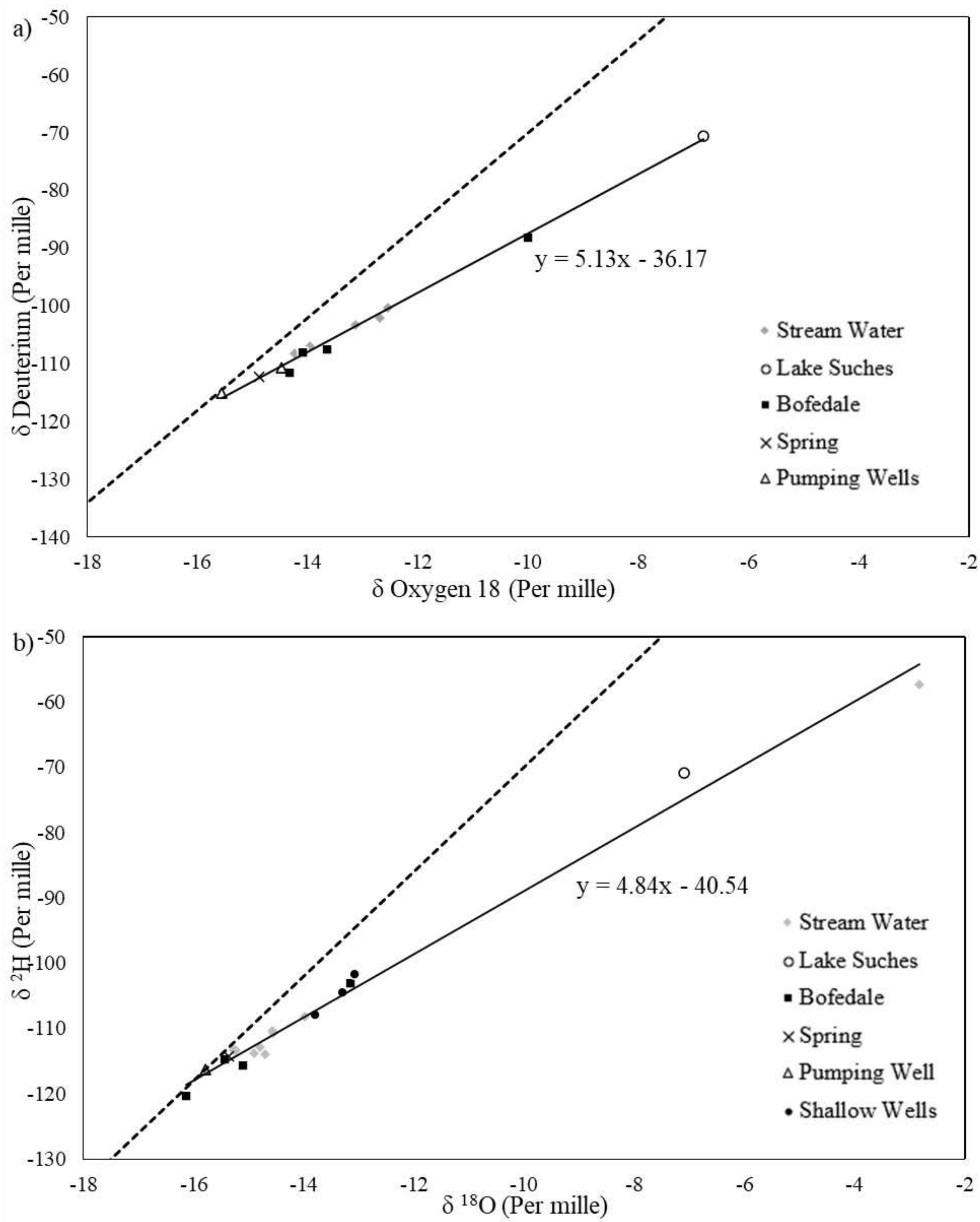

Figure 4.1: Water stable isotope sample results from the (a) January 2023 and (b) June 2023 sampling events plotted in δ^2H - $\delta^{18}O$ space. The GMWL is plotted as a dashed line, and the LEL is plotted as a solid line.

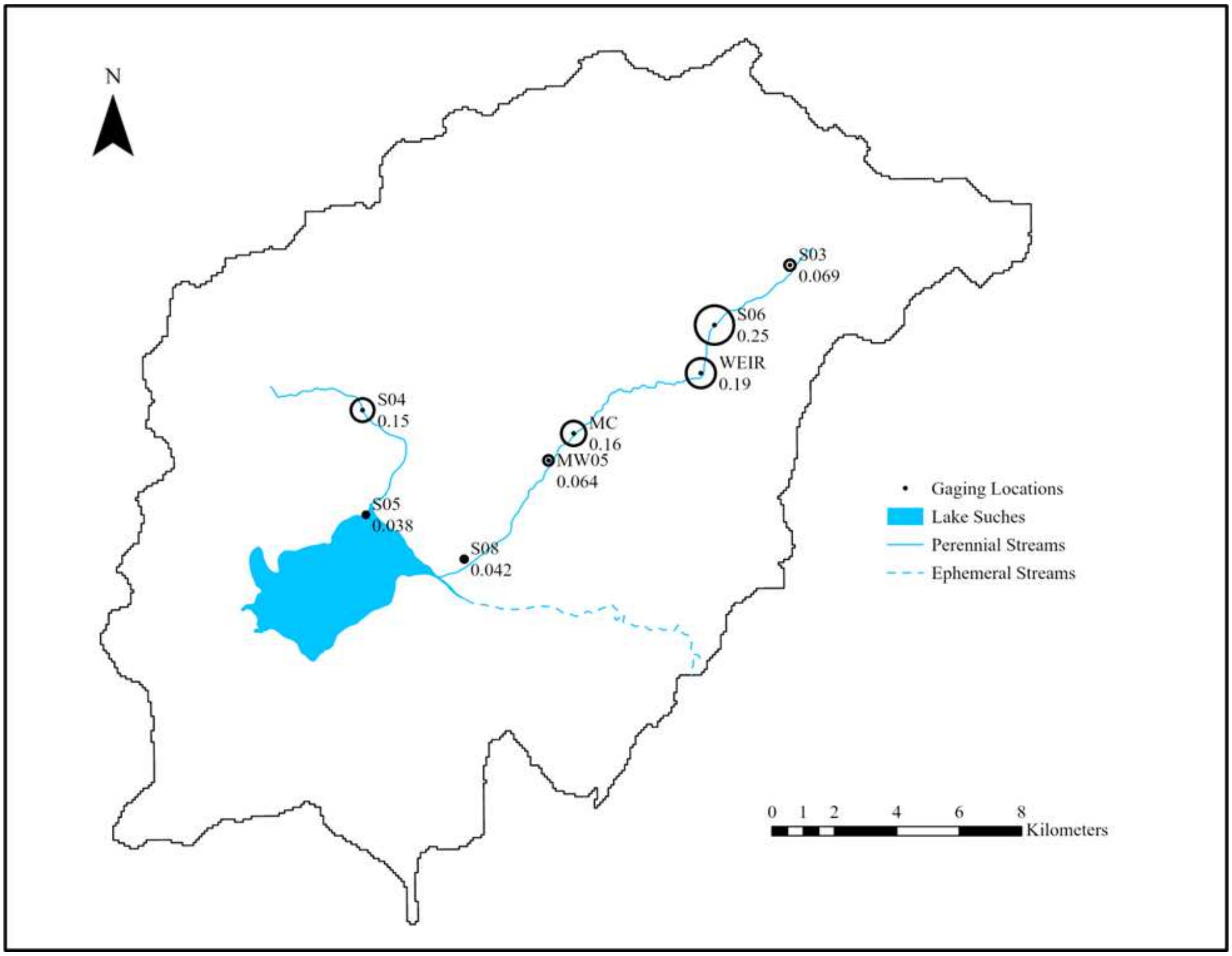

Figure 4.2: Gaging locations and measured streamflow values (m^3/sec), June 2023 gaging event. Circle size indicates the magnitude of streamflow observed at each location.

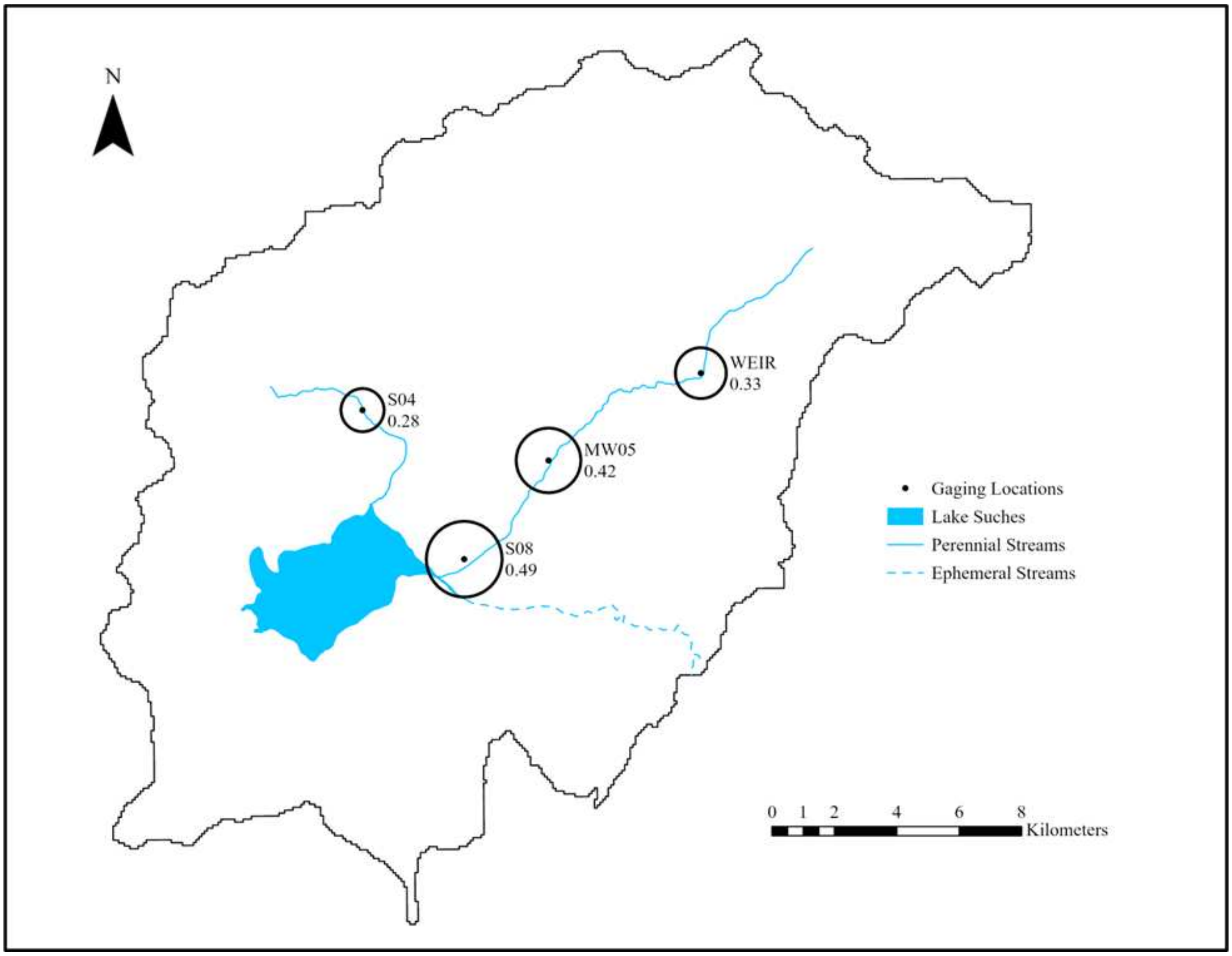

Figure 4.3: Gaging locations and measured streamflow values (m^3/sec), February 2024 gaging event. Circle size indicates the magnitude of streamflow observed at each location.

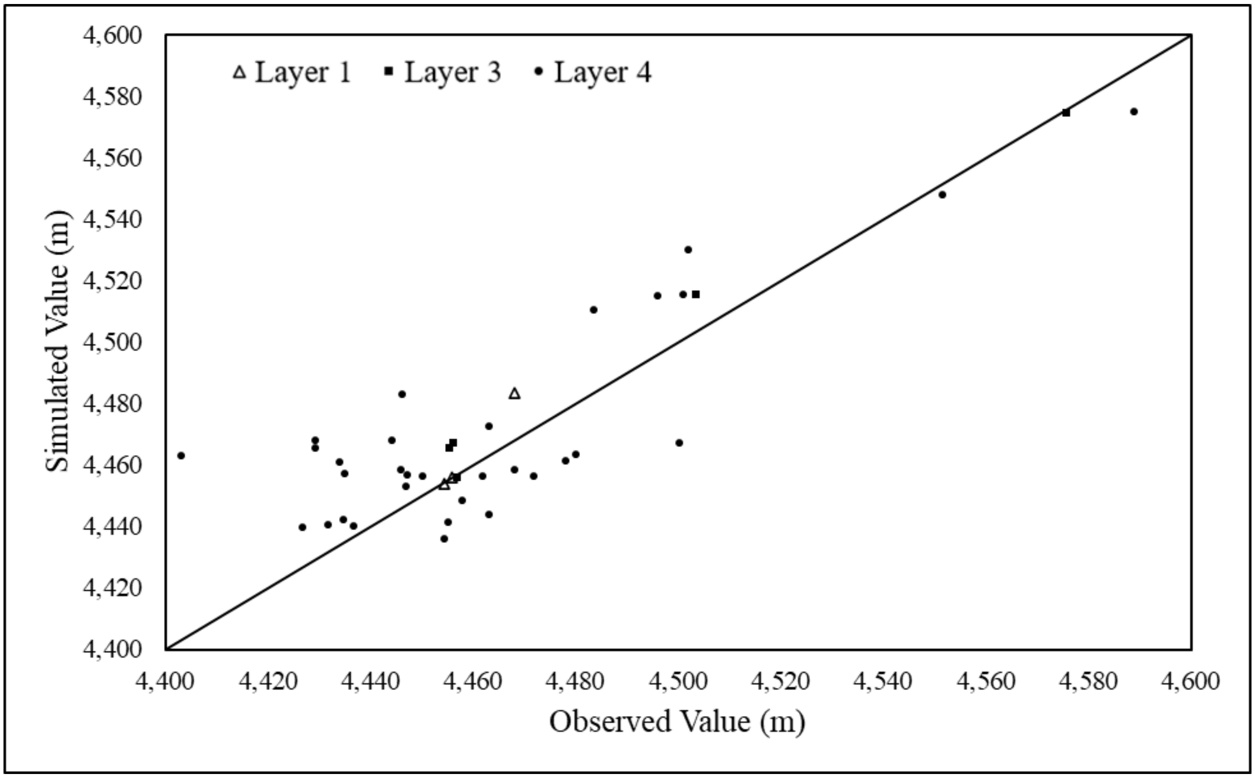

Figure 4.4: Simulated vs observed hydraulic head values in the base case recharge scenario (base case model used for calibration).

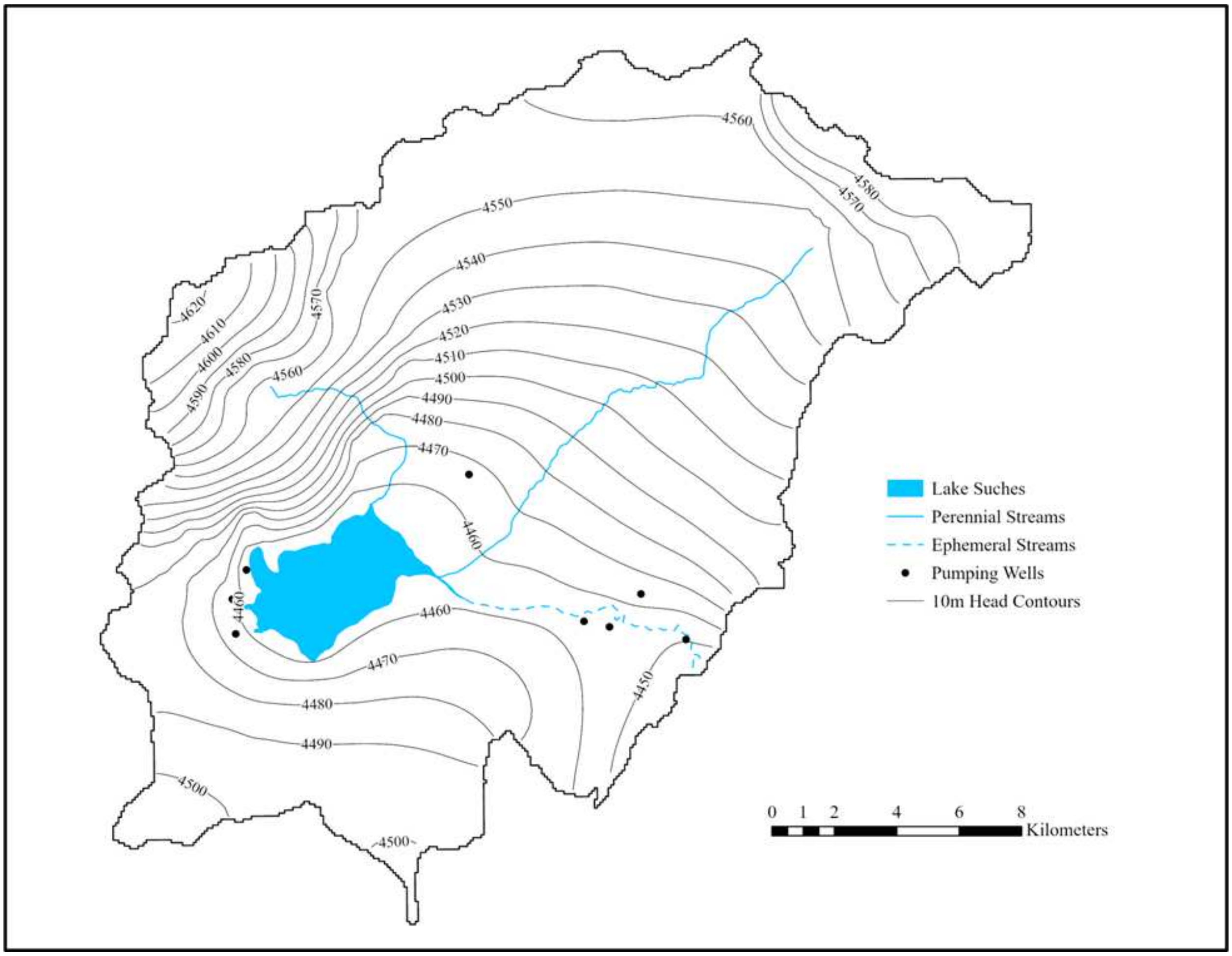

Figure 4.5: Simulated steady state predevelopment hydraulic head values in layer 4, base case scenario.

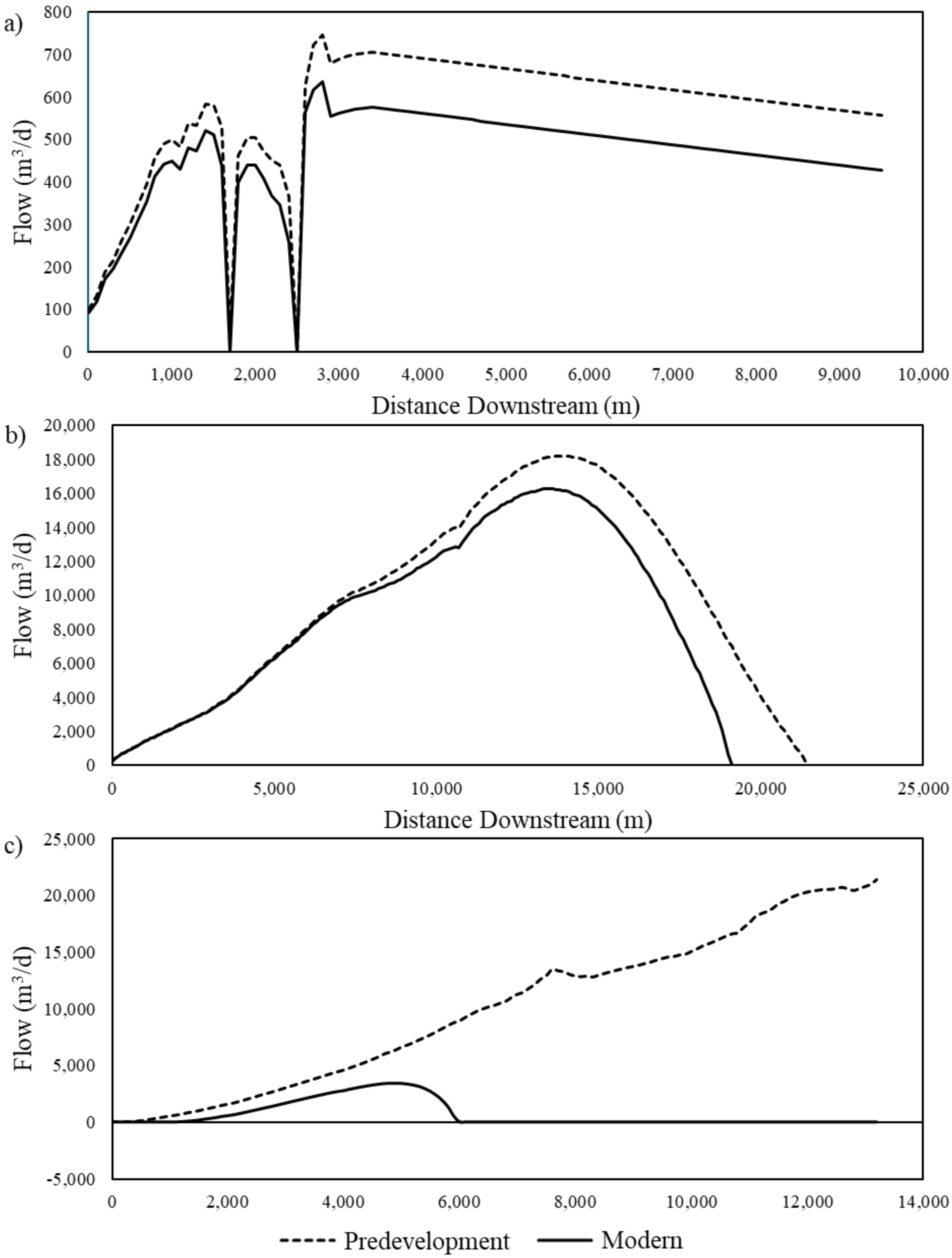

Figure 4.6: Simulated streamflow vs downstream distance in (a) Rio Huaytire, (b) Rio Japapunco, and (c) Rio Callazas. Results are provided for the base case model.

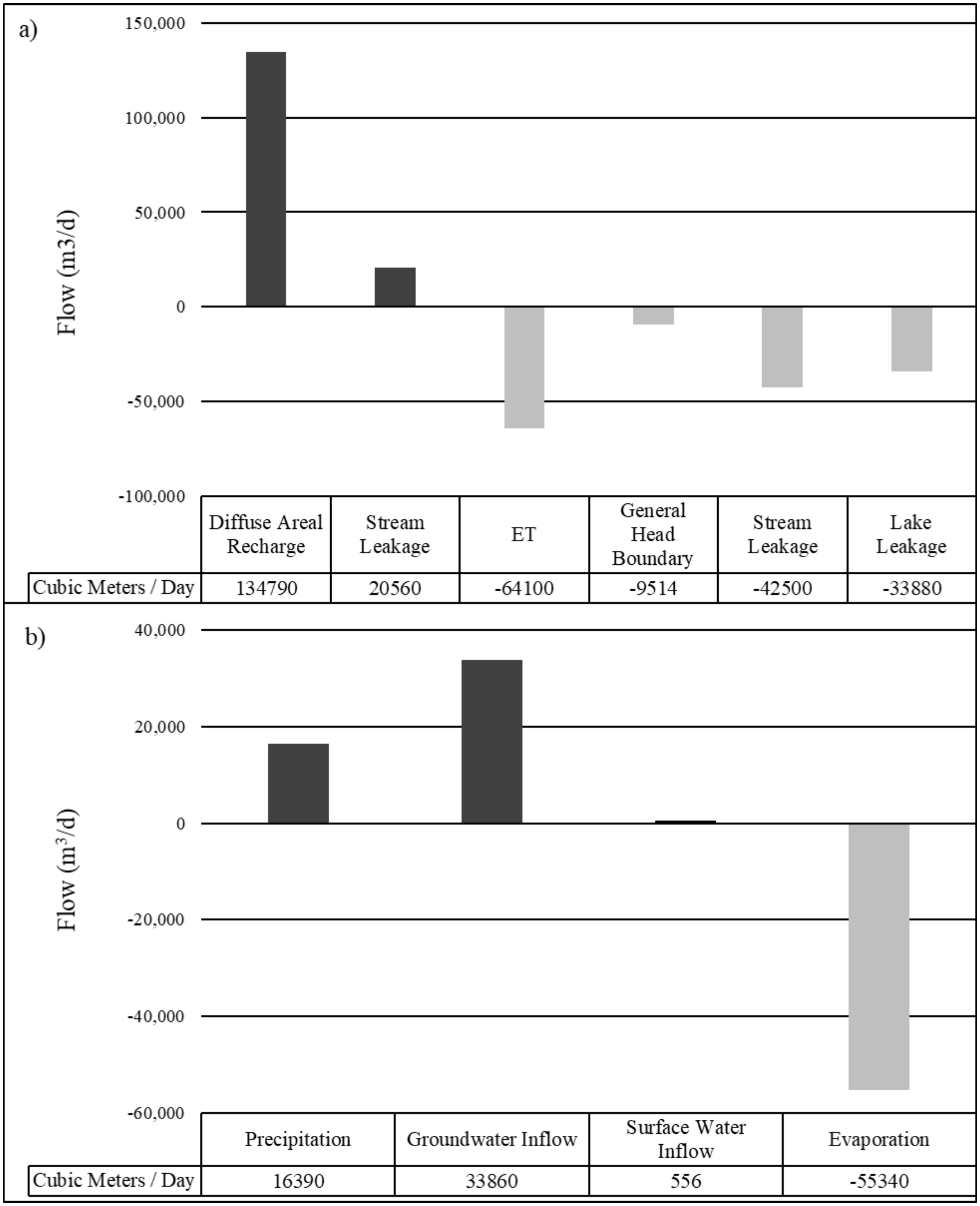

Figure 4.7: Simulated steady-state water budget for the aquifer system (a) and Lake Suches (b). Results are provided for the base case model.

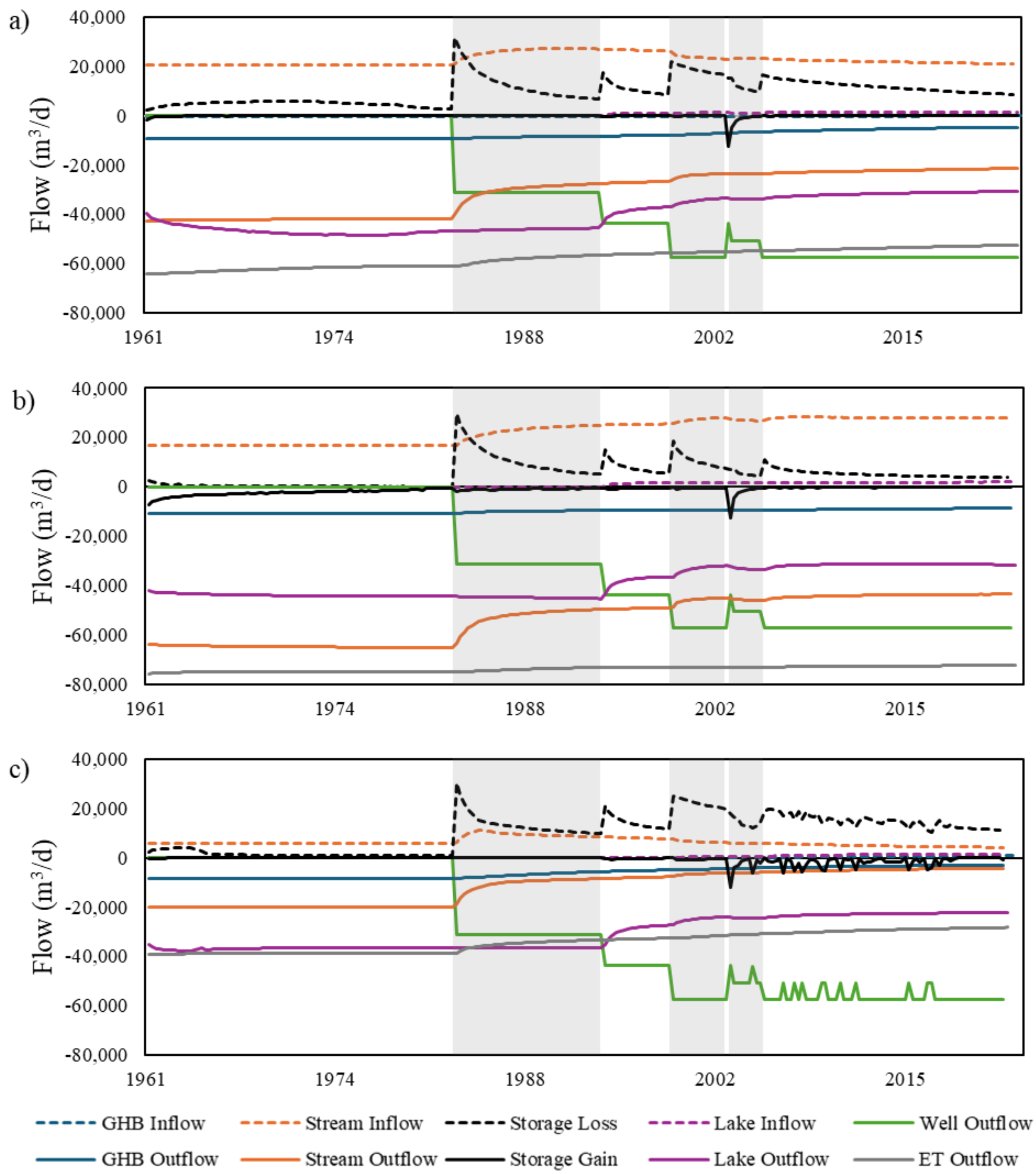

Figure 4.8: Simulated aquifer water budget for (a) base case, (b) high recharge, and (c) low recharge scenarios. Recharge derived from precipitation omitted for clarity; total recharge (constant through time) is 134,788, 180,418, and 94,907 m^3/day, respectively, in the base-case, high-recharge, and low-recharge scenarios. Starting in year 2004, well pumping in the low-recharge scenario fluctuates due to low simulated heads near well TP-5, TP-8, TP-9A, and TP-14. Gray shaded areas indicate stress periods.

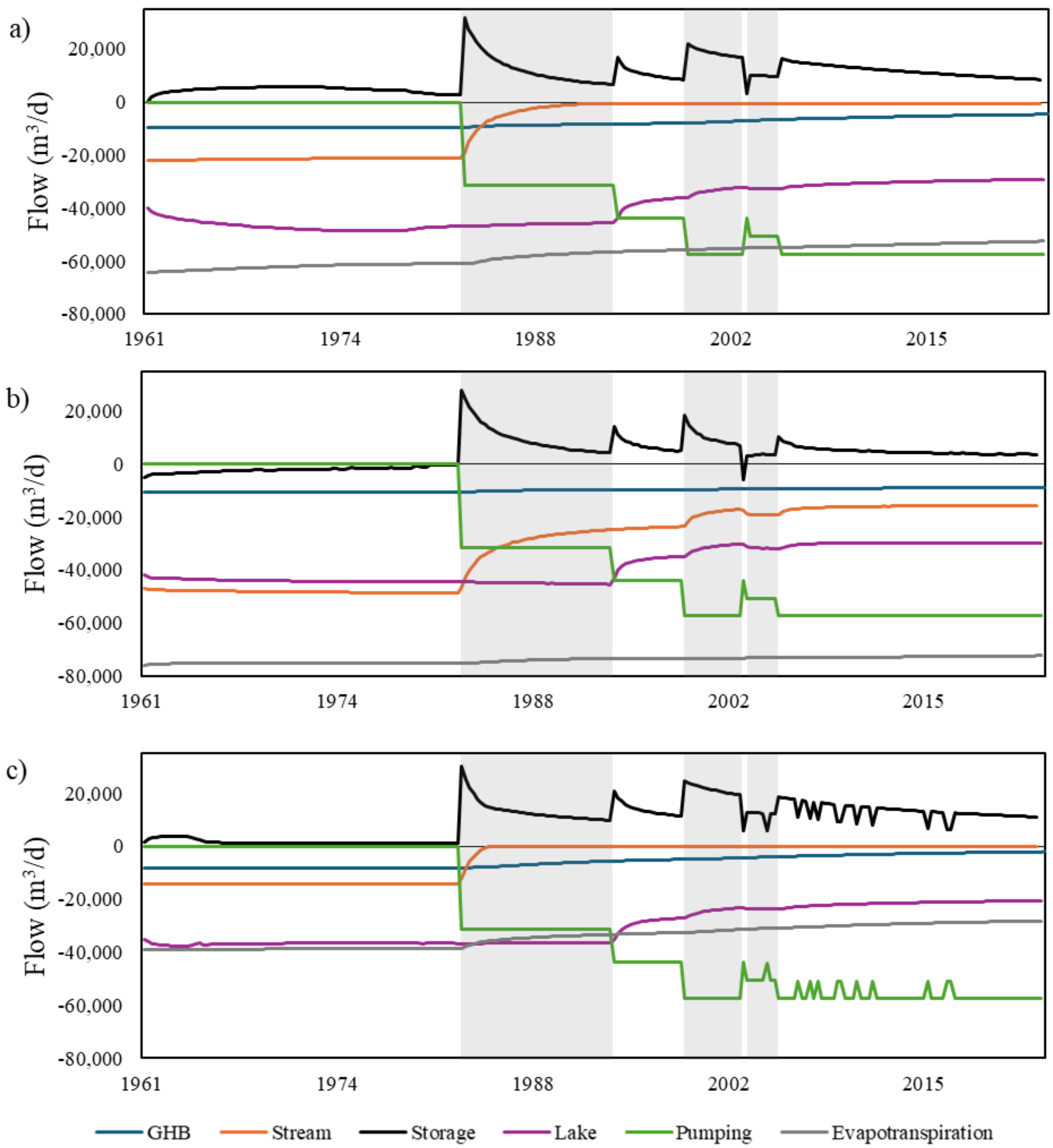

Figure 4.9: Simulated net water budget for the Huaytire Basin for a (a) base case, (b) high recharge, and (c) low recharge scenarios. Recharge derived from precipitation was omitted for clarity.

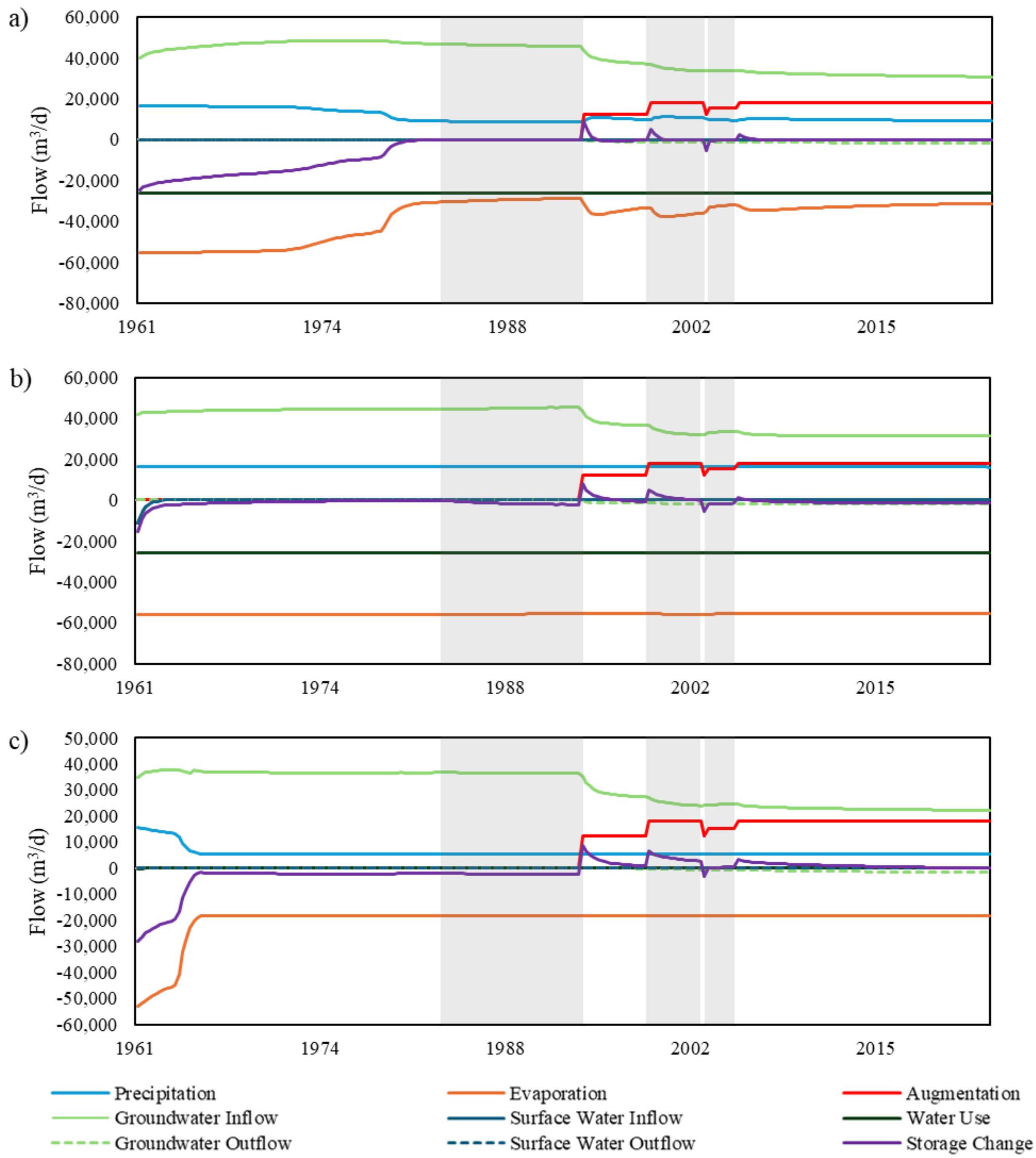

Figure 4.10: Simulated water budget for Lake Suches for (a) base case, (b) high recharge, and (c) low recharge scenarios.

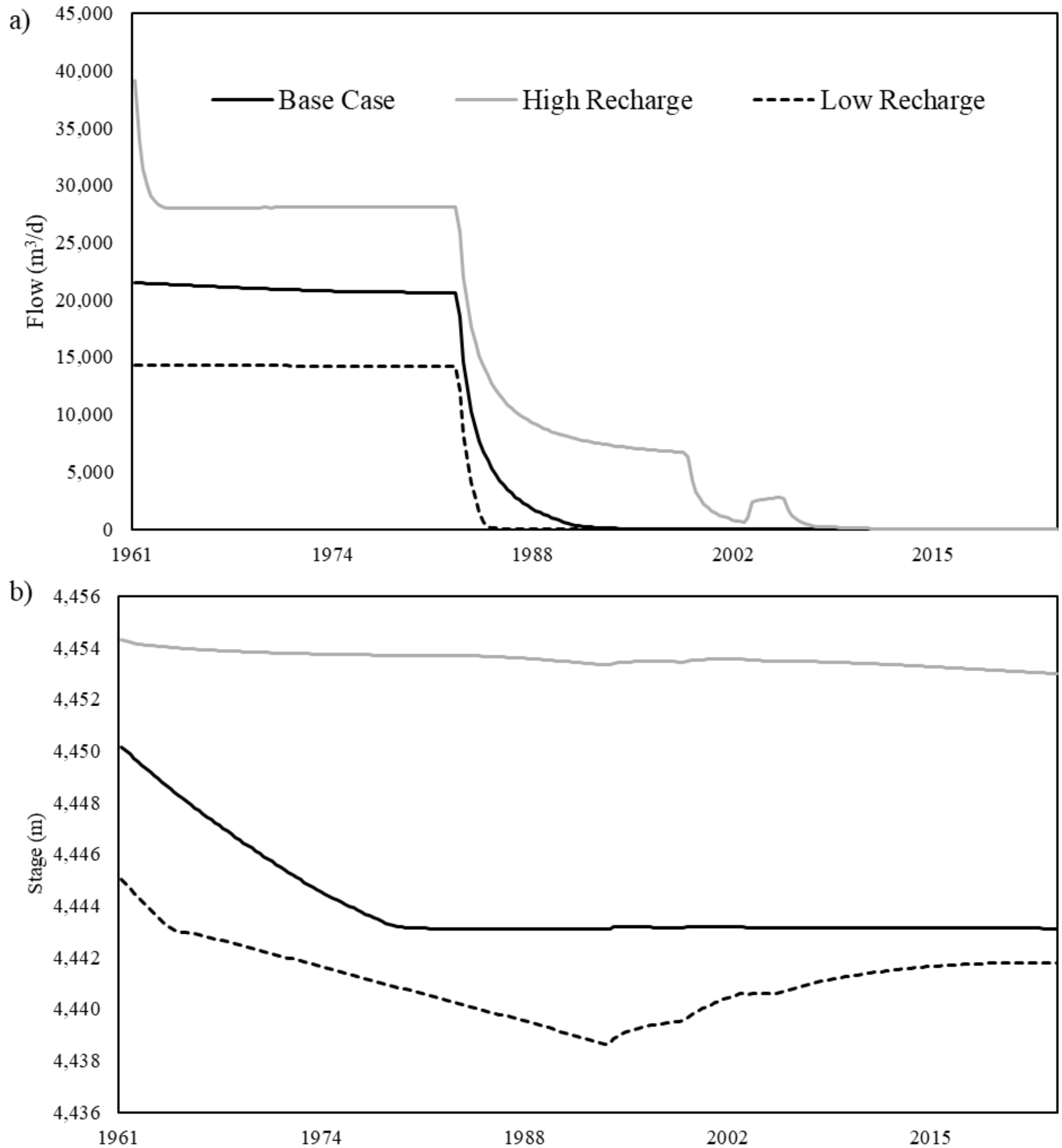

Figure 4.11: (a) Simulated surface water outflow in the Rio Callazas and (b) simulated lake stage in the base case, high recharge, and low recharge scenarios.

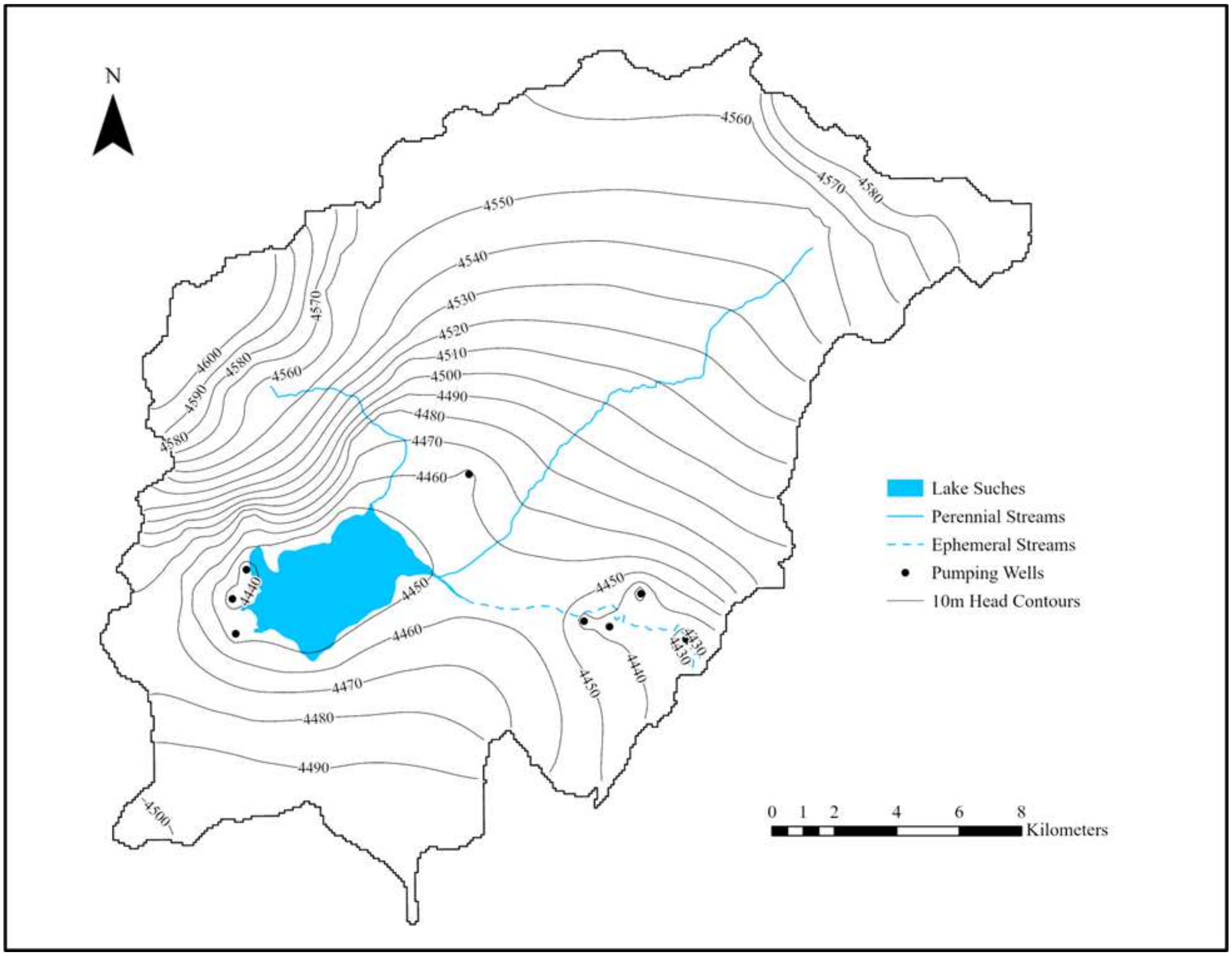

Figure 4.12: Simulated hydraulic head values in layer 4 at the end of the transient simulation (year 2024), base case model.

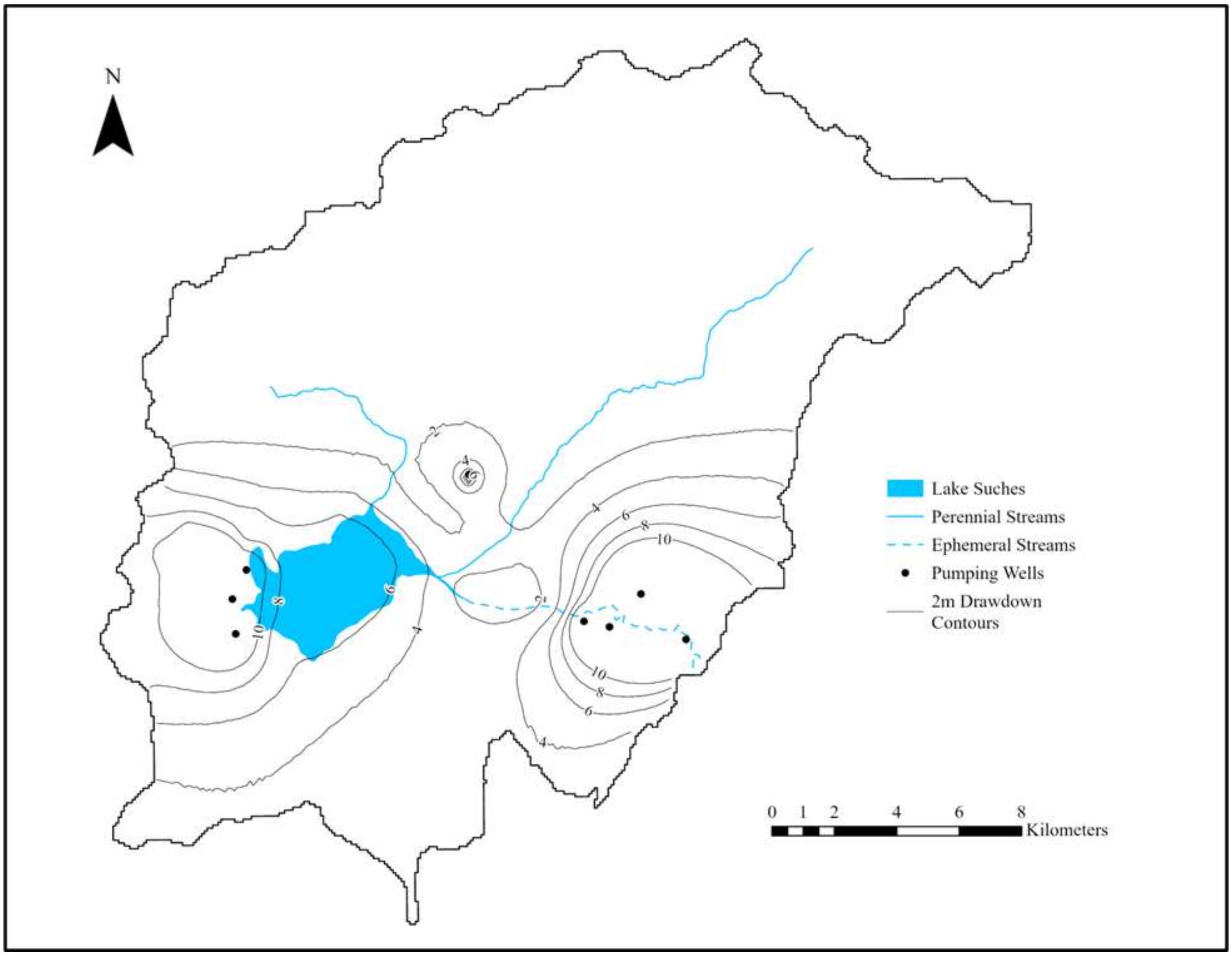

Figure 4.13: Simulated drawdown in Layer 4 at the end of the transient simulation.

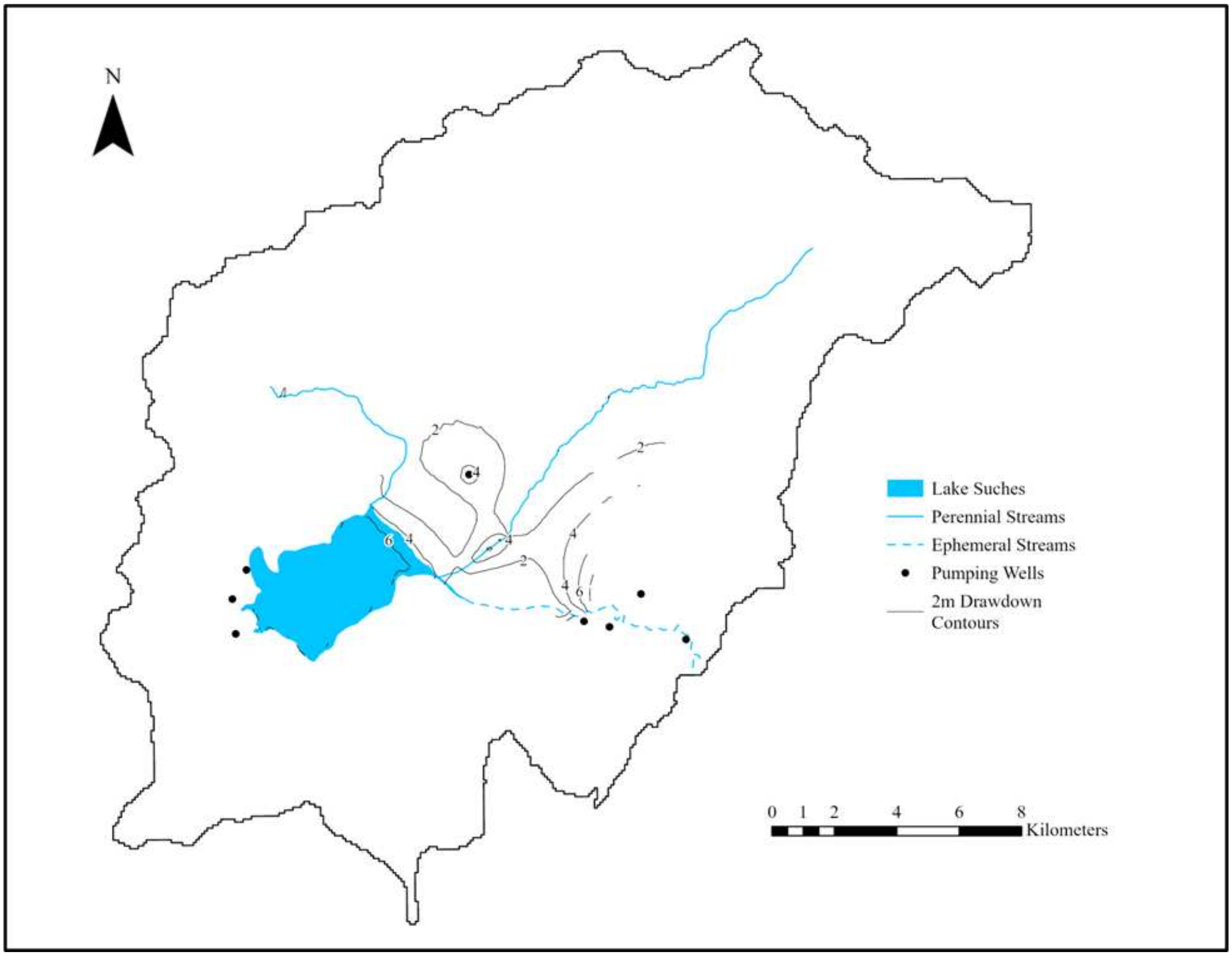

Figure 4.14: Simulated drawdown in Layer 1 at the end of the transient simulation.

CHAPTER 5: DISCUSSION

Over the past several decades, the Huaytire Basin has experienced hydrologic change marked by declining groundwater levels, reduced streamflow, and less vigorous wetland vegetation. These trends could be driven by multiple factors, including climate change, groundwater and surface water withdrawals from the basin, and grazing practices. In this study, an evaluation of potential climate effects was performed by analyzing historical temperature, precipitation, and evaporation data from the Tocco, Suches, and Pasto Grande weather stations. The influence of water withdrawal (groundwater pumping and Lake Suches diversions) was investigated in detail using numerical modeling. Grazing practices were not evaluated as part of this study.

5.1 Hydrologic impact of climate change in the Huaytire Basin

Available climate data for the Huaytire Basin as summarized in Chapter 2 includes temperature data collected at the Pasto Grande weather station (Elevation ~ 4,560 m amsl), evaporation data collected at the Tocco weather station (Elevation ~ 4,575 m amsl), and precipitation data collected at the Lake Suches weather station (Elevation ~ 4,555 m amsl) (Figures 2.1 – 2.3). While no significant trend is evident in precipitation, evaporation, or maximum monthly temperature values, minimum monthly temperature shows an increasing trend with a coefficient of correlation value of 0.21.

Higher temperatures could change the water budget in the Huaytire Basin by increasing the rate of evaporation from moist soil, increasing the rate of transpiration from plants, and increasing the rate of evaporation from surface water bodies, especially Lake Suches. The observed increase in mean minimum temperature may impact the water budget in the Huaytire Basin and contribute to observed hydrologic change in the basin. However, the magnitude of minimum monthly temperature change is small, and no trend was observed in maximum monthly temperature, evaporation, or precipitation, so the impact of climate change on the hydrology of the Huaytire Basin is expected to be minimal.

5.2 Hydrologic impact of groundwater and surface water pumping in the Huaytire Basin

As with any aquifer system, long-term groundwater pumping in Huaytire Basin also introduced fundamental changes to the water budget. Pumping must be offset by a reduction in aquifer storage, an increase in recharge (aquifer inflows), and/or a decrease in discharge (aquifer outflows) (Theis, 1940). When pumping begins, water is mostly derived from aquifer storage and drawdown occurs near the pumping well. Changes to the water budget begin when drawdown reaches a head-dependent boundary or source/sink flux. In certain cases with sustained pumping over a long period, a new steady state can be achieved when heads in the aquifer become stable and the pumping outflow term is balanced by increases in recharge and/or decreases in discharge. The sum of increased recharge and decreased discharge is often referred to as capture (Bredehoft, 2001).

In the Huaytire Basin, predevelopment groundwater outflows available for capture include outflow to Lake Suches, outflow to streams, outflow to evapotranspiration, and subsurface outflow across the basin outlet. The dynamics of these changes, including the magnitude and timing of capture from each outflow term, are difficult to predict in complex systems with a variety of boundary conditions and heterogeneous aquifer material. The numerical modeling results presented in Chapter 4 are useful for understanding the dynamic response of the Huaytire Basin aquifer and related hydrologic systems to groundwater pumping in the study area.

Lower simulated heads in the Huaytire Basin introduce changes to the surface water dynamics of simulated streams in the study area. Drawdown creates a lower hydraulic gradient between streams and the adjacent aquifer in gaining reaches and a higher hydraulic gradient between streams and the adjacent aquifer in losing reaches. Some reaches convert from gaining to losing over the duration of the simulation, and some reaches dry up completely (Figure 4.6). This results in streamflow depletion occurring in all three perennial streams included in the simulation, as inflow to streams is decreased and outflow from streams is increased. The Rio Callazas is the most severely impacted stream simulated in the model, and most of the simulated predevelopment discharge from the aquifer to the Rio Callaza is captured by pumping. This is largely because the Rio Callazas flows over a region of the model impacted by a cluster of four pumping wells producing a wide area of 10 meters or more of drawdown (Figures 4.13 and 4.14). The Rio Huaytire and Rio Japapunco are similarly impacted by drawdown on the Pampa Huaytire, though to a lesser degree due to their more distal location relative to pumping wells.

Outflow from Lake Suches is also reduced due to a decline in lake stage and related reduction in lake area and evaporation. Stage is dependent on the lake water budget which is impacted by groundwater and surface water development in two ways; water is removed from the lake via surface water diversion, and groundwater inflow is reduced because pumping-induced drawdown in the aquifer decreases the hydraulic gradient near the lake, thereby reducing groundwater discharge into the lake. Reduced groundwater discharge to Lake Suches due to drawdown is one example of capture. Evaporation outflow and precipitation inflow are also stage and area dependent and operate as a negative feedback on stage change. As stage falls due to changes in the lake water budget, the net evaporation rate (Evap. – Precip.) also falls as the area of the lake decreases. The reduction in net evaporation from Lake Suches as a response to pumping is another example of capture in the Huaytire Basin.

Phreatophytic evapotranspiration is another head dependent outflow available for capture in the Huaytire Basin. As drawdown occurs, the rate of evapotranspiration is reduced as hydraulic head falls between the land surface and the prescribed extinction depth. The difference between initial and final ET outflow is considered capture. The simulated reduction in ET in the transient simulation implies a decline in bofedal and pampa vegetation in response to groundwater pumping in the basin.

Groundwater outflow across the basin outlet changes when hydraulic head at the GHB becomes depressed due to drawdown and the hydraulic gradient between the GHB and the external constant head value is lowered. If hydraulic head at the GHB falls below the external constant head value, the hydraulic gradient is reversed, and groundwater may flow into the basin across the GHB. A significant reduction in groundwater outflow is observed over the duration of the transient simulation in addition to small amount of recharge induced from across the GHB. This change is also an example of capture in the Huaytire Basin.

5.3 Implications for Huaytire and downgradient communities

As introduced in Chapter 1, several anecdotal and observed hydrologic changes have previously been published broadly related to water quantity and quality in the Huaytire Basin and in downgradient systems. Bofedals and other groundwater dependent vegetation communities are reported to have declined in recent years, and streamflow in the Rio Callazas is reported to have diminished in magnitude. These impacts are often reported to be the result of groundwater and surface development in the Huaytire Basin. The results of the numerical groundwater flow model summarized in Chapter 4 indicate that groundwater and surface water pumping in the Huaytire Basin may produce hydrologic changes similar to those discussed in Chapter 1.

Surface water outflow across the basin outlet is eliminated in all three recharge scenarios over the duration of the transient simulation (Figure 4.11), consistent with recent (2023 – 2024) field observations of a dry channel within the basin study area. Groundwater outflow across the southeastern boundary, which may contribute baseflow to downstream gaining reaches of the Rio Callaza, was also significantly reduced (Figure 4.9, Figure 4.10). This result is consistent with reported streamflow deterioration in Rio Callazas downstream of the Huaytire Basin in recent years. In addition, widespread drawdown was also simulated in the model. The rate of simulated evapotranspiration was reduced over the duration of the transient simulation due to water table decline, implying a reduction in phreatophyte health or coverage in the Huaytire Basin. This result is also consistent with previous studies that have documented declining vegetation coverage/vigor in the basin (Oyague and Cooper, 2020; Bahamontes et al., 2021).

The results of the numerical model indicate that groundwater pumping from the Huaytire Basin may have negatively impacted water availability in the Rio Callazas and in the associated agricultural community of Candarave. A reduction in the flow of high-quality groundwater and surface water from the Huaytire Basin may also impact water quality in the Rio Callaza, which receives surface water contributions from several low quality streams containing unsafe levels of dissolved metals downstream of the study area. In addition, reduced phreatophyte coverage in the Huaytire Basin may be harmful to local pastoralists, who are dependent on shallow groundwater and healthy bofedals for successful camelid husbandry in the otherwise sparsely vegetated puna landscape.

5.4 Model Performance

Model calibration efforts yielded an acceptable MAE / Range value of 8.6%. The largest residuals between simulated and observed head values are generally associated with targets located on the Pampa Huaytire and represent areas where model simulated head values are too high. Model errors (nonzero residuals) are related to a variety of factors, including spatial discretization, uncertainty in hydraulic property values, and uncertainty in the magnitude and timing of source/sink fluxes. Regional groundwater flow models inherently require significant generalization and simplification of natural systems, and some degree of error is always expected. The Huaytire Basin numerical model performs adequately well to answer the basic motivating questions of this study with reasonable certainty.

With some exceptions, model generated streamflow is generally consistent with conditions observed in the field and with previously published interpretations of streamflow dynamics in the Huaytire Basin. Maximum simulated streamflow in the Rio Huaytire is two orders of magnitude lower than maximum observed values collected during both gaging events. Despite this deficiency, the presence of simulated streamflow in the Rio Huaytire represents a reasonable approximation of the natural system. The location of simulated gaining and losing reaches in both perennial streams is generally consistent with expected results as inferred from stream gaging and from previously published information. Underperforming streamflow simulation in the Rio Huaytire is not expected to have a significant impact on the key water budget results as summarized above.

Simulated streamflow patterns are more similar to conditions observed during the dry season gaging event than to conditions observed during the wet season gaging event. Gaging location S08, the furthest downstream gaging location on the Rio Japapunco, produced the highest observed streamflow value on the Rio Japapunco during the wet season gaging event and the lowest observed value during the dry season gaging event (Figure 4.2, Figure 4.3). Wet season gaging was performed during periods of intermittent rainfall, which may have produced runoff and streamflow conditions not explicitly simulated in the model. Dry season streamflow is dominated by baseflow and surface water-groundwater exchange and is therefore expected to provide a better target for streamflow simulated in the numerical model. Wet season S08 gaging information is therefore not considered as an appropriate target for model performance.

The Rio Callazas is dry under modern conditions, making it difficult to assess the reasonableness of simulated historic streamflow values. If simulated predevelopment streamflow generated in the Rio Callazas is unrealistically high, then less groundwater discharge along this stream would be available for capture, and the other head-dependent outflow terms in the aquifer water budget would see a greater reduction in magnitude to accommodate pumping. In this scenario, groundwater outflow across the southeastern GHB boundary is likely to see a more significant reduction in flow, and the implication for the Rio Callazas and downstream communities would be similar to the discussion presented above.

Accuracy of simulated lake stage is limited by the simple stage-volume calculation used by MODFLOW and the simplified bathymetry required by the structure of the finite difference grid. Lake Suches is simulated in the top two layers of the finite difference grid with a larger areal extent in Layer 1 than in Layer 2 to approximate lakebed geometry. When lake stage is simulated in layer 2, the lake is assumed to have a flat bottom with vertical sides and a uniform depth. When lake stage occurs in Layer 1, lake area is interpolated between the top of layer two and the top of layer one, and a greater amount of volume change is required to produce a similar change in lake stage. Despite these limitations, simulated lake stage is generally reasonable over the duration of the transient simulation as inferred from satellite imagery and bathymetry data published in Vining (2011).

5.5 Water Stable Isotopes

In general, water samples collected from pumping wells TP-12 and TP-15 are depleted relative to other samples in the dataset and plot close to the global meteoric water line (Craig, 1961) (Figure 4.1). This provides good evidence that deep groundwater in the Capillune Formation is isotopically very similar to precipitation water with little indication of isotopic enrichment along an evaporation line. If the global meteoric water line is a good approximation of isotopic variability in precipitation for the Huaytire Basin, then these results suggest that the deep aquifer in the vicinity of the sampled pumping wells is recharged via precipitation that infiltrates via relatively fast flow paths with minimal potential for evaporation, possibly through high elevation fractured igneous bedrock of the Barroso Group. It also suggests that groundwater produced by the pumping wells west of Lake Suches is not derived from Lake Suches surface water, which is very enriched relative to other samples in the dataset. These results are generally consistent with simulated surface water-groundwater dynamics in the basin. Only a small amount of seepage from Lake Suches to the aquifer occurs at the end of the transient simulation, equivalent to approximately 5% of groundwater inflow to the lake.

5.6 Groundwater Recharge Uncertainty Analysis

In general, aquifer recharge rates are highly uncertain. Model simulations conducted in this study considered a base case recharge rate of 9.7 cm/year in Zone 1 (25% of annual precipitation), with additional low-recharge and high-recharge scenarios that implemented rates equivalent to 15% and 32.5% of annual precipitation, respectively. Regions of the model exceeding 4,700 meters in elevation are assumed to experience higher precipitation rates than lower elevation regions, which is represented in the model by prescribing additional recharge (10% higher than Zone 1). An absolute lower boundary on the recharge flux was calculated by dividing the estimated annual volume of water lost to evaporation from Lake Suches, a relatively well constrained outflow, by the areal extent of the basin. This calculation yields a minimum recharge flux of 0.033 meters per year – a recharge ratio of approximately 8.5%. While this value represents the minimum recharge flux across the basin required to satisfy the net evaporation outflow from Lake Suches, it does not account for surface water outflow, groundwater outflow, or phreatophytic evapotranspiration, which are difficult to measure and poorly constrained in the Huaytire Basin. It is therefore reasonable to assume that the recharge ratio across the Huaytire Basin is higher than 8.5%.

Literature estimates of groundwater recharge on the altiplano are highly variable and site specific, making estimation of recharge in the Huaytire Basin uncertain. Few studies have attempted to quantify recharge on the Peruvian altiplano, although several authors have attempted to quantify groundwater recharge fractions in similar environments in neighboring Chile. de la Fuente et al. (2021) estimated a precipitation dependent recharge fraction ranging between 10% and 35% for various high Andean terminal basins located in northern Chile. Other studies conducted in northern Chile have estimated groundwater recharge fractions ranging between 2% and 21.5% of total precipitation (Kikuchi and Ferre, 2017; Uribe et al., 2015; Blin et al. 2022; Yanez-Morroni et al., 2022). Due to the uncertainty associated with estimating recharge on the altiplano, a range of recharge values were considered to analyze the sensitivity of key model results to the recharge parameter.

The low-recharge scenario model was unable to sustain pumping at the prescribed rate, and some pumping wells repeatedly dried and rewetted over the duration of the transient simulation. The large simulated drawdown and inability to sustain known pumping rates indicate that the prescribed recharge in this scenario was likely too low. Alternatively, it may suggest that the simulated transmissivity of the Capillune Formation is too low. Model runs with higher hydraulic conductivity values attempted during the sensitivity analysis produced unrealistically low heads across the model domain resulting in little or no streamflow in predevelopment simulations. This provides evidence that the calibrated hydraulic conductivity values for the Capillune Formation are appropriate, and that a higher recharge rate than the low-recharge scenario recharge rate is required to sustain pumping in the Huaytire Basin.

The results of the uncertainty analysis indicate that significant hydrologic impacts are expected to occur in the study area due to pumping regardless of prescribed recharge. The high-recharge scenario uses a recharge ratio close to the highest published value for similar environments in the Altiplano and represents an absolute upper boundary on the possible rate of recharge for the Huaytire Basin. Despite this, even in the high recharge scenario surface water outflow from the basin (Rio Callazas) is completely depleted over the duration of the transient simulation. The percentage of each remaining aquifer water budget outflow captured by pumping is highest for the low recharge scenario and lowest for the high recharge scenario. This suggests that, even if the estimated recharge rate used in the base-case scenario is higher than reality, the magnitude of capture due to pumping would be even greater than the simulated base case results summarized in Chapter 4.

5.7 Anthropogenic Basin Closure

The Huaytire Basin may be an example of partial anthropogenic basin closure as described by Pauloo et al (2021). Surface water outflow likely existed under predevelopment conditions as evidenced by the existence of a dry channel near the basin outlet, references to overflowing conditions in several publications, and the results of the predevelopment groundwater flow model. Surface water outflow from the Huaytire Basin does not occur under modern conditions, and the nearest instance of likely perennial streamflow in the Rio Callazas is located approximately 2-km downstream of the basin outlet. Simulated groundwater outflow across the basin outlet falls by more than 50% over the duration of the base case recharge simulation and is likely to continue to fall as the system approaches a new steady state condition. While ground water outflow is not completely captured in the transient simulation, the disappearance of surface water outflow from the Huaytire Basin is a significant event with broad ecological, economic and social implications for the Rio Callazas and associated communities, including the village of Candarave.

5.8 Implications for sustainability

Groundwater pumping outflow from the Huaytire Basin is occurring at approximately 42% of the presumed base case recharge rate. Significant reductions in each of the predevelopment outflow terms were simulated over the duration of the transient simulation in all three potential recharge scenarios. No scenario achieved a new steady state condition during the historical transient simulation, and the reduction in groundwater outflow to evapotranspiration, Lake Suches, and across the GHB is expected to increase in magnitude in the future. Because the rate of groundwater pumping is lower than the rate of recharge, aquifer drawdown will eventually stop and groundwater levels in the Huaytire Basin will stabilize around a new steady state condition. Assuming the modeled recharge rates are reasonably accurate, pumping from the basin can theoretically continue indefinitely at the current rate without depleting all groundwater in storage. However, this will come at the expense of significant additional reductions in phreatophytic vegetation, underflow to the Rio Callaza, and / or significant reduction Lake Suches areal extent. Given the impacts already observed in the Huaytire Basin and in downgradient communities, the current pumping regime may represent an unsustainable path.

CHAPTER 6: CONCLUSIONS

Southwestern Peru is a water stressed region requiring the careful application of well-informed water management strategies. Limited water resources in the area are generally derived from high elevation basins on the Altiplano and Andean highlands and experience intense competition agricultural, municipal, ecological, and industrial users. The disproportionate amount of water delivered from relatively humid headwater basins to lower elevation population centers and industrial users make water resource occurrence and management in high elevation basins deserving of scrutiny. In addition to their regional importance, water resources in highland areas are of local importance for the unique groundwater dependent ecosystems formed in some areas of the Altiplano and for maintaining the habitability of the region for human life.

The Huaytire Basin is a headwater basin in the Altiplano region of Southern Peru that has experienced more than 60 years of groundwater and surface water extraction related to mining activities. Development has been accompanied by observed hydrologic changes, including a decline in streamflow through the downgradient Rio Callazas and a deterioration in phreatophytic vegetation within the basin itself. Weather data collected from near the study area indicated that climate change was not an important driver of observed change in the Huaytire Basin. Our objective was to investigate pumping as a potential cause of hydrologic change in the study area using a numerical groundwater flow model.

A numerical model was developed using MODFLOW to simulate the hydrologic impact of surface water and groundwater withdrawals from the Huaytire Basin on the local hydrology. Groundwater recharge rates on the Altiplano are not well understood, and three recharge scenarios were considered to evaluate uncertainty associated with the recharge parameter. Head dependent flux values representing aquifer outflows saw significant reductions over the duration of the 63-year modeling period in all three recharge scenarios, and surface water outflow was eliminated in all three scenarios. In the base case recharge scenario, surface water discharge to gaining streams was reduced by 50%, groundwater outflow was reduced by 51%, groundwater discharge to Lake Suches was reduced by 9.5%, and phreatophytic evapotranspiration was reduced by 18%. These results demonstrate that groundwater and surface water extraction may be an important driver of the observed hydrologic changes in the Huaytire Basin and downgradient communities.

This study may have been improved with more rigorous and reliable information regarding the hydraulic properties and structure of aquifer materials occurring the basin, additional head targets and streamflow targets for model calibration, and better documentation of hydrologic changes within the basin and in downgradient systems. Future work should perform additional aquifer testing in the study area to better inform numerical modeling efforts, incorporate additional head targets acquired form local resource managers or users, and compile long term water quality and quantity data for the Rio Callazas to quantify possible trends and identify potential causes of water quality and quantity degradation in the region. Given the important social, economic, and ecological impact of water resource extraction from the Huaytire Basin, it is also recommended that future work explores revised management strategies, including lowering pumping rates or introducing managed aquifer recharge, to mitigate the impact of groundwater and surface water extraction in the Huaytire Basin.

LITERATURE CITED

Anderson, M. P., Woessner, W. W., and Hunt, R. J. (Eds.). (2015). Applied Groundwater Modeling (Second Edition). *Academic Press*. https://doi.org/10.1016/B978-0-08-091638-5.00018-3

Administracion Local del Agua Locumba (ALA) (2023). Scanned groundwater well inspection reports, Accessed February 2023

Bahamontes, J. F. C., Calizaya, D. S. Q., & Franco, M. S. S. (2021). Análisis multitemporal de la laguna Suches y del vigor de la vegetación del bofedal de Huaytire, Tacna. *Ciencia & Desarrollo*, *20*(1), Article 1. https://doi.org/10.33326/26176033.2021.1.1106

Balvin, D. (1995). Water, Mining and Pollution. The Southern Peru Case. Editorial Labor.

Beas, T. M. (1996). Lagunas alto andinas del sur del Peru: Caracteristicas quimicas. Ciencia & Desarrollo, 3, Article 3. https://doi.org/10.33326/26176033.1996.3.71

Bebbington, A., and Williams, M. (2008). Water and Mining Conflicts in Peru. *Mountain Research and Development*, 28(3), 190-195. https://doi.org/10.1659/mrd.1039

Benavides, B.G. (2014). *The Territorialization of a small community—The case of Huaytire, Peru* [Master thesis, The University of Bergen]. https://bora.uib.no/bora-xmlui/handle/1956/7993

Blin, N., Hausner, M., Leray, S., Lowry, C., and Suárez, F. (2022). Potential impacts of climate change on an aquifer in the arid Altiplano, northern Chile: The case of the protected wetlands of the Salar del Huasco basin. *Journal of Hydrology: Regional Studies*, *39*, 100996. https://doi.org/10.1016/j.ejrh.2022.100996

Bredehoeft, J. D. (2001). Why hydrogeologists model. *Ground Water*, 39(5), 617–618.

Clark, I., and Fritz, P. (1998). Environmental Isotopes in Hydrology. *Lewis Publishers*.

Consorcio Rio Locumba - CRL (2017). Estudio de Los Recursos Hidricos Superficiales y Subterraneos e Infraestructura Hidraulica para el Plan de Aprovechamiento en la Cuencs del Rio Locumba, en la Region de Tacna. Volument V, Estudio Hidrogeologico de la Cuenca del Rio Locumba.

Cooper, D. J., Sueltenfuss, J., Oyague, E., Yager, K., Slayback, D., Caballero, E. M. C., Argollo, J., and Mark, B. G. (2019). Drivers of peatland water table dynamics in the central Andes, Bolivia and Peru. *Hydrological Processes*, *33*(13), 1913–1925. https://doi.org/10.1002/hyp.13446

Craig, H. (1961). Isotopic Variations in Meteoric Waters. *Science*, *133*(3465), 1702–1703. https://doi.org/10.1126/science.133.3465.1702

Craig, H., & Gordon, L. I. (1965). *Deuterium and oxygen 18 variations in the ocean and the marine atmosphere*. Consiglio nazionale delle richerche, Laboratorio de geologia nucleare.

de la Fuente, A., Meruane, C., and Suárez, F. (2021). Long-term spatiotemporal variability in high Andean wetlands in northern Chile. *Science of The Total Environment*, *756*, 143830. https://doi.org/10.1016/j.scitotenv.2020.143830

Delgado, A. (2020). Quality assessment of surface water associated with a copper mine in Peru using grey systems. *International Journal of Advanced Trends in Computer Science and Engineering*, *9*(4), 6660–6668. https://doi.org/10.30534/ijatcse/2020/359942020

Doherty, J. (2015). PEST: Model-Independent Parameter Estimation (Version 14) [Software]. Watermark Numerical Computing. http://www.pesthomepage.org

Earle, L. R., Warner, B. G., & Aravena, R. (2003). Rapid development of an unusual peat-accumulating ecosystem in the Chilean Altiplano. *Quaternary Research*, *59*(1), 2–11. https://doi.org/10.1016/S0033-5894(02)00011-X

European Space Agency, Sinergise (2021). Copernicus Global Digital Elevation Model. Distributed by OpenTopography. https://doi.org/10.5069/G9028PQB. Accessed: 2024-07-04

Franco León, P., Oyague Passuni, E., Navarro Guzmán, M., Ignacio Apaza, J., Jove Chipana, C., Caceres Musaja, C., Franco Sulea, D. (2022). Bofedales de Huaytire y Anexos. Universidad Nacional Jorge Basadre Grohmann Fondo Editoria

Freeze, R. A., and Cherry, J. A. (1979). *Groundwater*. Prentice-Hall.

Garreaud, R., Vuille, M., & Clement, A. C. (2003). The climate of the Altiplano: Observed current conditions and mechanisms of past changes. *Palaeogeography, Palaeoclimatology, Palaeoecology*, *194*(1), 5–22. https://doi.org/10.1016/S0031-0182(03)00269-4

Geng, D.A. (2018). Inequalities in water governance in a context of mining extractivism. The case of the upper basin of the Locumba River (Tacna, Peru). In Overcoming inequalities in a fractured world: between elite power and social mobilization . (pp. 1 - 22). GENEVA. UNRISD. Retrieved from: https://cdn.unrisd.org/assets/legacy-files/301-info-files/99B57524B22716DDC125833C005AD4AC/Overcoming%20Inequalities%204b_Geng-Spanish---Final.pdf

Gies, E. (2021). Why Peru is reviving a pre-Incan technology for water. *BBC Future*. https://www.bbc.com/future/article/20210510-perus-urgent-search-for-slow-water

Harbaugh, A. W., Banta, E. R., Hill, M. C., and McDonald, M. G. (2000). MODFLOW-2000, The U.S. Geological Survey modular ground-water model: User guide to modularization concepts and the ground-water flow process (Report 00–92; Open-File Report). USGS Publications Warehouse. https://doi.org/10.3133/ofr200092

Hribljan, John, D. Cooper, Jeremy Sueltenfuss, E. Wolf, Katherine Heckman, Erik Lilleskov, and Rod Chimner. 2015. “Carbon Storage and Long-Term Rate of Accumulation in High-Altitude Andean Peatlands of Bolivia.” *Mires and Peat* 15:1–14.

Hvorslev, M.J., 1951. Time Lag and Soil Permeability in Ground-Water Observations, Bull. No. 36, Waterways Exper. Sta. Corps of Engrs, U.S. Army, Vicksburg, Mississippi.

Isch L., Edgar; Ingo Gentes; CAMAREN (Consortium); and WALIR (Organization). "Agua y servicios ambientales : visiones críticas desde los Andes." (2006). https://digitalrepository.unm.edu/abya_yala/556

Instituto Geológico, Minero y Metalúrgico - INGEMMET (1978) Geologia de los Cuadrangulos de Puquina, Omate, Huaytire, Mazo Cruz, y Pizacoma. *Boletin No.29*

Instituto Geológico, Minero y Metalúrgico - INGEMMET (2009) Hidrogeología de la cuenca del río Locumba. Presentación 29° Aniversario

Instituto Geológico, Minero y Metalúrgico - INGEMMET (1998) Hidrogeología de la cuenca del río Locumba. Mapa Hidrogeologico. Mapa No. 3.

Instituto Geológico, Minero y Metalúrgico - INGEMMET (2023). Geological Map of Peru https://hdl.handle.net/20.500.12544/3837

Josse, C., Cuesta, F., Navarro, G., Barrena, V., Cabrera, E., Chacón-Moreno, E., Ferreira, W., Peralvo, M., & A., S. (2009). *Ecosistemas de los Andes del Norte y Centro. Bolivia, Colombia, Ecuador, Perú y Venezuela*.

Kikuchi, C. P., and Ferré, T. P. A. (2017). Analysis of subsurface temperature data to quantify groundwater recharge rates in a closed Altiplano basin, northern Chile. *Hydrogeology Journal*, *25*(1), 103–121. https://doi.org/10.1007/s10040-016-1472-1

Knight Piesold Consultores S.A. (2000), Estudio de Impacto Ambiental del Proyecto Quellaveco. Preparado para Minera Quellaveco; 7 volúmenes.

Knight Piésold Consultores S.A. (2012). Modificación del Estudio de Impacto Ambiental – Optimización del Diseño y Operación de la Presa Vizcachas. Resumen Ejecutivo. Anglo American Quellaveco S.A. Proyecto Quellaveco.

Kohler, M. A., Nordenson, T. J., and Fox, W. E. (1955). Evaporation from pans and lakes. U.S. Department of Commerce, Weather Bureau Research Paper No. 38.

Kriegler FJ, Malila WA, Nalepka RF, Richardson W. (1969). Preprocessing transformations and their effects on multispectral recognition. In: Proceedings of the Sixth International Symposium on Remote Sensing of Environment, 13–16 October 1969, Ann Arbor, MI 97-131.

Kuznar, L. A. (1995). Awatimarka: The ethnoarchaeology of an Andean herding community. Cengage Learning.

Maidment, D. R., (1992) ‘Handbook of Hydrology.’ *McGraw-Hill, Inc*., New York.

McCall, M. K., Boni Noguez, A., Napoletano, B., & Rico-Rodríguez, T. (Eds.). (2021). Territorialising Space in Latin America: Processes and Perceptions. Springer International Publishing. https://doi.org/10.1007/978-3-030-82222-4

Meneses CAZ (2018). Gobierno de los recursos de uso común: Una historia de la regulación del agua en la cuenca alta de Locumba, 1950-2015. Masters Thesis, Pontifica Universidad Catolica del Perú, Lima, Perú.

Merritt, M. L., and Konikow, L. F. (2000). Documentation of a computer program to simulate lake-aquifer interaction using the MODFLOW ground water flow model and the MOC3D solute-transport model (Report 2000–4167; Water-Resources Investigations Report). USGS Publications Warehouse. https://doi.org/10.3133/wri004167

Observavtorio de las Empresas Transnacionales – OET (2008). PROGRAMA DE VIGILANCIA SOCIAL DE LAS EMPRESAS TRANSNACIONALES ANALISIS DE CASOS Y CONCLUSIONES DEL SEGUIMIENTO A TRANSNACIONALES

OECD (2021), *Water Governance in Peru*, OECD Studies on Water, OECD Publishing, Paris, https://doi.org/10.1787/568847b5-en.

Olson, D., Dinerstein, E., Wikramanayake, E., Burgess, N., Powell, G., Underwood, E., D’amico, J., Itoua, I., Strand, H., Morrison, J., Loucks, C., Allnutt, T., Ricketts, T., Kura, Y., Lamoreux, J., Wettengel, W., Hedao, P., & Kassem, K. (2001). Terrestrial Ecoregions of the World: A New Map of Life on Earth. *BioScience*, *51*, 933–938. https://doi.org/10.1641/0006-3568(2001)051[0933:TEOTWA]2.0.CO;2

Oyague Passuni, E., & Cooper, D. (2020). Peatlands of the Central Andes Puna, South America. *37*, 255–260.

Pauloo, R. A., Fogg, G. E., Guo, Z., & Harter, T. (2021). Anthropogenic basin closure and groundwater salinization (ABCSAL). *Journal of Hydrology*, *593*, 125787. https://doi.org/10.1016/j.jhydrol.2020.125787

Pérez-Jiménez, S. (2018). Impacto ambiental de la Compañía minera Southern Perú Copper Corporation en América Latina: Una aproximación histórica de comienzos del siglo XX a la actualidad. Revista Geográfica de América Central, 3(61E), Article 61E. https://doi.org/10.15359/rgac.61-3.25

Perla, C., (2012). Extracting from the Extractors: The Politics of Private Welfare in the Peruvian Mining Industry. [Ph.D., Brown University]. Retrieved October 17, 2023, from https://repository.library.brown.edu/studio/item/bdr:297720/PDF/

Porter GeoConsultancy. (2010). Andean Cu-Au-base metals province - Peruvian Andes PorterGeo Database - Ore Deposit Description

Prudic, D. E., Konikow, L. F., and Banta, E. R. (2004). A new streamflow-routing (SFR1) package to simulate stream-aquifer interaction with MODFLOW-2000.

Salem, J., Amonkar, Y., Maennling, N., Lall, U., Bonnafous, L., & Thakkar, K. (2021). An analysis of Peru: Is water driving mining conflicts? *Resources Policy*, *74*, 101270. https://doi.org/10.1016/j.resourpol.2018.09.010

Sandweiss, D., & Richardson, J. (2008). Central Andean Environments (pp. 93–104). https://doi.org/10.1007/978-0-387-74907-5_6

Shepley, M. G. (2024). Vertical hydraulic conductivity and layered heterogeneity: From measurements to models. *Hydrogeology Journal*, *32*(4), 1017–1042. https://doi.org/10.1007/s10040-024-02773-3

Southern Peru Copper Corporation (SPCC) (1974). El proyecto Cuajone: investigación y desarrollo de recursos hídricos subterráneos y sistema planificado de producción para el abastecimiento de agua

Southern Peru Copper Corporation (SPCC) (2009). Reporte Annual de Evaporaction, Estacion Tocco. Superintendencia de Recursos Hidricos

Southern Peru Copper Corporation - SPCC (2022) Caujone Operations Peru Technical Report Summary https://minedocs.com/22/Cuajone-TR-12312021.pdf

Squeo, F., Warner, B., Aravena, R., & Espinoza, D. (2006). Bofedales: High altitude peatlands of the central Andes. Revista Chilena de Historia Natural, 79, 245–255. https://doi.org/10.4067/S0716-078X2006000200010

Suárez, F., Oportus, T., Mendoza, M., Aguirre, I., Godoy, V., and Muñoz, J. F. (2024). Evaporation processes in the Silala River basin. *WIREs Water*, *11*(1), e1638. https://doi.org/10.1002/wat2.1638

Theis, C.V. (1940). The source of water derived from wells: Essential factors controlling the response of an aquifer to development. *Civil Engineer* 10, 277–280.

Tosi, Joseph A. 1960. Zonas de vida natural en el Perú; memoria explicativa sobre el mapa ecológico del Perú. Lima Instituto Interamericano de Ciencias Agrícolas de la OEA, Zona Andina.

Turnipseed, D.P., and Sauer, V.B. (2010). Discharge measurements at gaging stations: U.S. Geological Survey Techniques and Methods book 3, chap. A8, 87 p. (Also available at http://pubs.usgs.gov/tm/tm3-a8/.)

U.S. Geological Survery. *Geology and mineral resources of the Altiplano and Cordillera Occidental, Bolivia* (Report 1975; Bulletin). (1992). https://doi.org/10.3133/b1975

U.S. Geological Survey. (2024). Landsat 5 Collection 2 Level 2 (LT05_L2SP) [Data set]. Retrieved from https://earthexplorer.usgs.gov

Uribe, J., Muñoz, J. F., Gironás, J., Oyarzún, R., Aguirre, E., and Aravena, R. (2015). Assessing groundwater recharge in an Andean closed basin using isotopic characterization and a rainfall-runoff model: Salar del Huasco basin, Chile. *Hydrogeology Journal*, *23*(7), 1535–1551. https://doi.org/10.1007/s10040-015-1300-z

Vining, B.R. (2011). Ruralism, Land Use History, and Holocene Climate in the Suches Highlands, Southern Peru. Ph.D. Dissertation, Boston Univ., Boston, Massachusetts.

Vining, B.R. (2016) Pastoral Intensification, Social Fissioning, and Ties to State Economies at the Formative Period–Middle Horizon Transition in the Lake Suches Region, Southern Peru. Pp. 87–118 in *The Archaeology of Andean Pastoralism*.

Vining, B. R., Steinman, B. A., Abbott, M. B., and Woods, A. (2019). Paleoclimatic and archaeological evidence from Lake Suches for highland Andean refugia during the arid middle-Holocene. *The Holocene*, *29*(2), 328–344. https://doi.org/10.1177/0959683618810405

Viviroli, D., Dürr, H. H., Messerli, B., Meybeck, M., & Weingartner, R. (2007). Mountains of the world, water towers for humanity: Typology, mapping, and global significance. *Water Resources Research*, *43*(7). https://doi.org/10.1029/2006WR005653

Viviroli, D., Kummu, M., Meybeck, M., Kallio, M., & Wada, Y. (2020). Increasing dependence of lowland populations on mountain water resources. *Nature Sustainability*, *3*, 1–12. https://doi.org/10.1038/s41893-020-0559-9

Yáñez-Morroni, G., Suárez, F., Muñoz, J. F., and Lagos, M. S. (2024). Hydrological modeling of the Silala River basin. 1. Model development and long-term groundwater recharge assessment. *WIREs Water*, *11*(1), e1690. https://doi.org/10.1002/wat2.1690